UNIVERSITÉ DE SHERBROOKE
Faculté de génie

Département de génie mécanique

Analyse et optimisation d'un système de pompe à chaleur au CO_2 transcritique intégré avec un éjecteur diphasique

Analysis and optimization of a transcritical CO_2 heat pump system using a two-phase ejector

Thèse de doctorat
Spécialité: génie mécanique

Doctoral Thesis
Specialty: Mechanical Engineering

Sahar Taslimi Taleghani

Jury:
Mikhail Sorin (supervisor)
Sébastien Poncet (co-supervisor)
Nicolas Galanis (examiner)
Bernard Marcos (examiner)
Armin Hafner (examiner)
Brice Le Lostec (examiner)

Sherbrooke (Québec) Canada Janvier 2019

To my mother and father, Maryam and Saeed

To my sisters, Sara and Setareh

And to my spouse, Payam

RÉSUMÉ

L'objectif principal de ce projet de recherche est d'étudier en détail un système de pompe à chaleur transcritique au CO_2 utilisant un éjecteur diphasique pour améliorer l'efficacité énergétique et les performances du système.

Un cycle de CO_2 transcritique entraîne des pertes importantes lors de la détente (processus isenthalpique) ce qui explique de faibles performances thermodynamiques. Parmi les différents dispositifs de récupération des travaux d'expansion, un éjecteur est proposé pour récupérer une partie des travaux d'expansion dans le processus de régulation et améliorer l'efficacité du cycle. Par conséquent, il est important de comprendre les effets des performances de l'éjecteur ainsi que ses paramètres de fonctionnement pour parvenir à la conception optimale d'un système de réfrigération ou d'une pompe à chaleur.

Une étude comparative de différents cycles de réfrigération d'éjecteur au CO_2 transcritique a été réalisée et a montré que le cycle de récupération d'expansion de l'éjecteur (EERC) a le plus haut coefficient de performance (COP) et la plus haute efficacité exergétique par rapport aux autres cycles. Le COP et l'efficacité exergétique de l'EERC sont 23.3% supérieurs à ceux du cycle de recirculation de liquides (LRC). Ils sont respectivement 24.9% et 25,5% supérieurs à ceux du cycle de pression de refoulement du compresseur (CDPC) et sont respectivement 5.6 fois et 56.2% supérieurs à ceux et d'un cycle de réfrigération à jet de vapeur (VJRC). Il peut également améliorer le COP et l'efficacité exergétique de 23% et 24%, respectivement, par rapport à un cycle conventionnel.

Étant donné que les éjecteurs peuvent fonctionner dans différentes conditions de fonctionnement autres que le point critique, un modèle numérique détaillé a été développé pour évaluer les performances d'un éjecteur diphasique dans des conditions de simple et double « choking ». Le modèle a été validé avec succès à l'aide des données expérimentales disponibles dans la littérature ainsi que des données fournies par le laboratoire de technologie de l'énergie (LTE) d'Hydro-Québec. Ce modèle permet de prédire les performances de l'éjecteur pour une géométrie fixe (off-design) ainsi que pour des conditions de fonctionnement fixes (on-design).

L'évaluation de l'exergie de l'éjecteur diphasique au CO_2 a été réalisée pour les conditions de simple et double "choking" afin d'étudier l'impact de la contre-pression sur les pertes et les rendements exergétiques. Le comportement de trois mesures thermodynamiques, la production d'exergie, la consommation d'énergie et les pertes d'exergie, a été étudié. Les résultats de la comparaison de deux critères de performance exergétique (l'efficacité exergétique transitoire et l'efficacité exergétique de Grassmann) ont montré la présence d'une valeur maximale de l'efficacité exergétique transitoire autour du point critique. Il a également été déterminé que l'efficacité exergétique de Grassmann ne constitue pas un critère approprié pour évaluer les performances d'un éjecteur au CO_2 transcritique.

Enfin, un modèle de simulation d'un système de pompe à chaleur au CO_2 transcritique avec des échangeurs de chaleur à plaques pour le refroidisseur à gaz et l'évaporateur a été développé et validé expérimentalement. Un modèle de conception d'éjecteur diphasique a été intégré dans le modèle du système de pompe à chaleur pour analyser les différentes performances des systèmes de pompe à chaleur à éjecteur au CO_2. Ce modèle est basé sur les surfaces de transfert de chaleur réelles soumises à la contrainte d'une surface totale constante des échangeurs de chaleur. Les

effets des conditions de fonctionnement ainsi que des paramètres de conception de l'éjecteur, tels que le diamètre de la gorge de la buse primaire, le rapport de surface utile, le diamètre de sortie du diffuseur ainsi que le rapport de surface de transfert de chaleur sur les performances du système ont été étudiés. Les conditions optimales d'utilisation et les caractéristiques de l'éjecteur correspondant au COP maximal et à la capacité de chauffage maximale ont été obtenues afin de déterminer la conception optimale d'un cycle au CO_2 transcritique. Les rapports de surface de transfert de chaleur ont des effets importants sur le COP_h, la capacité de chauffage ainsi que sur la pression optimale du refroidisseur de gaz. Les caractéristiques de l'éjecteur ont des effets importants sur les performances optimales du système. Le diamètre de gorge de la buse primaire et le rapport de surface effective sont deux paramètres importants et peuvent être ajustés pour contrôler les conditions de fonctionnement lors de la conception des cycles à éjecteur. Cependant, le diamètre de sortie du diffuseur n'a pas d'effet significatif sur les performances du système. Le COP et la capacité de chauffage de la pompe à chaleur à éjecteur peuvent augmenter d'environ 17% et 20% respectivement en augmentant le ratio de la surface de transfert de chaleur. Les diamètres de gorge désirés et le rapport de surface efficace de l'éjecteur dans des conditions de fonctionnement données ont été obtenus dans la plage de 1.35 à 1.5 mm et de 7.8 à 8.3 respectivement. Les plages optimales du rapport d'entraînement et du rapport de pression sont également de 0.47 à 0.61 et de 1.16 à 1.35 respectivement.

Mots-clés: cycle de pompe à chaleur, éjecteur diphasique, CO_2, modèle thermodynamique, optimisation

ABSTRACT

The main objective of this research project is a detailed investigation of a transcritical CO_2 heat pump system using a two-phase ejector to improve energy efficiency and system performance.

A transcritical CO_2 cycle has large expansion losses due to an isenthalpic throttling process which causes the low thermodynamic performance of such systems. Among different expansion work recovery devices, an ejector is proposed to recover part of the expansion work in the throttling process and improve efficiency. Therefore, it is important to understand the effects of ejector performance as well as the operating parameters to reach an optimal design of a refrigeration or heat pump system.

A comparative study of different transcritical CO_2 ejector refrigeration cycles was performed under the same cooling capacity and showed that EERC (ejector expansion recovery cycle) has the highest COP and exergy efficiency compared to other cycles. The COP (resp. exergy efficiency) of EERC is approximately 23.3% (resp. 23.3%), 24.9% (resp. 25.5%) and 5.6 times (resp. 56.2%) higher than the corresponding COP and exergy efficiencies of liquid recirculation cycle (LRC), compressor discharge pressure cycle (CDPC) and vapor jet refrigeration cycle (VJRC). The integration of an ejector can also improve the COP and exergy efficiency by up to 23% and 24%, respectively compared to a conventional throttling valve cycle.

Since the ejectors may work at different operating conditions other than the critical point, a detailed numerical model was developed to evaluate the performance of a two-phase ejector under single choking and double choking conditions. The model was successfully validated with the experimental data available in the literature as well as the data provided by Hydro Québec's energy technologies laboratory (LTE). This model enables to predict the ejector's performance for a fixed geometry (off-design) as well as for fixed operating conditions (on-design).

The exergy evaluation of the CO_2 two-phase ejector was performed for both single and double choking conditions to investigate the impact of the back-pressure on the exergy losses and exergy efficiencies. The behavior of three thermodynamic metrics: exergy produced, exergy consumed and exergy losses was studied. The comparison results of two exergy performance criteria (transiting exergy efficiency and Grassmann exergy efficiency) illustrated the presence of a maximum value of transiting exergy efficiency around the critical point. It was also determined that the Grassmann exergy efficiency is not an appropriate criterion for the evaluation of a transcritical CO_2 ejector performance.

Lastly, a simulation model of a transcritical CO_2 heat pump system with plate heat exchangers for the gas cooler and the evaporator was developed and experimentally validated. A two-phase ejector design model was integrated into the model of the heat pump system to analyze the different performances of the CO_2 ejector heat pump systems. This model was based on the actual heat transfer areas under the constraint of constant total heat exchangers' area. The effects of the operating conditions as well as ejector design parameters such as primary nozzle throat diameter, effective area ratio, diffuser outlet diameter and also the heat transfer area ratio (the ratio of the gas cooler area to the evaporator area) on system performance were investigated. The optimum operating conditions and ejector characteristics corresponding to maximum COP and heating capacity were obtained in order to determine the optimum design of a transcritical CO_2 cycle. The heat transfer area ratios have important effects on COP_h, the heating capacity as well as the optimum gas cooler pressure. The ejector characteristics have

significant effects on the optimal performance of the system. The primary nozzle throat diameter and effective area ratio are two important parameters and can be adjusted to control the operating conditions for the design of ejector cycles. However the diffuser outlet diameter has no significant effect on the system performance. COP and heating capacity of the ejector heat pump can increase by approximately 17% and 20% respectively by increasing the heat transfer area ratio from 0.68 (A_{gc}=1.68 m^2, A_{ev}=2.46 m^2) to 4.7 (A_{gc}=3.41 m^2, A_{ev}=0.72 m^2). The desired throat diameters and effective area ratio of the ejector at given operating conditions were obtained in the range of 1.35-1.5 mm and 7.8-8.3 respectively. The optimal ranges of the entrainment ratio and pressure ratio were also 0.47-0.61 and 1.16-1.35 respectively.

Keywords: heat pump cycle, two-phase ejector, CO_2, thermodynamic model, optimization

ACKNOWLEDGMENTS

I would like to sincerely thank my supervisor, Prof. Mikhail Sorin for providing me an opportunity to do this project and his expertise, understanding and guidance during my work. I am also grateful to my co-supervisor Prof. Sébastien Poncet for his valuable support, guidance and encouragement. I am extremely thankful to such nice supervision and assistance of you both along the completion of my project.

I would like to express my profound gratitude to members of the jury, for their time to assess my work and their insightful suggestions and comments to improve it.

I would like to acknowledge my industrial partner, Dr. Hakim Nesreddine, at Hydro Québec's energy technologies laboratory (LTE) for his professional cooperation.

I am grateful to all my friends and colleagues who have supported me along the way and have given me good memories during the last 3 years.

I am profoundly grateful to my parents and my sisters who have provided me through moral encouragement and emotional support, as always for which my expression of thanks does not suffice.

Last, but not least, I owe my deep gratitude to my husband, Payam, for his great patience and personal support at all times.

TABLE OF CONTENTS

LIST OF FIGURES

LIST OF TABLES

CHAPTER 1

INTRODUCTION

1.1 Background and motivation

Energy saving and the use of clean energy sources have recently become significant issues. Increasing energy costs, ozone layer depletion and global warming have made an uncertain future for energy and global environment. Therefore the development of new technologies and the use of natural refrigerants with very low GWP coefficient help to find solutions for the future energy needs and reduction of the environmental impact.

All industrial sectors are developing systems to reduce greenhouse gas emissions. Carbon dioxide is an attractive alternative refrigerant in heating and refrigeration systems that has minimum impact on climate change [1]. In addition, it is not toxic, flammable and corrosive so it has no impact on the ozone layer. Using CO_2 as a refrigerant in heat pump systems is also competitive with other refrigerants [1]–[3]. It helps to decrease environmental phenomena and to improve energy savings. However, transcritical CO_2 compression cycle has a large throttling loss compared to the other refrigerants due to high-pressure change during expansion of a supercritical CO_2 to a subcritical state in an isenthalpic throttling process [4].

Ejector is a promising approach to be employed in a transcritical CO_2 cycle for expansion [5]. It has simple construction with no moving parts, robust and reliable operation. In an ejector, high-pressure motive (primary) stream expands in the primary nozzle into a low pressure and high velocity. This low pressure entrains a suction (secondary) stream into the mixing section. Inside the mixing section, the two streams exchange momentums and energies and then the uniform mixture compresses to a pressure higher than the inlet pressure of the secondary stream [6].

Since ejector is an important component in ejector refrigeration and heat pump systems, a better understanding of its performance is necessary to realize the potential to improve system efficiency [6]. There are numerous literature reviews which present ejector for CO_2 expansion work recovery but most of the existing works are limited to refrigeration cycle and global measurements to investigate overall system performance and energy efficiency improvement [7], [8]. Only a few of them worked on the optimization of a transcritical CO_2 ejector cycle considering both operating conditions and geometric parameters of the ejector. Thus because of this limited knowledge about CO_2 ejector systems, obtaining an optimum design methodology has received much attention of many researchers. This thesis presents an optimization study and detail investigation of a transcritical CO_2 heat pump cycle using an ejector. A two-phase ejector model is developed and incorporated into a heat pump cycle to reveal the effects of various parameters such as operating conditions, ejector geometry and heat transfer areas in a heat pump system. An ejector design model is developed to determine optimum design characteristics. An experimental study is performed to provide a validation of the analytical results of the heat pump and the ejector separately. Furthermore, a parametric study is presented based on the developed model to determine optimal design parameters and their effects on the system performance.

1.2 Objectives and approach

The main objective of the project is the analysis and optimization of a transcritical CO_2 heat pump system using a two-phase ejector and the detailed investigation of ejector characteristics to propose an efficient design improving the system performance.

This general objective includes the following specific objectives:

- Develop a detailed numerical model of a two-phase ejector using CO_2 as a refrigerant to predict the performance of an ejector under different operating conditions (single choking, double choking and critical point) and geometric parameters.
- Develop a simulation model of a CO_2 heat pump using plate heat exchangers.
- Perform the experimental analysis of a CO_2 heat pump and a two-phase ejector to validate the simulation models of the heat pump cycle as well as the ejector.
- Develop a simulation model of an ejector expansion transcritical CO_2 cycle to investigate the effects of ejector design parameters as well as operating conditions on the overall system performance.
- Perform a parametric study and optimization of a heat pump system with ejector including both operating conditions and ejector characteristics as well as heat exchangers areas.
- Identify the optimal design values to maximize the COP, heating capacity and ejector efficiency of a transcritical CO_2 ejector heat pump system.

1.3 Thesis outline

Chapter 2 of this thesis presents a review of the transcritical CO_2 systems and the principle of the ejector including modeling, governing equations, mixing theory, efficiency, critical mode and sound velocity.

Chapters 3 and 4 present the journal publications that were completed during the doctoral project. Chapter 5 is an article published in a conference proceeding. Chapter 6 is an article submitted for publication. These chapters include a section, “Avant-Propos”, which gives abstract, the status of the articles and their contribution to the thesis in French.

In chapter 3, a comparative study of different configurations of transcritical CO_2 ejector cycles is presented to identify the most efficient one. The COP, exergy efficiency and exergy destructions are calculated and compared for the expansion work recovery cycle (EERC), liquid recirculation cycle (LRC), compressor discharge pressure cycle (CDPC) and vapor jet refrigeration cycle (VJRC). Exergy analysis is also performed to determine the amount and locations of irreversibilities within different components of each cycle.

In Chapter 4, a detailed numerical model of a two-phase CO_2 ejector is presented to evaluate the ejector performance under different working conditions (single choking, double choking).

First, a new model is developed for a fixed geometry (off-design) which enables to predict the ejector's performance in both single and double choking conditions. Then, an ejector design model is developed to estimate its dimensions under fixed operating conditions (on-design). The ejector model is then validated using available experimental data in the literature as well as the data provided by Hydro Québec's energy technologies laboratory (LTE).

Chapter 5 presents an exergy analysis of a transcritical CO_2 two-phase ejector for different ejector's working conditions (single choking, double choking and critical point). The exergy losses and exergy efficiencies are evaluated for different back pressures. Two important metrics, exergy produced and exergy consumed are calculated based on transiting exergy. Grassmann exergy efficiency ($\eta_{ex,GR}$) and transiting exergy efficiency ($\eta_{ex,TR}$) for three different cases are compared to show the influence of transiting exergy flow inside a two-phase ejector.

In chapter 6, a model of a transcritical CO_2 heat pump cycle with plate heat exchangers for gas cooler and evaporator is simulated and experimentally validated. Then the ejector model is integrated within the heat pump system model to evaluate the system performance. Afterward, the parametric analysis is conducted to evaluate the effects of heat transfer areas, ejector characteristics and operating conditions on the COP and heating capacity of a transcritical CO_2 ejector heat pump system.

A summary of important conclusions as well as the future work of this study is expressed in chapter 7. Finally, an appendix and the references are given at the end of the thesis.

CHAPTER 2

STATE OF THE ART

This chapter presents a general review of a transcritical CO_2 cycle, the principle of an ejector and its important characteristics and applications of the ejector in expansion work recovery cycles. First, a transcritical CO_2 cycle is introduced and then the ejector performance and some of the important parameters for ejector modeling are described and finally, recent advancements in transcritical CO_2 ejector expansion system are presented.

2.1 History of CO_2

Carbone dioxide is an old refrigerant which was used in the refrigeration industry more than 100 years ago (1830-1930). However it disappeared after growing need for safety refrigerants and the first generation of synthetic refrigerants (CFCs). Due to chlorine contents in CFCs and their high ozone depletion potential (ODP), HCFCs with much lower ODP replaced CFCs. According to Montreal Protocol CFCs were phased out by January 1996 and HCFCs should be phased out by 2020. After phasing out of CFCs and HCFCs, HFC refrigerants were introduced. They have no ozone depletion potential but high global warming potential (GWP). After 1995 global warming has become an issue. Therefore, using natural refrigerant such as CO_2 has become more important. The historical cycle of the refrigerants is shown in Figure 2.1. Nowadays, the divers to use natural refrigerants are as follows:

- Kyoto protocol (1997) to reduce the emission of greenhouse gases
- EU commission F-Gas regulation to use natural working fluids (NWF) (2014)
- Montreal Protocol on GWP refrigerates (2016)
- Accelerated phasedown of HFCs
- Ban on HFCs
- Governmental restrictions and tax on HFCs

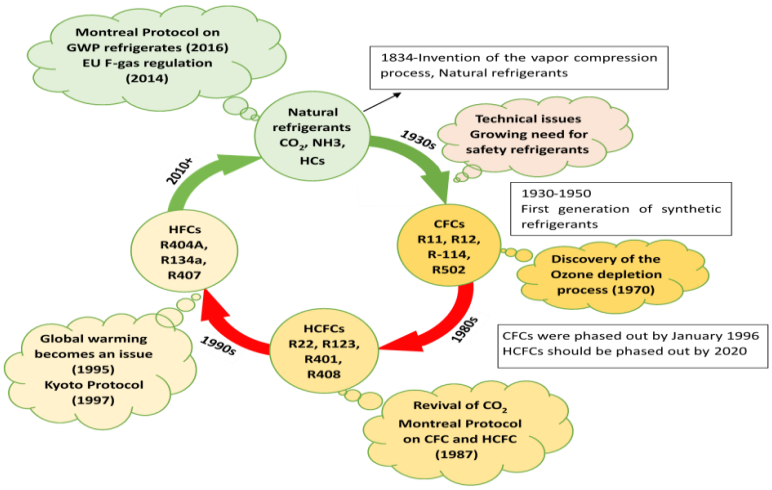

Figure 2.1 Historical cycle of the refrigerants

2.2 Transcritical CO_2 cycle

Carbone dioxide is a natural refrigerant that is secure, reliable, inexpensive and available. It is not toxic, flammable or corrosive so it has a global warming potential (GWP) of 1 and no impact on the ozone layer. Furthermore, it has a low critical temperature and high working pressure. The critical temperature and pressure are 31.1˚C and 73.7 bars respectively. Figure 2.2 shows the phase diagram of CO_2. The vapor pressure of CO_2 is much higher and its volumetric refrigeration capacity is 3 to 10 times larger than CFC, HCFC, HFC and HC refrigerants used in the different refrigeration applications. This feature results in a compact size for the compressor and less material consumption for the piping operating with CO_2 [1], [2], [9].

The performance of carbon dioxide is different from other refrigerants used in conventional vapor compression refrigeration and heat pump systems due to its application in transcritical cycles. For a saturating temperature above the critical temperature along with high pressure, the cycle is referred to transcritical [2]. A conventional cycle works under the critical point. Heat absorption occurs in the evaporator at low pressure and heat rejection occurs in the condenser at high pressure but in the transcritical cycle, heat rejection takes place in the gas cooler at a pressure above the critical point. Compared to a subcritical cycle, a CO_2 transcritical cycle has larger expansion losses of an isenthalpic throttling process because of the large pressure difference between heat rejection and heat absorption that causes low performance of the cycle [10]. A conventional refrigeration cycle and the corresponding pressure-specific enthalpy diagrams at subcritical and transcritical cycles are shown in Figure 2.3.

In a CO_2 transcritical cycle, a high-pressure change occurs when the supercritical CO_2 expands to subcritical state yielding a greater throttling loss compared to other refrigerants. Throttling loss can be reduced in different ways. One of the promising ways is to include an ejector. An ejector expansion device can replace the throttling valve to recover the expansion losses and increase the cycle efficiency. It increases the suction pressure of the compressor that results in reducing the compressor work.

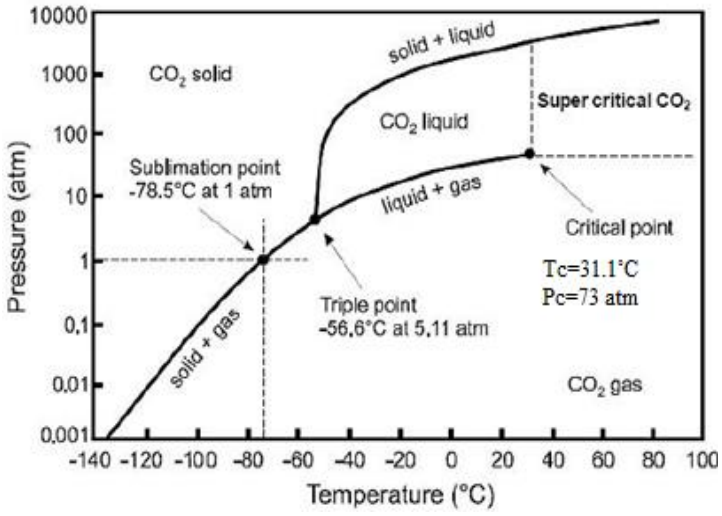

Figure 2.2 Phase diagram of CO_2

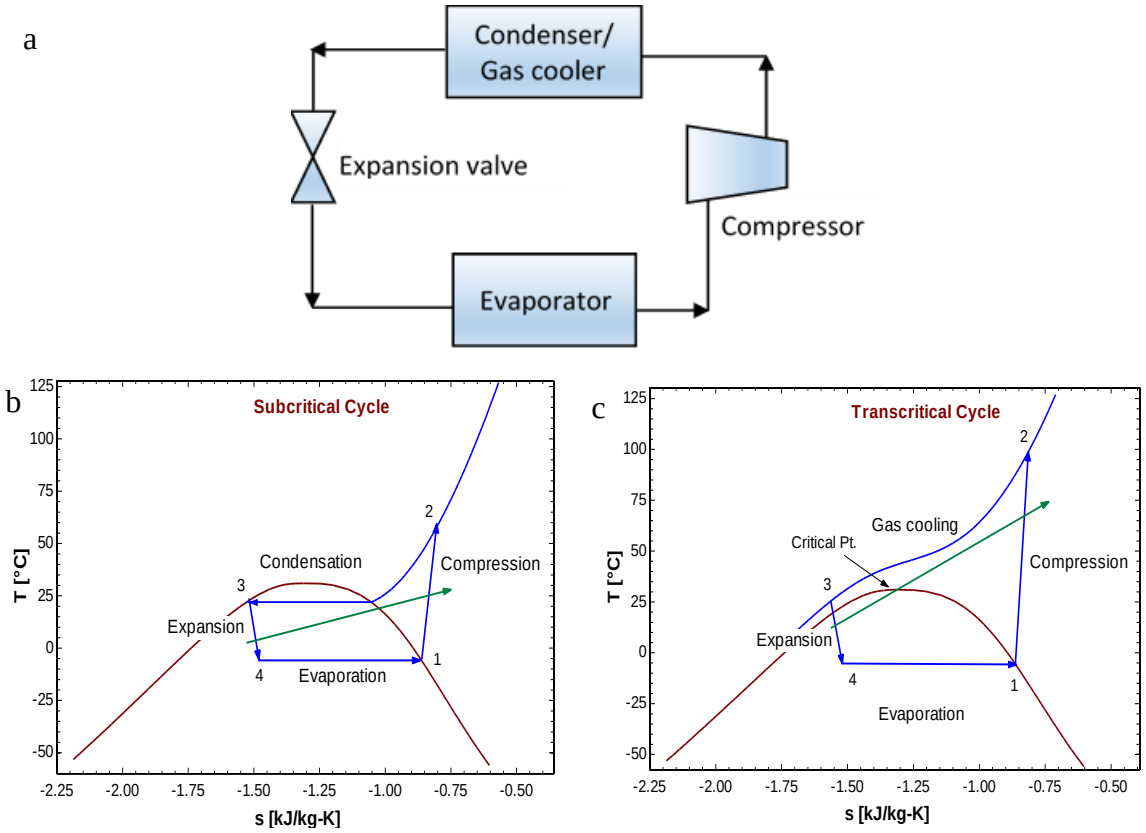

Figure 2.3 a) Conventional refrigeration cycle; Pressure-specific enthalpy diagrams: b) subcritical cycle, c) transcritical cycle

2.3 Principle of an ejector

An ejector is a simple and reliable device with no moving part, which can be used in refrigeration and heat pump systems. Using ejector in air conditioning and refrigeration systems based on low-grade energy has been studied since the mid-1950s. Understanding the ejector performance is vital to determine the size, capability, cost and performance of the whole system. It is also important to investigate the ejector characteristics for optimization purpose to obtain appropriate operating conditions and geometrical parameters and improve the system performance. Due to the specific geometry and operating conditions of the ejector, complex flow phenomena may occur including supersonic conditions, shock occurrence, turbulent mixing, two-phase flow (in some cases) and shock-boundary layer interactions. Thus the understanding of the ejector theory is not yet very clear. It requires to use conservation equations of mass, energy and momentum, some gas dynamic equations, state equations, isentropic relations as well as some appropriate assumptions in the description of the flow and mixing within the ejector.

Schematic of an ejector is shown in

Figure 2.4. A typical ejector comprises a primary nozzle, a secondary nozzle, a mixing section and a diffuser. Working process of an ejector can be explained as follows. The primary stream expands through a converging-diverging nozzle from high pressure into a supersonic speed and very low pressure in the mixing section. Its internal energy converts to kinetic energy during acceleration.

The low pressure of the primary stream at the nozzle exit plane entrains the secondary stream into the mixing chamber and its velocity increases. Then two streams mix. They exchange momentum, kinetic and internal energies and become a uniform stream. The mixture of the two streams further converts its kinetic energy into internal energy and increases its pressure toward the diffuser exit to a pressure higher than the initial secondary inlet pressure. The ejector performance is defined by two global parameters [11]:

$$\text{Entrainment ratio, (ER)} = \frac{\text{mass of secondary flow}}{\text{mass of primary flow}} \tag{2.1}$$

$$\text{Pressure ratio , } (P_{ratio}) = \frac{\text{static pressure at diffuser exit}}{\text{static pressure at secondary inlet}} \tag{2.2}$$

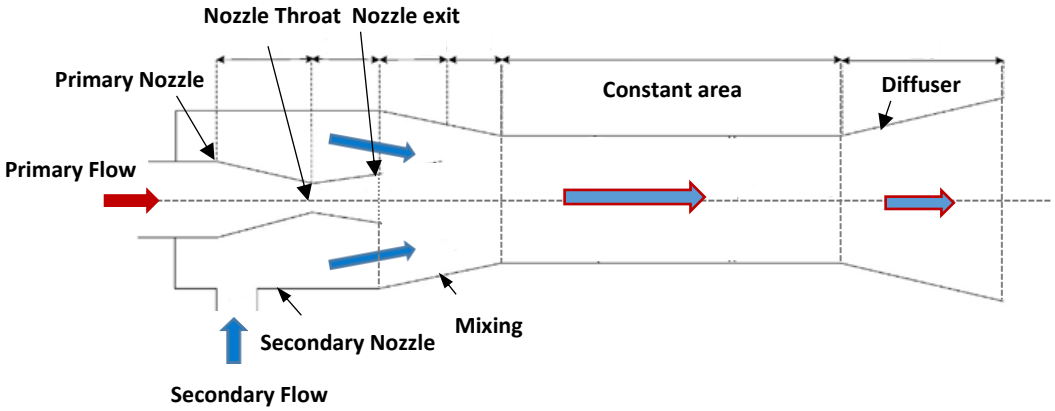

Figure 2.4 Schematic of an ejector

2.4 Modeling of a two-phase ejector

Different models of the ejectors exist according to assumptions, governing equations, auxiliary conditions, mixing mechanism and solution methods. Thermodynamic modeling is a simple way to solve the equations in one dimension. It is also easily integrated into a system. Conservation equations of mass, momentum and energy, some gas dynamic equations, state equations, isentropic relations as well as some appropriate assumptions, initial and boundary conditions are used to solve the flow within the ejector. Some assumptions that are usually employed to simplify the problem are as follows: adiabatic walls of the ejector, steady state flow, isentropic or polytropic efficiencies for the nozzles and the diffuser, stagnation points of the streams at inlets and outlet of the ejector, friction losses in the mixing chamber, and dissipation coefficient for mixing losses. Most ejector models presented for CO_2 two-phase flows are based on a homogeneous equilibrium model in which both gas and liquid are in thermodynamic and mechanical equilibrium. It means that both phases have the same pressure, temperature, velocity, turbulence kinetic energy and turbulence dissipation [5], [7], [12]–[17]. Although there are some works on the non-homogeneous (heterogeneous) formulation of a CO_2 two-phase fluid, flow patterns in CO_2 two-phase ejectors

have not been well studied and recorded so far. The design of a two-phase ejector requires advanced knowledge on flow pattern, mass, momentum, energy transfer, shock waves propagation, phase change mechanism and turbulence models. Moreover, each assumption made by the heterogeneous flow model is not completely certain and may be far from real cases. On the other hand, the homogeneous flow model showed it could be a reliable alternative in different situations [18], [19].

Under ideal conditions, the general equations which are used in each section of the ejector are as follows:

Conservation of mass

$$\sum \rho_i u_i A_i = \sum \rho_e u_e A_e \tag{2.3}$$

Conservation of momentum

$$P_i A_i + \sum \dot{m}_i u_i = P_e A_e + \sum \dot{m}_e u_e \tag{2.4}$$

Conservation of energy:

$$\sum \dot{m}_i (h_i + {}^{u_i^2}/_2) = \sum \dot{m}_e (h_e + {}^{u_e^2}/_2) \tag{2.5}$$

2.5 Mixing theory inside the ejector

The ejector can be defined according to the position of its nozzle exit (NXP). There are two feasible methods, first is the constant area mixing ejector in which the nozzle exit is located within the constant area mixing section. The mixing of the primary and secondary streams occurs inside the constant area section. The second one is the constant pressure mixing where the nozzle exit is located within the converging part of the mixing chamber or suction chamber and the mixing occurs at a constant pressure.

Figure 2.5 shows a constant area and a constant pressure mixing. A normal or oblique shock wave may also occur if there is a supersonic flow mixture inside the constant mixing section that causes a pressure rise and a subsonic flow in the entrance of the diffuser.

The constant pressure and constant area theories have been first developed by Keenan et al. [20]. Their work is based on a one-dimensional (1-D) design of the ejector. For the constant pressure mixing model, they assumed that the primary and secondary flows reach the same pressure at the nozzle exit and then mixing occurs with constant pressure. They also reported that a constant pressure mixing gives better performance of a model than a constant area mixing model and the constant area model provides generally a better agreement with experimental results. However, there are some models in which mixing occurs with both pressure and area changes [21], [22].

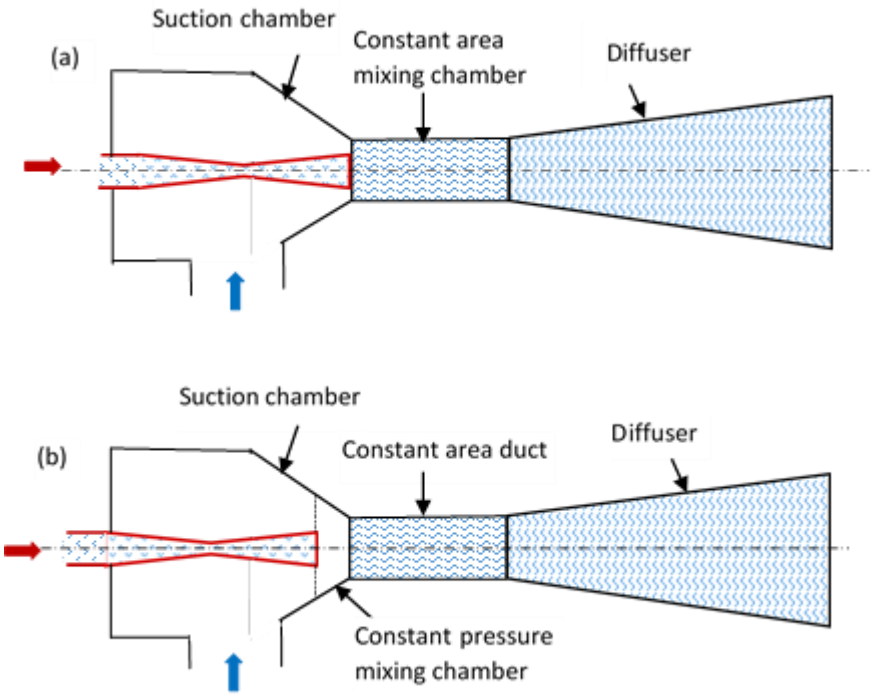

Figure 2.5 Schematic of an ejector with (a) constant area mixing, (b) constant pressure mixing

2.6 Ejector component efficiencies

In the thermodynamic model, it needs to implement some coefficients as an approximation to account for the effects of a non-isentropic process, frictional and mixing losses. Isentropic coefficients (η_p, η_s, η_d) are used to account for non-ideal processes in the nozzles and diffuser. The effects of frictional and mixing losses are also taken into account by using a coefficient (η_{mix}) in the momentum equation. These parameters are highly dependent on the ejector design and configuration. Therefore it is not possible to extract them easily. They can be determined by CFD and experiments by matching the test and analytical results. Since the ejector model is highly dependent on the efficiency coefficients of the ejector components, it is important to improve the methods for estimating actual ejector coefficients and determine their effects on the ejector geometry. Neither Keenan et al.[20] nor Munday and Bagster [23] have considered irreversibilities due to friction in their works.

Huang et al. [24] conducted experiments using a heat driven system for 11 different ejector specifications using R141b. they determined the ejector component efficiencies by matching experimental data with simulation results of a 1-D ejector model. The constant values for the primary and secondary nozzle efficiencies and an empirical relation for the mixing efficiency were obtained.

CFD modeling was firstly used to determine ejector efficiencies by Varga et. al. [25] for water as a working fluid in air conditioning systems. The simulated enthalpies and isentropic process were

compared to determine the primary nozzle, suction nozzle and diffuser efficiencies. They concluded that the primary nozzle efficiency was only dependent on the nozzle throat diameter and it was independent of operating conditions. The suction efficiency was also constant and just reduced when the pressure was above a critical value. The diffuser efficiency depends on the condenser conditions and increases by increasing the back pressure. The mixing efficiency increases with the back pressure until a critical value and then decreases significantly. They also obtained an optimal value of area ratio for ejector performance according to operating conditions.

Liu and Groll [26] studied ejector efficiencies based on a model of two-phase flow ejector and measured data. They established empirical relations for the isentropic efficiencies of the primary and secondary nozzles, and the efficiency of the mixing section. Their results showed that ejector component efficiencies highly depend on geometries and operating conditions. The range of 0.5-0.93 was obtained for the primary nozzle, 0.37-0.9 for the secondary nozzle and 0.5-1 for the mixing section. A transcritical CO_2 refrigeration cycle with a controllable ejector at different geometrical and operating conditions was used in their study. The motive nozzle efficiency was dependent on the ejector throat diameter. The suction nozzle efficiency was affected by the motive nozzle throat diameter, primary nozzle exit position, and outdoor air temperature while the mixing efficiency was varied by the primary nozzle exit position and outdoor air temperature.

The values of the component efficiencies used in recent works for the modeling of two-phase CO_2 ejector are summarized in Table 2.1.

Table 2.1 Component efficiencies from literature in a CO_2 two-phase ejector

Authors	η_p	η_s	η_d	η_{mix}
Ameur et al. [12]	0.85	0.85	0.7	0.97
Elbel and Hrnjak [27]	0.8	0.8	0.8	
Elbel and Hrnjak [13]	0.9	0.9	0.9	
Lawrence and Elbel [28]	0.8	0.8	0.75	
Li and Groll [7]	0.9	0.9	0.8	
Ksayer [29]	0.85	0.85	0.75	
Fangtian and Yitai [30]	0.9	0.9	0.8	
Manjili and Yavari [31]	0.7	0.7	0.8	0.95
Deng et al. [8]	0.7	1	0.8	
Sarkar [16]	0.8	0.8	0.75	
Zhang and Tian [32]	0.9	0.9	0.8	

Galanis and Sorin [33] first introduced constant polytropic efficiencies in the ejector (which is used in aerodynamic processes of turbine and compressor) instead of the constant isentropic efficiencies. They used polytropic efficiencies for expansion processes in the nozzles and compression process in the diffuser to consider the effect of the pressure ratio through off-design operation in a 1-D thermodynamic model. It was later used successfully for real gases for single-phase ejectors [21],

[34], [35]. Haghparast et al. [35] also showed that the replacement of isentropic efficiencies by polytropic efficiencies within 1-D ejector models provides more accurate results.

2.7 Overall ejector efficiency

It is difficult to determine the efficiencies of the ejector components from experimental data. For single-phase ejectors, a commonly used efficiency is given by ASHRAE [36]. It is defined as the total enthalpy gained by the primary and secondary streams from the secondary inlet to diffuser outlet divided by the total enthalpy available for recovery from the primary stream inlet to the primary nozzle outlet.

$$\eta_{ejec} = \frac{\dot{m}_p + \dot{m}_s}{\dot{m}_p} \frac{h_{d,out} - h_{s,in}}{h_{p,in} - h_{p,out,is}} \tag{2.6}$$

Although this efficiency definition works well for single phase ejectors, however, it doesn't give reasonable efficiency values for two-phase ejectors due to negative and large magnitude enthalpy change between the diffuser outlet and the secondary inlet in the numerator.

A definition of the ejector performance as a function of the entrainment ratio was proposed for two-phase ejectors by Elbel and Hrnjak [27]. An ejector work recovery efficiency is calculated as the amount of expansion work recovery divided by the maximum amount that could be recovered:

$$\eta_{ejec} = \frac{W_{rec}}{W_{rec,max}} = \frac{\dot{m}_s}{\dot{m}_p} \frac{h(P_{d,out}, s_{s,in}) - h_{s,,in}}{h_{p,in} - h(P_{d,out}, s_{p,in})} \tag{2.7}$$

There are other efficiency definitions for two-phase ejector [37]–[39] but all require the knowledge of the mixing section pressure while the efficiency of Elbel and Hrnjak (Eq. 2.7) does not require it. It only depends on the inlet and outlet conditions of the ejector. This efficiency definition has been used by other researchers [40], [41].

2.8 Sound velocity in a two-phase fluid

Calculation of the sound velocity is very important to obtain Mach number (M) under critical flow conditions and analyzing chocking phenomena. In single-phase compressible flows, it can be obtained by:

$$a^2 = \left(\frac{\partial P}{\partial \rho}\right)_s \tag{2.8}$$

$$M = \frac{u}{a} \tag{2.9}$$

where u is the flow velocity and a is the sound velocity. The Mach number is equal to one at the throat of the ejector nozzle in a single-phase reversible flow.

In a two-phase flow, the speed of sound is not easy to calculate especially near the liquid saturation line where liquid and vapor gradients increase very rapidly at a nonlinear rate. In two-phase flows, pressure and temperature are not independent and the sound velocity depends on the physical properties and interphase area of the fluid.

Wood [42] proposed the following relation for the sound velocity, which was imposed by a homogeneous two-phase model. This model has been used in extensive publications [43]:

$$a^2 = \frac{1}{\bar{\rho}} \frac{1}{(\frac{\alpha_v}{\rho_v a_v^2} + \frac{1-\alpha_v}{\rho_l a_l^2})} \tag{2.10}$$

where α_v is gas volume fraction (void fraction) defined by:

$$\alpha_v = \frac{V_v}{V_v + V_l} \tag{2.11}$$

Yazdani et al. [43] used the relation proposed by Brennen [44] based on the change of volume fraction in thermodynamic relations including homogeneous equilibrium and homogeneous frozen expression:

$$\frac{1}{\rho a^2} = \frac{\alpha_v}{P}\left[(1-\epsilon_v)f_v + \epsilon_v g_v\right] + \frac{1-\alpha_v}{P}\epsilon_l g_l \tag{2.12}$$

Where ρ is the average density of the two-phase fluid, f and g are the thermodynamic properties that can be calculated from local pressure, density and enthalpy of the fluid [44].

In another work, Nakagawa et al. [45] proposed the following relation:

$$a^2 = \frac{P}{\alpha_v(\alpha_v\rho_v + (1-\alpha_v)\rho_l)} \tag{2.13}$$

Ameur et al. [12] reviewed several relations for the computation of the two-phase velocity and proposed a relation for the sound velocity relied on the homogeneous two-phase model:

$$a^2 = \frac{1}{\rho^2}\left[x\frac{1}{\rho_v^2}(\frac{\partial\rho_v}{\partial P})_s + (1-x)\frac{1}{\rho_l^2}(\frac{\partial\rho_l}{\partial P})_s\right]^{-1} \tag{2.14}$$

where

$$\rho = \frac{1}{\bar{v}} = \alpha_v\rho_v + (1-\alpha_v)\rho_l \tag{2.15}$$

$$\bar{v} = xv_v + (1-x)v_l \tag{2.16}$$

Lund and Flatten [46] established a hierarchy of relaxation models to calculate sound velocities in two-phase flows. They studied the influence of equilibrium assumptions on the propagation of

pressure waves. They imposed three sound velocities: a pressure equilibrium (p equilibrium), a temperature equilibrium (P, T equilibrium) and a phase transfer equilibrium (P, T, μ equilibrium). They used the simulated results for the CO_2 transport in the pipeline and concluded that the pressure and temperature relaxed model is in good agreement with experiments and can be used in the numerical simulations. Zheng et al. [47] used this dynamic model to consider the chocking of the primary flow through the nozzle throat in a transcritical CO_2 ejector expansion cycle. This model considered an equilibrium pressure and temperature but no equilibrium of the chemical potentials:

$$a^{-2} = a_w^{-2} + \frac{\rho}{T}\frac{C_{p,v}C_{p,l}(\zeta_l - \zeta_v)^2}{C_{p,v} + C_{p,l}} \tag{2.17}$$

$$a_w^{-2} = \rho\left(\frac{\alpha_v}{\rho_v a_v^2} + \frac{\alpha_l}{\rho_l a_l^2}\right) \tag{2.18}$$

$$\zeta_k = \left(\frac{\partial T}{\partial P}\right)_{s_k} = \frac{T\beta_k v_k}{C_{p,k}} \tag{2.19}$$

$$C_{p,k} = \rho_k \epsilon_k c_{p,k} \tag{2.20}$$

where k refers to each phase. Figure 2.6 shows the velocity of sound used in different papers in terms of the void fraction for CO_2 at a pressure of 3682.9 kPa.

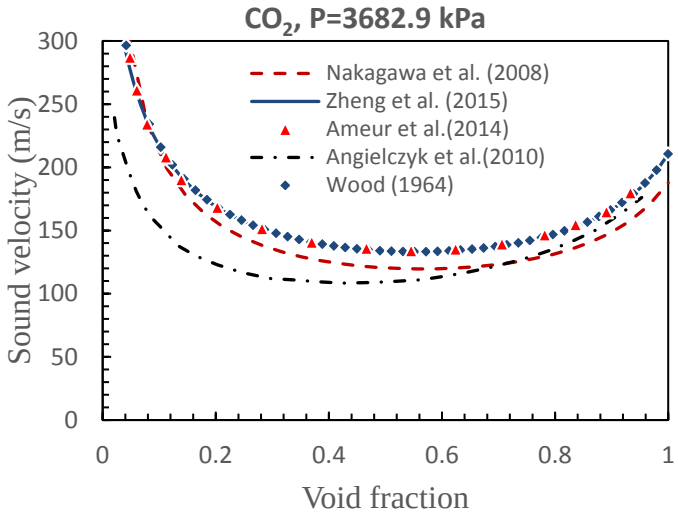

Figure 2.6 Sound velocity of two-phase CO_2 as a function of the void fraction

2.9 Choking phenomena in the ejector

According to Keenan et al.'s [20] assumption, the two streams mix together inside the suction chamber and the mixing pressure is constant from the nozzle exit to the inlet of the constant area. However, this theory is unable to analyze the choking of the secondary flow under the critical operating mode.

Munday and Bagster [23] further assumed a constant pressure mixing in which the primary flow expands after exiting from the primary nozzle. It creates a hypothetical throat area (effective area) for the secondary flow downstream of the nozzle exit (Figure 2.7, section y-y) where the secondary flow reaches a sonic velocity and chocks at this point. After the choking of the secondary flow, the mixing process of the two streams starts and completes at the end of the mixing chamber. Due to the supersonic flow downstream of the mixing section, there is a train of shock waves that cause a compression effect and a sudden drop in flow speed.

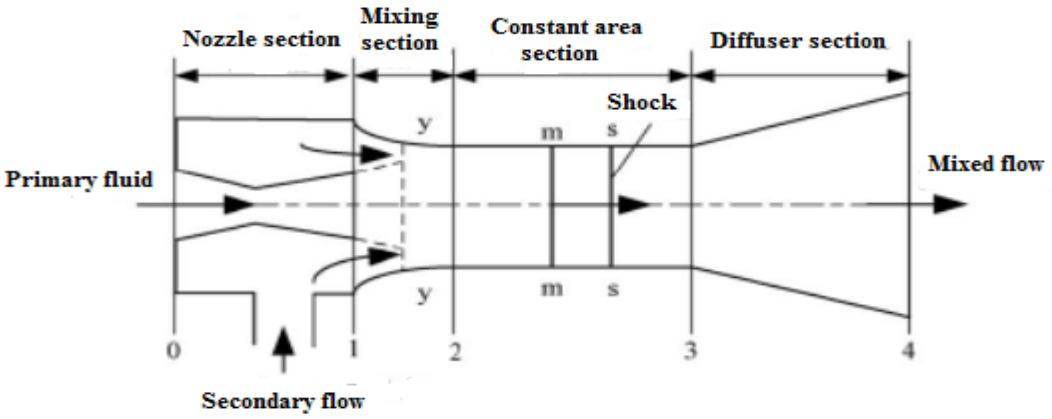

Figure 2.7 Structure of the ejector used by Munday and Bagster [23]

Huang et al. [24] introduced a critical mode model for an ideal gas based on Munday and Bagster's [23] model. According to their model, there are two choking phenomena in the ejector; one in the primary flow through the primary nozzle throat and the other in the secondary flow, which is the result of the acceleration of the entrained flow from its stagnation point. Detail information about the critical mode of the ejector and its effect on the ejector modeling are presented in chapter 4 (Figure 4.3).

2.10 Transcritical CO_2 ejector expansion work recovery systems

Nowadays, it is very important to recover waste heat and transfer it to useful energy (heating, cooling, etc.). A heat pump system provides heat by transferring it from one area to another (or lower temperature level to a higher temperature level). It is used for heat recovery from different sources in various industrial and residential applications to improve energy efficiency. In a subcritical heat pump, the low critical temperature reduces the performance and heat capacity of the system due to the limitation of the operating temperature range and low enthalpy of the vaporization at a temperature less or near the critical temperature [4]. Since CO_2 can operate in a transcritical system due to high working pressure, CO_2 heat pumps can work at a higher pressure than most other refrigerants. It has an advantage of high vapor density and high volumetric heating capacity, which causes the same heating capacity as other working fluids is obtained by a smaller volume of CO_2. This results in a smaller and more compact system. A review study of transcritical CO_2 refrigeration systems for supermarket applications was carried out by Gullo et al. [48]. A

transcritical two-phase ejector integrated into a refrigeration or heat pump cycle is used to improve the system performance by recovering some part of the expansion losses.

In 2003, a Japanese corporation (Denso) introduced a patent employing two-phase ejector in a transcritical CO_2 heat pump and introduced it to the market [49]. Nowadays their heat pumps are manufactured by several companies. Though the first commercial applications have been introduced to the market [50], there is still a need to work in the field of ejector technology in the future. Recent ejector researches focused on the development of advanced models, investigation of alternative ejector cycles, applications of ejector work recovery cycles in real systems and control strategies [50].

Ju et al. [51] developed a simple thermodynamic CO_2 ejector model for analyzing operating conditions in a CO_2 heat pump water heater. They used a two-phase model with constant mixing pressure and obtained 16% higher COP than a conventional system. The ejector entropy production was found 22% of the total entropy of the system that indicated the importance of a good design of the ejector in such a system.

A simultaneous heating and cooling application was investigated by Sarkar et al. [52]. They developed a transcritical CO_2 heat pump model to study the effects of the compressor speed, the inlet temperature of the external fluids to the evaporator and the gas cooler, the discharge pressure of the compressor and heat transfer area ratio on the COP of a heat pump system. The established results offered the guidelines for the design and optimization of a heat pump system. In a further investigation, Sarkar [16] developed a thermodynamic model with an ejector constant area mixing model for the optimization of two different cycles: a standard ejector expansion transcritical CO_2 heat pump cycle and a modified cycle that feeds back some part of the separator vapor to the evaporator. The optimization was based on COP maximization for simultaneous cooling and heating applications. It was found that both cycles had similar results except at low evaporator temperatures where the modified cycle was less efficient. The results also showed the more significant effect of the gas cooler outlet temperature than the evaporator temperature on the performance of the cycle.

There are limited works on the effect of the ejector geometry using CO_2 in the literature. Elbel and Hrnjak [27] conducted an experimental study of a transcritical CO_2 ejector refrigeration system using a variable motive nozzle throat and compared the results with conventional expansion valve system under different ejector's diffuser angle, high side pressures and ambient outdoor temperature. Their results showed an increase in both cooling capacity and COP up to 8% and 7% respectively in the ejector system. The COP was maximized at an optimum gas cooler pressure, however, the maximum ejector efficiency occurred at a pressure much lower than this optimum gas cooler pressure. The highest ejector efficiency was obtained at the smallest diffuser angle of 5°. It was justified by a trade-off between kinetic energy losses by vortex formation in larger diffuser angles and frictional pressure drop losses in smaller diffuser angles.

The effect of the mixing length on the performance of a two-phase CO_2 ejector refrigeration cycle was investigated by Nakagawa et al. [40] with and without internal heat exchanger (IHX). They used an ejector with a constant rectangular cross-section and three different mixing lengths (5, 15 and 25mm). The ejector efficiency and COP exhibited a minimum value for 5 mm and a maximum value for 15 mm. However, increasing the length of the mixing section had a negative effect on

COP. The COP was improved by up to 26% with IHX using the 15 mm length. However, increasing further the mixing length lowered the COP by 10%.

Nakagawa et al. [53] experimentally investigated the two-phase flows of CO_2 in the diverging part of a rectangular converging-diverging nozzle to analyze decompression boiling process for different angles and inlet conditions. They proved that the pressure distribution curve approached the calculated isentropic homogeneous equilibrium (IHE) curve for divergence angles larger than 0.306˚ with high inlet temperatures above 35˚C. However, for divergence angles smaller than 0.306˚ and inlet temperatures below 35˚C, the pressure distribution was different from that calculated by IHE which indicated that the boiling process occurred at non-equilibrium state.

Angielczyk et al. [54] developed the homogeneous relaxation model (HRM) for a two-phase CO_2 flow through the ejector motive nozzle. The pressure distribution along the nozzle was calculated for three different nozzle geometries and compared with experimental data of Nakagawa et al. [53]. The model was more consistent than the homogeneous equilibrium model (HEM) in terms of propagation velocity and therefore speed of sound prediction. Even though their results were in agreement with experiments downstream the throat, they could not validate their model upstream and in the nozzle throat.

Yazdani et al. [43] presented a non-homogeneous mixture model for CO_2 two-phase flows inside an ejector. A commercial CFD platform was implemented to formulate the conservation equations of mass, momentum, and energy for the mixture density and mass averaged velocity. The phase-change model was also used to account for the non-equilibrium transition to a two-phase regime. The evaporation/condensation rate was obtained from the dynamics of bubble growth including boiling and cavitation. The results showed that the cavitation portion of phase change was generally small but could be dominant near the walls and at the motive nozzle throat. The slip model was recognized to be not efficient to predict the overall ejector performance.

Palacz et al. [55] studied the accuracy of homogeneous equilibrium model using CFD based on the expansion of CO_2 through two-phase ejectors for a vast range of ejector operating conditions. The experimental tests were carried out for the validation of the simulated results in terms of mass flow rates. It was concluded that the accuracy of the HEM varied for different operating conditions. The results were more accurate for operating conditions close to or above the critical point of CO_2. Moreover, with the decreasing temperature and decreasing distance to the saturation line, the model accuracy decreased.

Smolka et al. [17] developed a homogeneous model of CO_2 two-phase flow. A robust numerical solution was developed to simulate the two-phase flow with real gas properties compared with well-known multi-phase models, such as the Euler–Euler or the mixture models. An enthalpy based equation (instead of temperature based) was used in the mathematical model. Local pressure distributions in the mixing chamber and diffuser and the mass flow rates of primary and secondary flows were obtained and validated with the experiments. It was reported that heterogeneous model was unstable with unacceptable computation times. This model was then used by Palacz et al. [41] to optimize a CO_2 ejector mixing section. They used two optimization algorithms, a genetic algorithm (GA) and an evolutionary algorithm (EA) to optimize a CO_2 ejector mixing section. The optimization was based on maximizing the ejector efficiency. The result demonstrated the high

relation between ejector performance and mixing section diameter as the larger length of the mixing section was obtained in the optimal design.

More complicated models (heterogeneous considering phase change such as evaporation/ condensation) may give more details of the two-phase flow nature but they are computationally too expensive for optimization purpose.

2.11 Nomenclature

		Subscripts	
A	Cross section area, mm^2	d	Diffuser
a	Sound velocity, m s^{-1}	e	Exit
c_p	Specific heat, J kg^{-1} K^{-1}	ejec	Ejector
ER	Entrainment ratio	in	Inlet
h	Specific enthalpy, kJ kg^{-1}	is	Isentropic
$\dot{m}$	Mass flow rate, kg s^{-1}	l	Liquid
M	Mach number	max	Maximum
P	Pressure, kPa	mix	Mixing
P_{ratio}	Pressure ratio (pressure lift)	p	Primary
s	Specific entropy, kJ kg^{-1} K^{-1}	rec	Recovery
u	Velocity, m s^{-1}	s	Secondary
V	Volume, m^3	th	Ejector throat
W	Work rate, kW	tot	Total
Greek symbols		v	Vapor
α	Volume void fraction	**Abbreviation**	
β	Thermal expansion coefficient, K^{-1}	1-D	One dimentional
ϵ	Interacting fraction	CFD	Computational fluid dynamics
η	efficiency	COP	Coefficient of performance
μ	Chemical potential, J kg^{-1}	HEM	Homogeneous equilibrium model
ρ	Density, kg/m^3	HRM	Homogeneous relaxation model
v	Specific volume, m^3 kg^{-1}	IHE	Isentropic homogeneous equilibrium
x	Quality	IHX	Internal heat exchanger
		NXP	Nozzle exit position

CHAPTER 3

ENERGY AND EXERGY EFFICIENCIES OF DIFFERENT CONFIGURATIONS OF THE EJECTOR-BASED CO_2 REFRIGERATION SYSTEMS

3.1 Avant-propos

Auteurs et affiliation:

- Sahar Taslimi Taleghani: étudiante au doctorat, Université de Sherbrooke, Faculté de génie, Département de génie mécanique.
- Mikhail Sorin: professeur, Université de Sherbrooke, Faculté de génie, Département de génie mécanique.
- Sébastien Poncet: professeur, Université de Sherbrooke, Faculté de génie, Département de génie mécanique

Date d'acceptation: 1 Janvier 2018

État de l'acceptation: version finale publiée.

Revue: International Journal of Energy Production and Management

Titre français: Efficacités énergétiques et exergétiques des différentes configurations de systèmes frigorifiques à base d'éjecteur au CO_2

Contribution au document: Cet article contribue à la thèse en comparant différents cycles d'éjecteurs au CO_2 transcritiques afin de trouver le cycle le plus efficace du point de vue thermodynamique.

Résumé français: Le dioxyde de carbone (CO_2) est un remplacement approprié aux réfrigérants classiques en raison de ses faibles effets sur le réchauffement de la planète. Cependant, son application dans un cycle traditionnel de réfrigération par compression conduit à de faibles performances thermodynamiques en raison des pertes de dilatation importantes dans un processus d'étranglement. L'utilisation d'éjecteurs permet de réduire ces pertes. De nombreux scénarios de cycles basés sur des éjecteurs ont été proposés. Parmi eux, quatre configurations différentes peuvent être distinguées: un cycle de récupération du travail d'expansion (EERC), un cycle de recirculation des liquides (LRC), un cycle croissant de pression de décharge du compresseur (CDPC) et un cycle de réfrigération à jet de vapeur (VJRC). Cette étude traite de l'analyse comparative de ces cycles. Afin d'étudier les performances des cycles, les simulations numériques sont développées à l'aide du logiciel EES. Deux critères de performance, l'efficacité énergétique (COP) et l'efficacité exergétique sont évalués pour chaque cycle. Les valeurs les plus élevées de

ces critères indiquent le cycle le plus efficace du point de vue thermodynamique. Les résultats montrent que l'EERC présente l'efficacité la plus élevée en matière de COP et d'exergie par rapport aux autres cycles. Par exemple, le COP de l'EERC est 3.618 et l'efficacité énergétique est de 9.68%. Le COP (resp. efficacité exergétique) est d'environ 23.3% (resp. 23.3%), 24,9% (resp. 25.5%) et 5.6 fois (resp. 56.2%) supérieur aux rendements énergétiques et exergétiques correspondants aux cycles LRC, CDPC et VJRC. De plus, en comparaison avec un cycle basique, le COP et l'efficacité exergétique de l'EERC sont supérieurs de 23% et 24% respectivement. L'analyse exergétique détaillée du cycle EERC a permis de localiser les composants où se produisent les principales pertes exergétiques. Les pertes les plus importantes se produisent dans l'évaporateur (environ 33% de la destruction totale de l'exergie du cycle), suivi par le compresseur (25.5%) et l'éjecteur (24.4%).

3.2 Abstract

Carbon dioxide (CO_2) is an appropriate replacement for conventional refrigerants due to its low global warming effects. However, its application within a traditional refrigeration compression cycle leads to low thermodynamic performance due to the large expansion losses in a throttling process. The application of ejectors allows reducing these losses. Many scenarios of ejector-based cycles have been proposed. Among them, four different configurations may be distinguished: an expansion work recovery cycle (EERC), a liquid recirculation cycle (LRC), an increasing compressor discharge pressure cycle (CDPC) and a vapor jet refrigeration cycle (VJRC). This study deals with the comparative analysis of these cycles. In order to study the performance of the cycles, the numerical simulations are developed using EES software. Two performance criteria, energy efficiency (COP) and exergy efficiency are evaluated for each cycle. The highest values of these criteria point to the most thermodynamically efficient cycle. The results show that the EERC has the highest COP and exergy efficiency compared to other cycles. For example, the COP of the EERC is 3.618 and the exergy efficiency is 9.68%. The COP (resp. exergy efficiency) is approximately 23.3% (resp. 23.3%), 24.9% (resp. 25.5%) and 5.6 times (resp. 56.2%) higher than the corresponding energy and exergy efficiencies of LRC, CDPC and VJRC. Moreover, in comparison with a basic throttling valve cycle, the COP and exergy efficiency in EERC are higher up to 23% and 24% correspondingly. The detailed exergy analysis of EERC cycle has pinpointed the equipment where the major exergy losses take place. The largest losses occur in the evaporator (about 33% of the total exergy destruction of the cycle) followed by the compressor (25.5%) and the ejector (24.4%).

3.3 Introduction

Carbon dioxide (CO_2) is an appropriate replacement for conventional refrigerants due to its low global warming effects. One of the disadvantages of the cycle is a large exergy loss due to an important pressure reduction during expansion of CO_2 from the supercritical to the subcritical state in a throttling valve. Among different devices for expansion work recovery, ejector is a favorable equipment, which enables to reduce losses by recovering part of the expansion work in a throttling process and improve the cycle's efficiency.

The first application of two-phase ejector to the transcritical CO_2 cycle was first described by Gay [56]. It was proposed to replace the expansion valve by a two-phase ejector to reduce the losses due to the throttling process.

Kornhauser [5] was the first to develop a one-dimensional and homogeneous model of a two-phase ejector using R12 as a refrigerant in the ejector expansion refrigeration system (EERS). Li and Groll [7] adapted the Kornhauser's model for an ejector used within a transcritical CO_2 air-conditioning system.

A thermodynamic exergy analysis of transcritical CO_2 ejector refrigeration system was performed by Fangtian and Yitai [30]. They evaluated COP and exergy destruction of the system. Their results showed an improvement of 30% in COP and decreasing exergy loss more than 25% compared to the conventional system.

The present study is focused on a thermodynamic comparative analysis of the performance of the different transcritical CO_2 ejector cycles to identify the most efficient one. The COP, exergy efficiency and exergy destructions are calculated and compared for the expansion work recovery cycle (EERC), liquid recirculation cycle (LRC), increasing compressor discharge pressure cycle (CDPC) and vapor jet refrigeration cycle (VJRC). Exergy analysis is employed to determine the amount and locations of irreversibilities within different components of each cycle.

3.4 Ejector applications for transcritical CO_2 cycles

Different applications of the ejector in CO_2 air-conditioning and refrigeration systems used in this study are as follows:

Ejector for utilization of low-grade energy (vapor jet ejector systems, VJRC)

Ejectors for expansion work recovery cycle (standard two-phase ejector, EERC)

Ejectors for liquid recirculation cycle (LRC)

Ejector for increasing compressor discharge pressure (CDPC)

3.4.1 Vapor jet ejector systems (VJRC, single-phase ejectors)

In the vapor jet cycle, a pump, a generator, and an ejector replace the compressor. A fraction of the liquid from the condenser is pumped to a high pressure and temperature. The fluid absorbs heat at a constant pressure from a low-grade energy source in the generator. The heated flow expands in a primary nozzle to a high velocity and a low pressure. This low pressure entrains the secondary flow from the evaporator into the mixing chamber of the ejector. The irreversible mixing of the two fluids occurs in the mixing chamber depending on the ejector geometry at the constant pressure or at the constant area. Finally, the flow decelerates in the diffuser by converting the remaining kinetic energy into the pressure increase. The vapor exiting the diffuser is condensed at a constant pressure. The liquid at the condenser exit is pumped to the generator. The vapor is sent through the metering valve to the evaporator.

The main advantage of the VJRCs is that they can produce a refrigeration effect by using the low-grade waste heat for heating the primary flow in the generator.

Compared to a conventional system, for the same pressure increase, the work of the liquid pump in the VJRC is less than the compressor work and it does not also require any lubrication [57]. The schematic of a transcritical CO_2 VJRC and corresponding temperature-specific entropy diagram are shown in Figure 3.1 It can be seen the flow through the mixing section and the diffuser remains vapor so the ejector works in a single-phase mode.

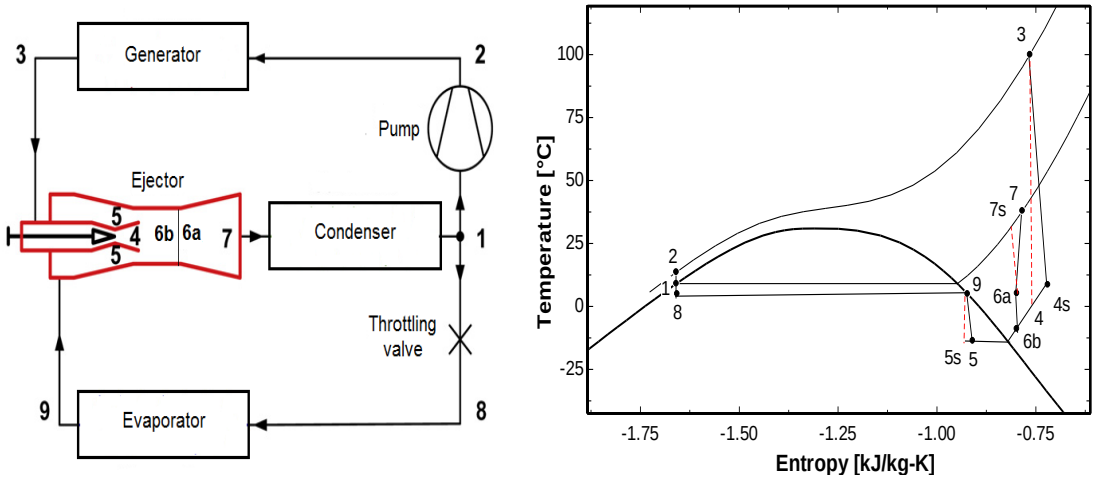

Figure 3.1 Transcritical CO_2 vapor jet refrigeration cycle and corresponding Temperature-Specific entropy diagram

3.4.2 Two-phase ejectors for expansion work recovery (EERC)

A two-phase ejector can be used in vapor compression systems for recovery of the expansion work by reducing the throttling losses to improve the performance of the system.

As shown in Figure 3.2, the subcritical CO_2 coming from the vapor port of the separator is compressed to high pressure and temperature to the supercritical state. It releases heat in the gas cooler. After the gas cooler exit, the stream enters the primary nozzle of the ejector and expands at the mixing section. The secondary vapor stream pre-accelerates into the mixing section. The mixture then flows through the diffuser which causes a compression before entering the separator. Vapor portion of the two-phase flow returns to the compressor while the pressure of the liquid portion is reduced through the metering valve before entering the evaporator. The stream absorbs heat in the evaporator before it enters the ejector.

EERC has two main advantages. First, the cooling capacity increases because the isentropic expansion inside the primary nozzle in comparison to an isenthalpic expansion valve of a conventional system has a larger enthalpy difference. Second, the compressor work is decreased due to the increase of the suction pressure of the compressor resulting in COP improvement.

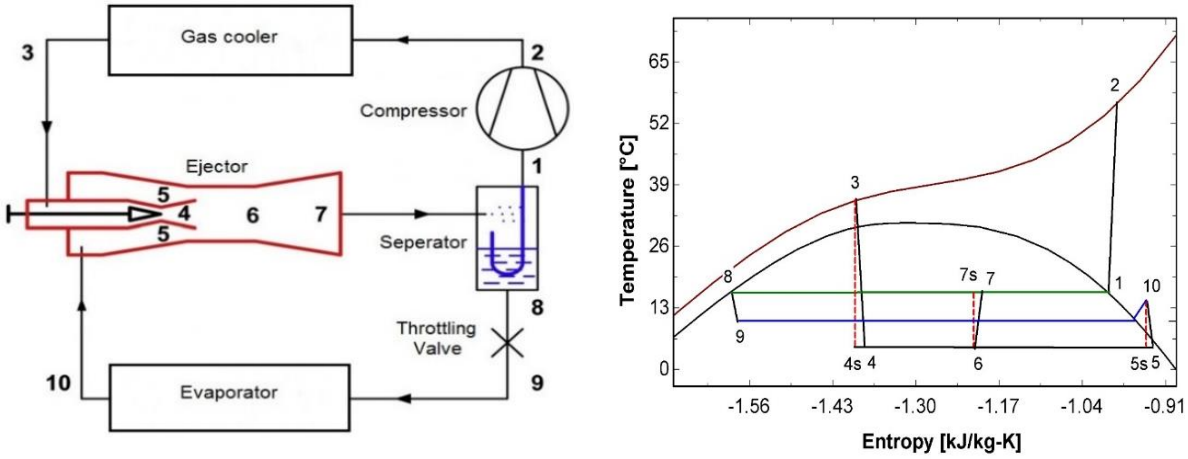

Figure 3.2 Transcritical CO_2 ejector expansion recovery cycle and the corresponding temperature-specific entropy diagram

3.4.3 Two-phase Ejectors for liquid recirculation (LRC)

In this cycle, the ejector is used to recirculate liquid and improve the evaporator performance. It was first patented by Phillips [58] and later by Lorentzen [59]. Figure 3.3 shows a schematic of the cycle and corresponding T-S diagram for transcritical CO_2. The expansion work recovered by the ejector is used to liquid recirculation. The amount of COP improvement by using liquid recirculation is dependent on the working fluid used. There is also an optimum value for every system and operating condition because with increasing the recirculation both the heat transfer coefficient and the pressure drop increase [28].

Lawrence and Elbel [28] studied two applications of the two-phase ejector cycle for CO_2 as a working fluid: first was liquid recirculation cycle that used the ejector to improve the evaporator performance and other was a standard two-phase ejector that used work recovery of the ejector to increase the compressor pressure. The COP improvement of 3% through CO_2 ejector was obtained in the recirculation cycle as it could reach up to 25% in a standard two-phase ejector to directly unload the compressor pressure.

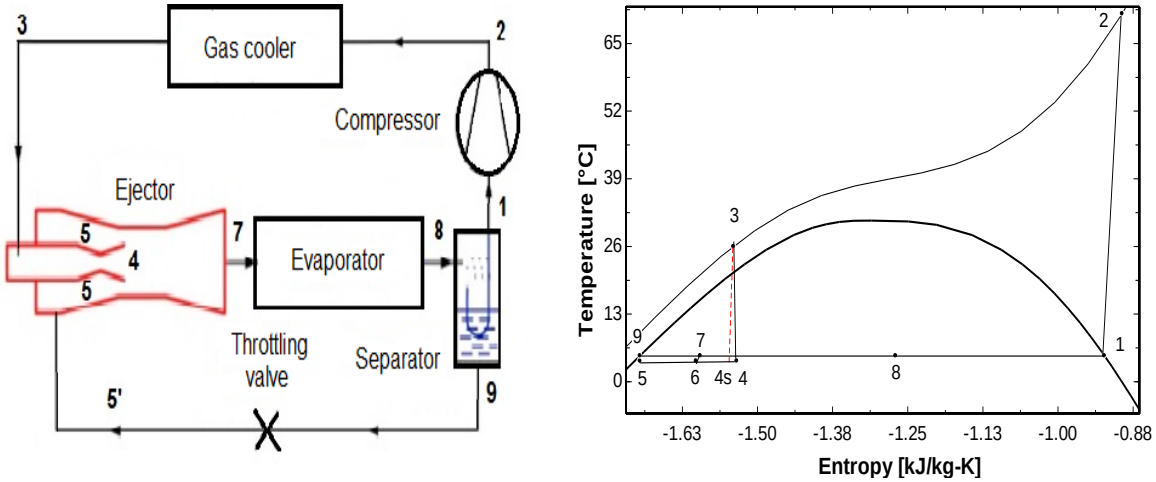

Figure 3.3 Transcritical CO_2 liquid recirculation cycle and the corresponding temperature-specific entropy diagram

3.4.4 Two-phase ejector for increasing compressor discharge pressure (CDPC)

This innovative cycle was recently introduced by Bergander [60]. In this cycle, ejector is used as a second stage compressor. Unlike standard two-phase ejector which increases the suction pressure of the compressor, in this cycle, the ejector is used to increase the compressor discharge pressure. In a subsequent work, Bergander [61] developed a thermodynamic ejector model for R22 and conducted experiments that showed 16% COP improvement. In this cycle, there is a two-phase flow inside the ejector, liquid for the primary flow and vapor for the secondary one. The primary flow enters the ejector after exiting the pump and mixes with the secondary flow that comes from the compressor. The flow at the exit of the ejector enters the gas cooler. The layout of this cycle and the corresponding T-S diagram are presented in Figure 3.4.

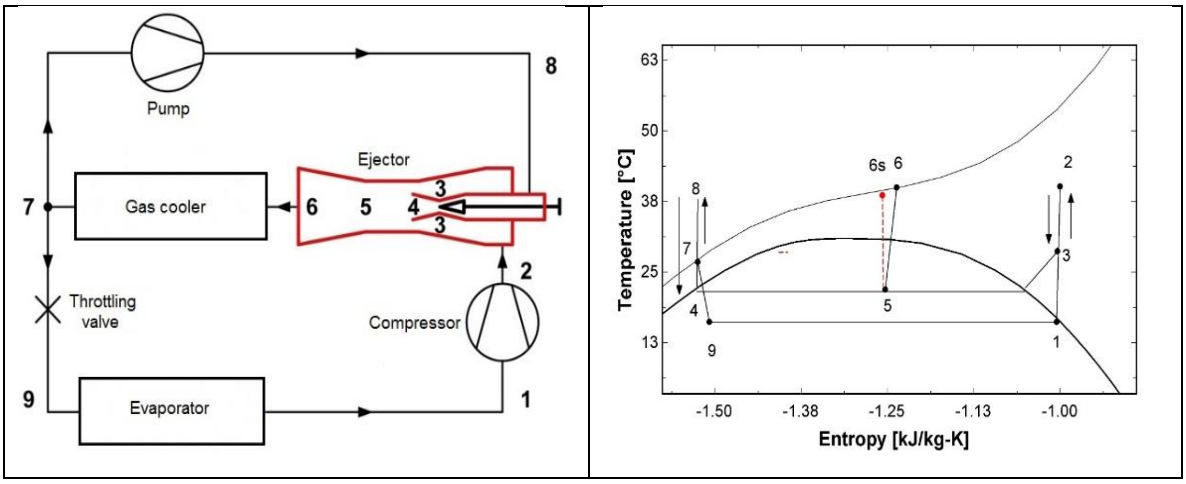

Figure 3.4 CO_2 transcritical ejector cycle to increase the compressor discharge pressure and corresponding temperature - specific entropy diagram

3.5 Exergy analysis of different ejector cycles

The exergy analysis of the ejector cycles introduced in section 2 is carried out to investigate the exergy destruction of the different components of the system to determine the maximum performance and potential improvements of the cycles.

3.5.1 Modeling of two-phase flow ejector

Different models of the ejectors exist according to assumptions, governing equations, auxiliary conditions, mixing mechanism and solution methods. Thermodynamic modeling is a simple way to solve the equations in one dimension. It is also easily integrated into a system.

Conservation equations of mass, energy and momentum, some gas dynamic equations, state equations, isentropic relations as well as some appropriate assumptions, initial and boundary conditions are used to solve the flow within the ejector. Some assumptions that are usually employed to simplify the problem are as follows: adiabatic walls of the ejector, steady state flow, isentropic efficiencies for the nozzles and the diffuser, stagnation points of the streams at inlets and outlet of the ejector and mixing coefficient for mixing losses.

Most ejector models presented for CO_2 two-phase flows are based on a homogeneous equilibrium model in which both gas and liquid are in thermodynamic and mechanical equilibrium. It means that both phases have the same pressure, temperature, velocity, turbulence kinetic energy and turbulence dissipation rate [5], [7], [12]–[17].

3.5.1.1 Assumptions and calculation procedure

The thermodynamic model of the two-phase ejectors (EERC, LRC, CDPC, section 3.4.2~3.4.4) is based on the following assumptions:

1. Flow is one-dimensional, steady state and adiabatic through the ejector.
2. The homogeneous equilibrium is assumed for two-phase flow.
3. The CO_2 thermodynamic and transport properties of the primary and secondary flows are obtained from real fluids properties.
4. Flow losses in the pipes and heat exchangers are negligible.
5. Kinetic energies of the refrigerant are negligible at the ejector inlet and outlet
6. Friction losses are defined in terms of isentropic efficiencies in the nozzles, diffuser and mixing.
7. Mixing occurs under a constant pressure in the ejector mixing section with the assumption that the fluid momentum is conserved.
8. Pressure loss of the secondary flow is assumed ΔP=1bar for EERC, LRC, CDPC.
9. Critical-mode operation is applied for VJRC and normal shock takes place at the end of the constant area mixing chamber [62], [63].
10. The secondary inlet flow is considered as a saturated vapor in EERC, saturated liquid in LRC, superheated vapor in CDPC.
11. The heat sink temperature (or the ambient temperature, T_0) is 35˚C for EERC, LRC, and CDPC and $(T_{gen,in} + T_{gen,out})/2 + 5℃$ for VJRC; the heat source temperature is 27˚C.

The constant parameters used in the simulations of the cycles are shown in Table 3.1. An engineering equation solver (EES) program is used to solve the proposed models in section 2 which combines non-linear equations with thermo-physical property functions.

The modeling of the ejector expansion recovery cycle is based on one unit of mixing refrigerant mass flow in the mixing sector of the ejector. Therefore, the primary mass flow from the gas cooler is $1/(1 + ER)$ and the secondary mass flow from the evaporator is $ER\ /\ (1\ +\ ER)$.

Table 3.1 Constant parameters used in the simulation

Pressure of gas cooler	88 bar	Cooling capacity	72 kW
Temperature of gas cooler exit	36°C	Efficiency of nozzles	0.8
Temperature of evaporator	5°C	Efficiency of diffuser	0.8
Temperature of generator exit (VJRC)	100°C	Efficiency of mixing	0.95
Pressure of generator (VJRC)	88 bar	Efficiency of compressor	0.75
Pressure of evaporator	39.69 bar	Efficiency of pump	0.75

The model is solved according to the relationship between the vapor quality of the ejector outlet and the entrainment ratio. The solution converges when Eq. (3.1) is satisfied to maintain a balance between liquid and vapor in the expansion recovery cycle:

$$x_{out,diff} = \frac{1}{1 + ER} \tag{3.1}$$

First, the properties at different states of the cycles are calculated. In EERC, according to Figure 3.2 the specific enthalpy at gas cooler and evaporator exit (h_3, h_{10}) are defined. The motive flow expands to mixing pressure with a nozzle efficiency η_{pn} defined as:

$$\eta_{pn} = \frac{h_3 - h_4}{h_3 - h_{4s}} \tag{3.2}$$

Where

$$h_{4s} = f(P_{evap} - \Delta P, s_3) \tag{3.3}$$

By applying energy conservation law between state 3 and 4 the velocity at state 4 is obtained:

$$\frac{1}{2}u_4^2 = h_3 - h_4 \tag{3.4}$$

The velocity of secondary flow (u_5) is calculated in the same way as that of the primary flow and then the velocity of mixed flow is determined by the momentum equation in mixing chamber according to:

$$u_6\, m_6 = m_4 u_4 + m_5 u_5 \tag{3.5}$$

The mixing efficiency is defined as [64]:

$$\eta_{mix} = \frac{\frac{1}{2}m_4 u_{4'}^2}{\frac{1}{2}m_4 u_4^2} \tag{3.6}$$

Where $u_{4'}$ is the corrected velocity at state 4 which takes into account the mixing loss.

The energy conservation between two inlets and outlet of the ejector is as follows:

$$m_3 h_3 + m_{10} h_{10} = m_7 h_7 \tag{3.7}$$

The energy conservation between inlet and outlet of the diffuser is described as:

$$\frac{1}{2} u_6^2 + h_6 = h_5 \tag{3.8}$$

The diffuser efficiency is defined as:

$$\eta_{diff} = \frac{h_{7s} - h_6}{h_7 - h_6} \tag{3.9}$$

The pressure and quality at the ejector outlet (state 7) are obtained as

$$p_7 = f(s_6, h_{7s}) \tag{3.10}$$

$$x_7 = f(p_7, h_7) \tag{3.11}$$

This quality satisfies the Eq. (3.1). The cooling capacity of the cycles (Figures 3.1~3.4) can be written:

$$Q_{evap} = m_{evap}\left(h_{out,evap} - h_{in,evap}\right) = \frac{ER}{(1 + ER)}\left(h_{out,evap} - h_{in,evap}\right) \tag{3.12}$$

The compressor power consumption is

$$W_{comp} = m_{comp}\left(h_{out,comp} - h_{in,comp}\right) = \frac{1}{(1 + ER)}\left(h_{out,comp} - h_{in,comp}\right) \tag{3.13}$$

The gas cooler capacity is:

$$Q_{gc} = \dot{m}_{gc}\left(h_{out,gc} - h_{in,gc}\right) = \frac{1}{(1 + ER)}\left(h_{out,gc} - h_{in,gc}\right) \tag{3.14}$$

The cooling coefficient of performance (COP_c) for EERC and LRC is obtained using:

$$COP_C = \frac{Q_{evap}}{W_{comp}} \tag{3.15}$$

For the cycle including the pump (CDPC) the COP_c is defined as

$$COP_C = \frac{Q_{evap}}{W_{comp} + W_{pump}} \tag{3.16}$$

For vapor jet refrigeration system, VJRC, it is expressed as

$$COP_C = \frac{Q_{evap}}{Q_{gen} + W_{pump}} \tag{3.17}$$

3.5.1.2 Exergy calculations

The exergy in all states is calculated based on the unit mass flow of mixing refrigerant in the ejector:

$$ex_k = m_k . [(h_k - h_0) - T_0 \cdot (s_k - s_0)] \quad (3.18)$$

Where m_k is the mass flow at the cycle state k. The exergy destructions in the various processes are calculated as follows:

Compressor:

$$ex_{loss,comp} = ex_{in,comp} - ex_{out,comp} + W_{comp} \quad (3.19)$$

Gas cooler:

$$ex_{loss,gc} = ex_{in,gc} - ex_{out,gc} + Q_{gc}. [1 - \left(\frac{T_0}{T_{sink}}\right)] \quad (3.20)$$

Ejector:

$$ex_{loss,ej} = ex_{in,pn} + ex_{in,sn} - ex_{out,diff} \quad (3.21)$$

Evaporator:

$$ex_{loss,evap} = ex_{in,evap} - ex_{out,evap} + Q_{evap}. [1 - \left(\frac{T_0}{T_{source}}\right)] \quad (3.22)$$

Throttling valve:

$$ex_{loss,th} = ex_{in,th} - ex_{out,th} \quad (3.23)$$

The total exergy destruction is calculated using:

$$ex_{loss,tot} = ex_{loss,comp} + ex_{loss,ej} + ex_{loss,th} + ex_{loss,evap} + ex_{loss,gc} + ex_{loss,gen}\ (VJRC) + ex_{loss,cond}(VJRC) \quad (3.24)$$

The exergy efficiency of the cycles is evaluated as:

$$\eta_{ex} = 1 - \frac{ex_{loss,tot}}{W_{comp}} \quad (3.25)$$

For the cycle includes the pump, CDPC, exergy efficiency is as following:

$$\eta_{ex} = 1 - \frac{ex_{loss,tot}}{W_{comp} + W_{pump}} \quad (3.26)$$

For VJRC (Figure 3.1), exergy efficiency and total exergy loss are calculated by:

$$\eta_{ex} = 1 - \frac{ex_{loss,tot}}{W_{pump}+ex_{Q,ge}+ex_{Q,cond}} \quad (3.27)$$

$$ex_{loss,tot} = ex_{loss,pump} + ex_{loss,gen} + ex_{loss,cond} + ex_{loss,ej} + ex_{loss,th} + ex_{loss,evap} \quad (3.28)$$

Where $ex_{Q,gen}$ and $ex_{Q,cond}$ are exergy transfer by heat in generator and condenser respectively which are defined as:

$$ex_Q = Q.[1 - \left(\frac{T_0}{T}\right)] \quad (3.29)$$

3.6 Results

The comparison of the results for four transcritical CO_2 refrigeration cycles is presented below. Exergy destructions and exergy efficiencies of the cycles are calculated under constant cooling capacity and corresponding parameters listed in Table 3.1.

As shown in Tables 3.2 and 3.3, the EERC has the highest COP and exergy efficiency. For the high-side pressure of 88 bar, the COP for EERC is 23.3%, 24.9% and 5.6 times higher than the COP for LRC, CDPC and VJRC, respectively.

It is also shown that EERC improves the COP by up to 23.1% compared to basic cycle without the ejector while the COP of LRC and CDPC remains almost constant and for VJRC, the COP is very low. For given operating conditions, the pressure ratio of EERC is also the largest among other cycles.

Table 3.3 shows the exergy losses in each component and exergy efficiency of all cycles. It can be noticed that EERC has the maximum exergy efficiency. The entrainment ratio and pressure ratio are 0.564 and 1.15 for EERC respectively. The exergy loss in the evaporation process is the largest one in this system while for LRC and VJRC, the largest loss occurs in the ejector.

The throttling exergy loss in the basic cycle is 7.69 KJ kg^{-1} that constitutes 34.07% of the total exergy loss. However, it is only 0.34 $KJkg^{-1}$, 1.88% of the total exergy loss in EERC and the ejector's exergy loss is also 4.383 KJ kg^{-1}, 24.4% .The sum of these two losses is 26.28% of the total exergy loss of the system which is less than the throttling loss in the conventional cycle. The exergy loss in compressor and gas cooler are also reduced in EERC and it is almost constant in the evaporator.

The use of liquid recirculation in refrigeration system improves the entrainment ratio compared to EERC, however, COP and exergy efficiency remain constant compared to conventional cycle. Therefore despite a large amount of work that can be recovered with the CO_2 ejector, there is not the COP improvement for LRC.

The CDPC simulation shows that the ejector integration with this cycle is not efficient. It is due to the fact that the pressure lift is accomplished mainly by the compressor not the ejector. The pressor ratio is obtained 1.01 for this cycle.

The jet refrigeration cycle (single phase ejector, Figure 3.1) achieves the lowest COP and the lowest exergy efficiency compared to other cycles. The low COP value around 0.65 is obtained. The high exergy losses of heat transfer in condenser (16.2%) and generator (16.9%) result in low exergy efficiency.

Table 3.2 Comparison of the ejector's performance of the cycles

Device	Ejector performance				
	EERC	LRC	CDPC	VJRC	BC
COP	3.618	2.935	2.896	0.6476	2.938
ER	0.564	0.641	1.558	0.921	-
P_{ratio}	1.15	1.03	1.01	1.11	-

Table 3.3 Exergy destructions and exergy efficiencies of the cycles (P_{gc} = 88 bar, T_{evap} = 5˚C, Q_{evap}=72 kW)

Device	Exergy Loss, kW									
	EERC		LRC		CDPC		VJRC		BC	
	Loss, kW	%	Loss, kW	%	Loss, kW	%	Loss, kW	%	Loss, kW	%
Compressor	4.58	25.5	5.539	24.55	5.475	23.86	-	-	5.533	24.5
Gas cooler	2.817	15.68	3.515	15.55	1.679	7.317	-	-	3.511	15.55
Ejector	4.382	24.38	7.705	34.08	2.082	9.074	12.82	43.91	-	-
Valve	0.338	1.878	-	-	7.696	33.54	0.2198	0.753	7.696	34.07
evaporator	5.854	32.57	5.847	25.86	5.847	25.48	5.808	19.89	5.847	25.88
Generator	-	-	-	-	-	-	4.931	16.89	-	-
condenser	-	-	-	-	-	-	4.73	16.2	22.59	-
Pump	-	-	-	-	0.165	0.72	0.686	2.35	-	-
Total	17.97	100	22.61	100	22.94	100	29.2	100	24.51	100
W_{comp}	19.9	-	24.53	-	24.19	-	-	-	-	-
W_{pump}	-	-	-	-	0.668	-	2.558	-	-	-
$ex_{Q,evap}$	-1.919	-	-1.919	-	-	-	-1.919	-	-1.919	-
$ex_{Q,gen}$	-	-	-	-	-	-	8.8	-	-	-
$ex_{Q,cond}$	-	-	-	-	-	-	19.76	-	-	-
Q_{gen}	-	-	-	-	-	-	108.6	-	-	-
η_{ex}	-	9.683	-	7.856	-	7.718	-	6.197	-	7.831

3.7 Conclusion

A comparative study based on the first and second laws of thermodynamics is performed for different transcritical CO_2 refrigeration cycles that use an ejector: EERC, LRC, CDPC and VJRC. The analysis for given conditions led to the following conclusions:

- Transcritical CO_2 refrigeration cycles, EERC has the highest COP and exergy efficiency. For the given operating conditions, it improves the COP and exergy efficiency by up to23% and 24%, respectively, compared to the basic throttling cycle.

- In EERC, the irreversibility loss of the expansion process is significantly reduced compared to basic throttling valve cycle and as a result the exergy efficiency is increased.

- The COP of EERC is improved by up to 23.3%, 24.9% and 5.6 times compared to the LRC, CDPC and VJRC.

- The exergy loss in the evaporation process is the largest loss in EERC, whereas for LRC and VJRC the ejection process has the largest loss.

- The use of liquid recirculation improves entrainment ratio compared to EERC, however, COP and exergy efficiency decrease.

- CO_2 can gain more benefit from EERC compared to other cycles. CO_2 ejector liquid recirculation cycle and VJRC has a low potential for COP improvement.

- Ejector is not effective in the cycle for increasing compressor discharge pressure because the pressure lift is mainly accomplished by the compressor.

3.8 Acknowledgments

This project is a part of the Collaborative Research and Development (CRD) Grants Program at 'Université de Sherbrooke'. The authors acknowledge the support of the Natural Sciences and Engineering Research Council of Canada, Hydro-Québec, Rio Tinto, Alcan and Canmet ENERGY Research Center of Natural Resources Canada.

3.9 Nomenclature

		subscripts	
ER	Entrainment ratio	0	Dead state in the exergy analysis
Ex	Exergy	C	Cooling
Ex_Q	Exergy transferred by heat	comp	Compressor
H	Specific enthalpy, kJ kg^{-1}	cond	Condenser
LRC	Liquid recirculation cycle	diff	Diffuser
M	Mass flow rate, kg s^{-1}	ej	Ejector
P	Pressure, bar	evap	Evaporator
P_{ratio}	Pressure ratio (pressure lift)	gc	Gas Cooler
Q	Heat rate, kW	gen	Generator
S	Specific entropy, kJ kg^{-1} K^{-1}	in	Inlet
T	Temperature, K	mix	Mixing
U	Velocity, m s^{-1}	out	Outlet
VJRC	Vapor jet refrigeration cycle	pn	Primary Nozzle
W	Work rate, kW	sn	Secondary Nozzle
X	Quality	th	Throttling
ΔP	Pressure drop, bar	tot	Total
Greek symbols		**Abbreviation**	
η	Isentropic efficiency	BC	Basic cycle without ejector
ρ	Density, kg m^{-3}	CDPC	Compressor discharge pressure cycle
η_{ex}	Exergy efficiency	COP	Coefficient of performance
		EERC	Expansion work recovery cycle
		LRC	Liquid recirculation cycle
		VJRC	Vapor jet refrigeration cycle

CHAPTER 4

MODELING OF TWO-PHASE TRANSCRITICAL CO_2 EJECTORS FOR ON-DESIGN AND OFF-DESIGN CONDITIONS

4.1 Avant-propos

Auteurs et affiliation:

- Sahar Taslimi Taleghani: étudiante au doctorat, Université de Sherbrooke, Faculté de génie, Département de génie mécanique.

- Mikhail Sorin: professeur, Université de Sherbrooke, Faculté de génie, Département de génie mécanique.

- Sébastien Poncet: professeur, Université de Sherbrooke, Faculté de génie, Département de génie mécanique

Date d'acceptation: 21 Octobre 2017

État de l'acceptation: version finale publiée.

Revue: International Journal of Refrigeration

Titre français: Modélisation d'éjecteurs au CO_2 transcritique diphasique en régimes on- et off-design

Contribution au document: Cet article contribue à la thèse par une modélisation détaillée des éjecteurs au CO_2 diphasique dans différentes conditions de fonctionnement (régimes "single et double choking").

Résumé en français: Les éjecteurs diphasiques au CO_2 sont utilisés comme composants de récupération du travail d'expansion dans les systèmes de réfrigération ou de pompes à chaleur. Un nouveau modèle thermodynamique a été développé pour les conditions dites "single" et "double choking" afin de concevoir de tels éjecteurs et d'étudier leurs performances. Ce modèle, basé sur le modèle d'équilibre homogène (HEM), résout les équations de conservation utilisant des propriétés réelles des fluides. Les irréversibilités dues au frottement dans les buses et le diffuseur sont prises en compte par des rendements polytropiques. Les performances d'un éjecteur diphasique sont prédites pour une géométrie d'éjecteur fixe et selon les spécifications de fonctionnement de l'admission dans des conditions hors design. Le modèle peut également évaluer les dimensions de l'éjecteur pour des conditions de fonctionnement d'entrée et de sortie données (on-design). Les résultats sont comparés et validés par rapport aux données expérimentales publiées. Les effets des irréversibilités sur les dimensions de l'éjecteur sont étudiés en détail.

4.2 Abstract

This model, based on the homogeneous equilibrium model (HEM), solves the conservation equations using real fluid properties rather than ideal gas assumptions. The irreversibilities due to friction in the nozzles and the diffuser are accounted for by polytropic efficiencies. The performance of a two-phase ejector is predicted for a fixed ejector geometry and given inlet operating specifications at off-design conditions. The model can also evaluate the ejector dimensions for given inlet and outlet operating conditions (on-design). The results are compared and validated against published experimental data. The effects of the irreversibilities on the ejector dimensions are investigated in detail.

4.3 Introduction

Saving energy and the using clean energy sources have recently become significant issues. Increasing energy costs, ozone layer depletion and global warming have made the future uncertain for energy and the global environment. Therefore, the development of new technologies and the use of natural refrigerants with very low global warming potential (GWP) coefficients will help face future energy needs while reducing their environmental impact.

Carbon dioxide is an attractive alternative refrigerant in heating and refrigeration systems. It has minimal impact on climate change. In addition, it is not toxic, flammable or corrosive and has no impact on the ozone layer. Therefore, using this refrigerant in ejector systems helps to decrease environmental impact while reducing energy consumption. However, the transcritical CO_2 compression cycle has a large throttling loss compared to the other refrigerants due to the high-pressure change during expansion in the throttling process from a supercritical CO_2 to a subcritical state.

An ejector offers a promising approach by their use in the transcritical CO_2 cycle for the recovery of the expansion losses. It has a simple construction with no moving parts, making it robust with reliable operation [6]. Figure 4.1 shows the schematic of an ejector. A typical ejector comprises a primary nozzle, a secondary nozzle, a mixing section and a diffuser.

The ejector's theory was first proposed by Keenan and Neumann [65]. They developed a 1-D model based on conservation equations, as well as the respective theories associated with mixing, gas dynamics, and ideal gases. According to Keenan et al.'s assumption [20], the two streams mix together inside the mixing chamber and the mixing pressure is constant between the primary nozzle exit and the inlet of the constant area duct. However, this theory is unable to analyze the choking of the secondary flow when the ejector operates at critical conditions.

Munday and Bagster [23] further assumed constant pressure mixing in which the primary flow expands after exiting the primary nozzle. It creates a hypothetical throat (effective area) for the secondary flow downstream of the primary nozzle exit (Figure 4.1, cross section "sm") where the secondary flow reaches sonic velocity and chokes. After the choking of the secondary flow, the mixing process of the two streams starts and completes at the end of the mixing chamber. Huang et al. [24] introduced a critical mode model for an ideal gas based on Munday and Bagster's [23] model. According to the Huang model, there were two choking phenomena inside the ejector; one

in the primary flow through the primary nozzle throat and the other in the secondary flow which results from the acceleration of the entrained flow from its stagnation point.

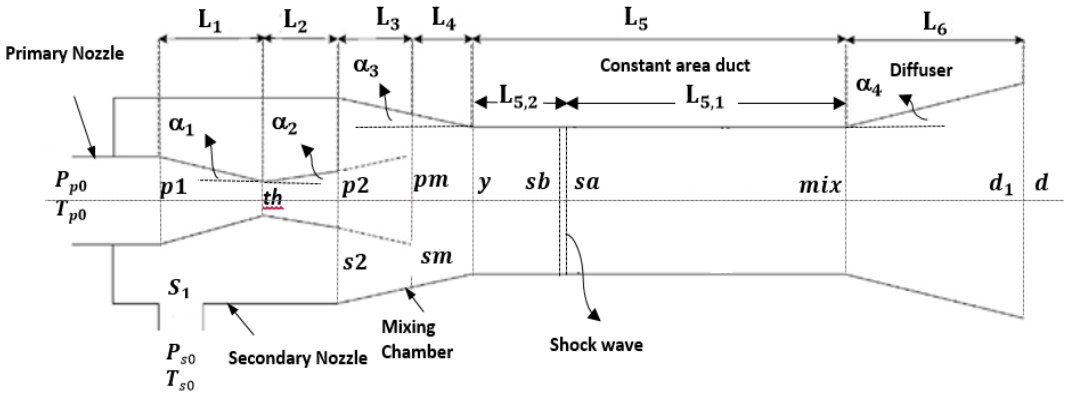

Figure 4.1 Schematic of an ejector with relevant notations

Neither Keenan et al [20] nor Munday and Bagster [23] considered irreversibilities due to friction. In the 1-D analysis of Huang et al. [24], they conducted experiments in a heat driven single-phase system using R141b, for 11 different ejector specifications. They determined different efficiencies by matching experimental data with simulations.

The performance improvement of a two-phase ejector cycle was first described in the patent of Gay [56]. In this cycle, the expansion valve is replaced by a two-phase ejector to reduce the throttling losses associated with the use of an expansion valve. Using transcritical CO_2 systems to improve the performance and the energy efficiency was considered in the late 1980s. The layout of a standard two-phase transcritical CO_2 cycle and the corresponding temperature-specific entropy diagram are shown in Figure 4.2.

There are numerous literature reviews which present ejectors for CO_2 expansion work recovery, but most are limited to global measurements to obtain improvements in cycle performance, energy and exergy efficiency [5], [7], [30], [32].

Kornhauser [5] was the first to develop a one-dimensional and homogeneous model of a two-phase ejector, using refrigerant R12 in the ejector expansion refrigeration cycle (EERC). The homogeneous equilibrium model (HEM) was assumed, with constant pressure mixing of the two streams considered at a pressure lower than that of the evaporator. He introduced efficiencies for the ejector components to account for deviation from the isentropic process. The shock effects were considered in these efficiencies. This model has been used in many two-phase ejector models available in the literature [7], [13]–[16].

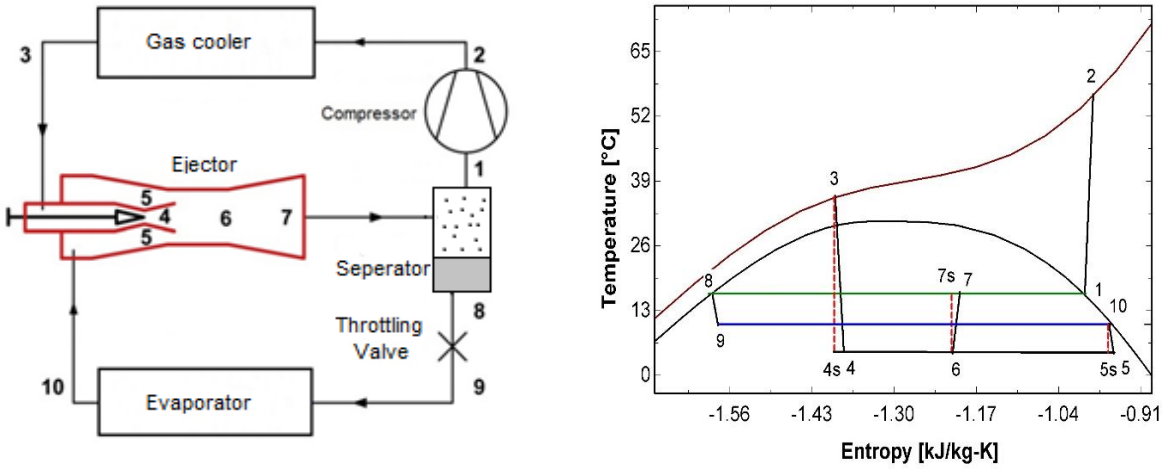

Figure 4.2. Transcritical CO_2 cycle and corresponding temperature-specific entropy diagram

Li and Groll [7] employed a two-phase ejector model based on the Kornhauser's model for a transcritical CO_2 air-conditioning system. They reported COP (Coefficient of Performance) improvement of up to 16%.

Elbel and Hrnjak [13] also used Kornhauser's model in their simulation to investigate the effects of the internal heat exchanger (IHX) on the performance of a transcritical CO_2 ejector system. Their results illustrated system performance improvements (COP and cooling capacity) by using an ejector and IHX in a conventional system.

A thermodynamic and exergy analysis of the transcritical CO_2 ejector refrigeration system was performed by Fangtian and Yitai [30]. Their results showed an improvement of 30% in COP and a decrease in exergy losses of 25% compared to conventional systems. Liu and Groll [26] studied ejector efficiencies based on a two-phase ejector model of two-phase flow ejector and measured data. They showed that ejector component efficiencies highly depend on geometries and operating conditions.

Zhang and Tian [32] presented a thermodynamic model of the ejector transcritical CO_2 refrigeration cycle to investigate the effect of the suction nozzle pressure drop (SNPD) on the performance of the cycle. They recorded a 45% increase in COP compared to the basic cycle through the optimization of the SNPD value and a 43% reduction in the ejector exergy losses.

Ameur et al. [12] proposed a thermodynamic approach to model a two-phase ejector. They used a mass flux maximizing criterion for double-choking at the nozzle throats instead of an approximate calculation of the sound velocity. Constant isentropic efficiencies, as well as three geometrical parameters, were considered in their model. Comparison of the results with experimental values showed good agreement. However, there is neither detailed information about the calculation of shock wave nor about adapting the assumptions and geometrical parameters of their model with the experimental devices.

Smolka et al. [17] developed a computational homogeneous model of CO_2 two-phase flow through a heat pump system. They proposed a mathematical model using an enthalpy based equation. Local

pressure distributions in the mixing chamber and the diffuser and the mass flow rates of the primary and secondary flows were obtained and validated for two types of ejectors, one for single-phase R141b and the other for two-phase CO_2 ejector.

Yazdani et al. [43] developed a CFD code accounting for the real properties of CO_2 in an expansion work recovery ejector to obtain an ejector design model. To model the two-phase flow, they implemented a non-homogeneous mixture model and validated the obtained entrainment ratio and pressure recovery against experimental data. The effect of the slip model on the pressure distribution is shown as a series of expansion waves along the axis, although it has a negligible effect on the overall performance of the ejector. Palacz et al. [55] used the CFD model to study the accuracy of the HEM based on the expansion of CO_2 through a two-phase ejector for a wide range of operating conditions. Two-phase evaporation in supersonic CO_2 ejectors was studied by Giacomelli et al. [66]. More complicated CFD models may give more details of the two-phase flow nature but they are computationally too expensive specifically for optimization purposes [67].

The ejectors may work at different operating conditions other than the critical point in double chocking or single chocking as shown in Figure 4.3.

For a fixed geometry and constant ejector input conditions, the back pressure that gives the maximum entrainment ratio defines the double choking condition. In this case, the maximum entrainment ratio remains constant while the back pressure decreases from its critical point. In double choking condition both the primary and the secondary flows are choked. This means that the mass fluxes reach their maximum values at their respective nozzle throats. The case for which the secondary flow is not choked is called the single choking condition in which changing the back pressure results in changing the entrainment ratio. If the back pressure is higher than a limited pressure, a backflow occurs and the ejector is in the malfunction mode.

The present study proposes a detailed 1-D model for evaluating the performance of a two-phase CO_2 ejector for both single chocking and double choking conditions. Therefore it is more complete than all previous thermodynamic models which are limited to a certain case (either single chocking [5], [32], [47] or double choking [12]). It is the first time that the performance of a two-phase ejector is investigated in both conditions.

First, a new model is proposed to predict the ejector's performance for a fixed geometry (off-design). This model is able to simulate a two-phase ejector in both single and double choking conditions. It is validated using experimental data available in literature.

Second, the model is developed for the design of a two-phase ejector, ie the computation of its dimensions under fixed operating conditions (on-design). The model is also validated and used for the parametric analysis to evaluate the effect of polytropic efficiency variations on the sizes of the primary and secondary nozzles and of the diffuser. This model which refers to the critical point of the ejector is then used for the predictions of the ejector's performances under different possible cases.

Constant polytropic efficiencies will be used for the expansion and compression processes in the nozzles and the diffuser to take into account the effect of the pressure ratio on the irreversibilities. The concept of polytropic efficiency was first introduced by Galanis and Sorin [33] for single-

phase ejectors working with perfect gases. It was later used successfully for real gases by Khennich et al. [34] and Samaké et al. [21] for single-phase ejectors.

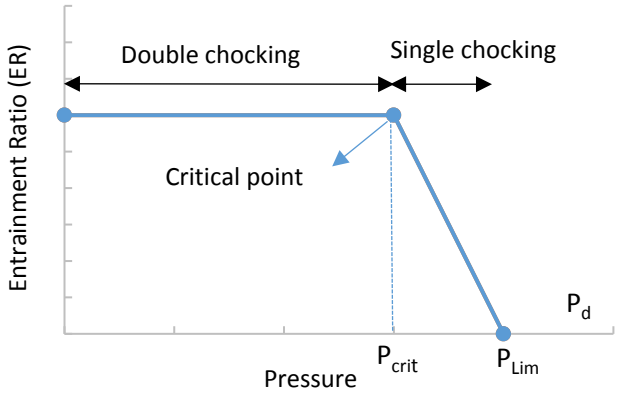

Figure 4.3 Critical mode of an ejector

4.4 Thermodynamic Modeling

In an ejector, the high-pressure primary stream (P_{p0}) expands in the primary nozzle to become a low-pressure stream with high velocity (P_{p2}). This low pressure entrains a suction (secondary) stream (P_{s0}) into the mixing section (P_{s2}). The two streams exchange momentum and energy inside the mixing section and then the uniform mixture is compressed to the value higher than the inlet pressure of the secondary stream (P_d).

Since the ejector is a key component in an ejector refrigeration or heat pump cycle, it is important to quantify its performance in the cycle. Two common parameters are used to evaluate ejector's performance: the ability to entrain the secondary flow inside the ejector, defined as the entrainment ratio ($ER = \dot{m}_s/\dot{m}_p$), and the ability to increase the suction pressure that is known as the pressure ratio ($P_{ratio} = P_d/P_{s0}$). This section describes the assumptions and governing equations as well as the procedure used to model the ejector.

4.4.1 Assumptions

Different models of the ejectors exist according to the assumptions, governing equations, auxiliary conditions, mixing mechanism and solution methods. Conservation equations of mass, energy and momentum, gas dynamic equations, state equations, isentropic relations as well as some appropriate assumptions, initial and boundary conditions are used to solve the flow within the ejector. The assumptions which are employed to simplify the problem in the proposed two-phase ejector model are listed below:

- Flow is one dimensional, adiabatic and steady state throughout the ejector.
- Heat transfer between the streams and walls is neglected.

- The homogeneous equilibrium model is assumed for the two-phase flow. This means that the two phases are in dynamic and thermal equilibrium and all fluid properties and velocities are constant across a cross-section area. This assumption is believed to be reasonable due to high average velocities and small ejector dimensions which result in good phase mixing [12].

- The CO_2 thermodynamic and transport properties of the primary and secondary flows are obtained from real fluid properties using the fundamental equation of state developed by Span and Wagner [68].

- The inlet velocities of the primary and secondary flows are negligible (stagnation conditions).

- Constant polytropic efficiency coefficients are used to account for friction losses in the nozzles and the diffuser.

- The friction losses in the mixing chamber are negligible, however, a friction factor is calculated for constant area duct.

- Mass flux maximization criterion is used for both nozzles, as previously done for single- [21], [33], [34] and two-phase ejectors [12].

- Both primary and secondary fluids are choked at design condition (double choking).

- A normal shock wave takes place at the inlet of constant area duct and the mixing of two streams is complete before the shock occurrence.

- The flow at the diffuser inlet is subsonic and decelerates toward the exit stagnation conditions where the pressure is higher than at the secondary inlet. Supersonic conditions at the diffuser inlet are of little practical interest in the refrigeration and heat pump applications in which compression ratio is important.

4.4.2 Model of a two-phase ejector for fixed geometry (off-design)

In this section, a two-phase CO_2 ejector is described for a given geometry while the operating conditions of the primary and secondary flows vary. The model is based on double choking conditions for the critical mode. It is assumed that the secondary flow is choked inside the mixing chamber (cross section "sm", Figure 4.2) [21], [23]. It is also proposed a method to calculate the properties at the diffuser outlet for the case in which the secondary flow does not choke in the mixing chamber (single chocking condition).

The corresponding flowchart is shown in Figure 4.4. As determined in the flowchart, the input parameters of the model are:

- Temperature and pressure of the primary flow

- Temperature and pressure of the secondary flow

- Primary nozzle, secondary nozzle and diffuser efficiencies ($\eta_{pol,p}, \eta_{pol,s}, \eta_{pol,d}$)
- Geometry of the ejector: length of the constant area duct (L_5), throat diameter (D_{th}), mixing diameter (D_{mix}), diffuser exit diameter (D_{d1})

The calculation starts with a preliminary value for entrainment ratio then the quality is computed at the ejector exit. The solution converges for design conditions when Eq. (4.1) is satisfied to maintain a balance between liquid and vapor in the expansion recovery cycle.

$$x_d = 1/(1 + ER) \tag{4.1}$$

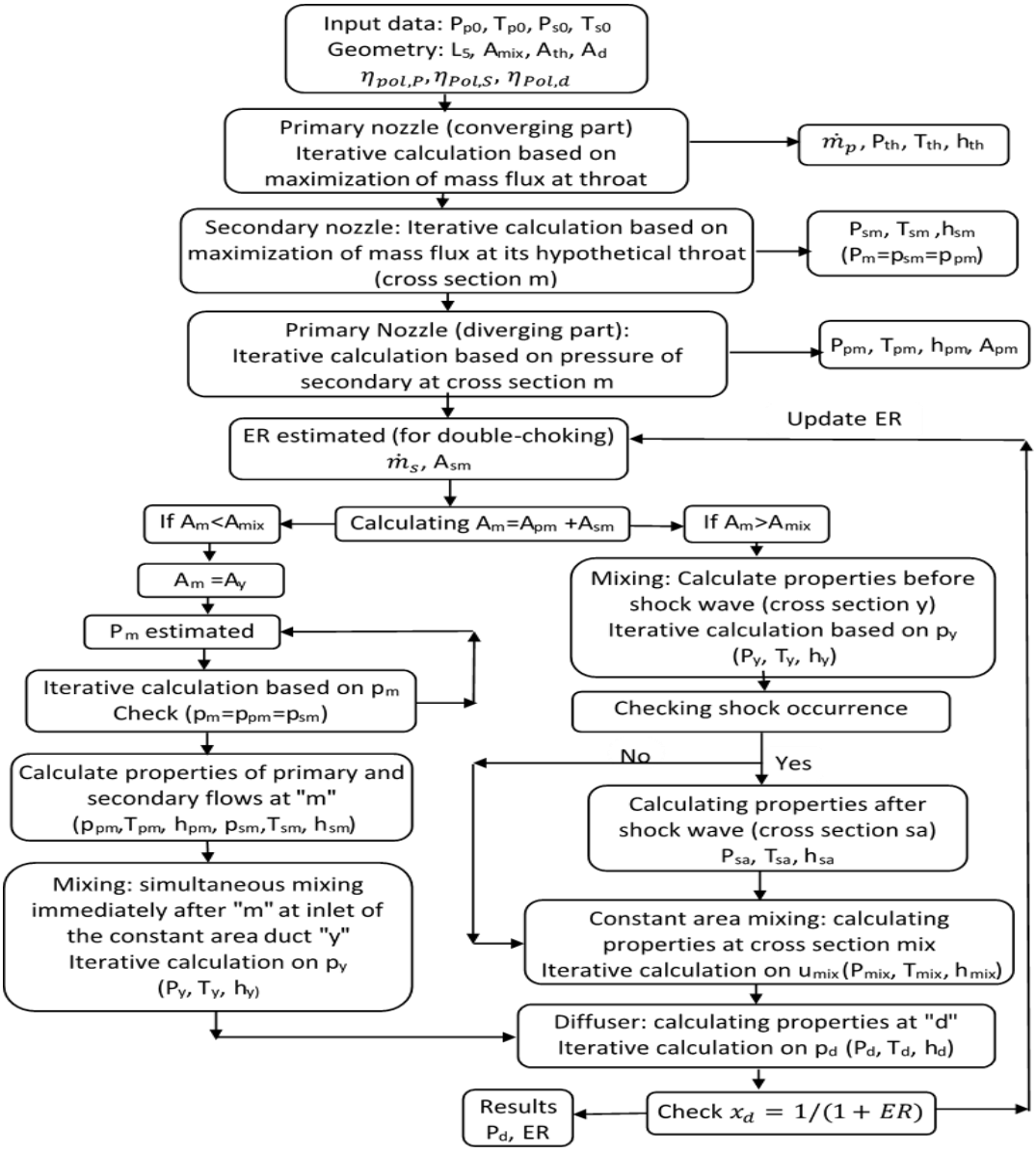

Figure 4.4 Procedure for CO_2 two-phase ejector modeling for a fixed geometry

The sound velocity proposed by Lund and Flatten [46] is used to estimate the Mach number in different cross sections of the ejector. Their velocity model assumes pressure and temperature equilibrium, but not equilibrium of the chemical potentials [47]:

$$a^{-2} = \rho\left(\frac{\epsilon_v}{\rho_v a_v^2} + \frac{\epsilon_l}{\rho_l a_l^2}\right) + \frac{\rho}{T}\frac{C_{p,v}C_{p,l}(\zeta_l - \zeta_v)^2}{C_{p,v} + C_{p,l}} \tag{4.2}$$

$$\zeta_k = \left(\frac{\partial T}{\partial P}\right)_{s_k} = \frac{T\beta_k v_k}{C_{p,k}} \tag{4.3}$$

$$C_{p,k} = \rho_k \epsilon_k c_{p,k} \tag{4.4}$$

$$\epsilon_v = \frac{1}{1+\left[\frac{1-x}{x}\right]\frac{\rho_v}{\rho_l}} \tag{4.5}$$

where a_v and a_l are single phase sound velocity of a saturation vapor and liquid , ϵ_v and $\epsilon_l = 1 - \epsilon_v$ are the void fraction of the vapor and liquid phases in homogeneous flow , respectively and k refers to each phase.

Primary and secondary nozzles (cross sections "th", "pm","sm")

The iterative solution starts with an estimated nozzle throat pressure and continues incrementally decreasing the pressure to the point where the mass flux reaches its maximum value. The polytropic efficiency coefficient is obtained as the isentropic efficiency of an elemental process and takes into account the effect of pressure ratio on the entropy increase during expansion and compression processes. The acceleration of the primary and secondary streams are calculated using the definition of the polytropic efficiencies as well as the conservation of mass, momentum and energy (Figure 4.5b). In the divergent part of the primary stream, the pressure is assumed to reach the same pressure as secondary stream at its hypothetical throat (cross section "sm"). After calculating the pressure at cross-section "m", a value for the entrainment ratio is estimated and the mass flow rate of secondary flow is determined. Then the secondary flow area at "sm" and therefore the total area of the primary and secondary flows are obtained ($A_m = A_{pm} + A_{sm}$).

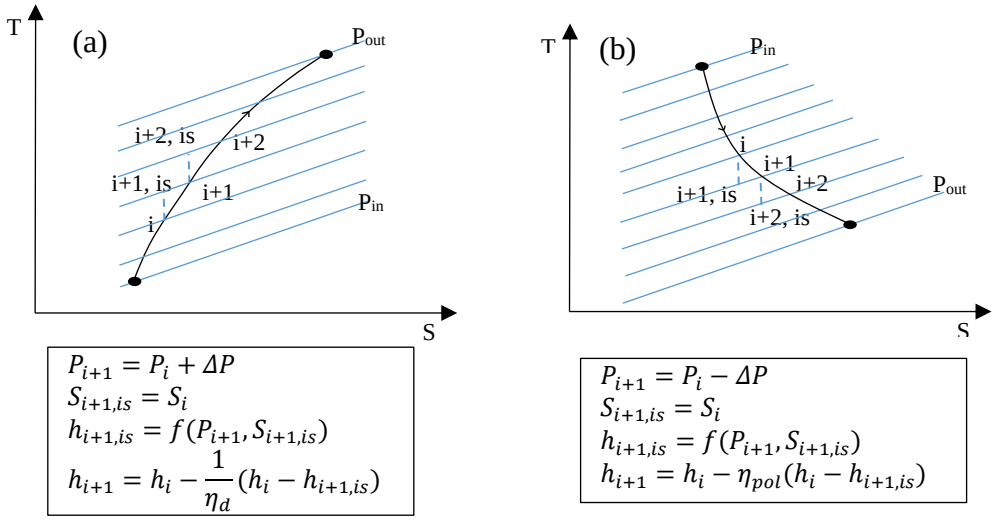

Figure 4.5 Definition of the polytropic efficiency to evaluate the flow properties; (a) diffuser (b) nozzles

Mixing chamber (cross section "y")

The interaction between two streams begins and the supersonic flow slows down in this area. First, the area of the cross section "m" (A_m) is compared to given mixing area ($A_y = A_{mix}$). For $A_m > A_y$, the choking of the secondary stream occurs in the mixing chamber. The iteration starts with an estimated value of the exit pressure at cross section "y" and then the pressure is corrected until satisfying mass conservation at this cross section. Unlike the previous models [5], [7], [13], [47] the proposed one does not use the assumption of the constant mixing pressure. By imposing momentum balance in this area, one gets:

$$u_y(\dot{m}_s + \dot{m}_p) + P_y A_y = (P_{sm}A_{sm} + P_{pm}A_{pm}) + (\dot{m}_s u_{sm} + \dot{m}_p u_{pm}) - F_{ym} \quad (4.6)$$

F_{ym} is the axial force on the fluid due to the pressure along the walls of mixing chamber.

For $A_m < A_y = A_{mix}$, the secondary flow doesn't choke in the mixing chamber. This case works at single chocking condition (sloped part of Figure 4.3). To model this particular case, it is assumed that both primary and secondary flows reach a constant pressure at cross section "m" immediately before "y" ($P_{pm} = P_{sm} = P_m$, $A_m = A_y$). A value is estimated for P_m and the iteration starts from the primary nozzle throat to obtain the properties of the primary flow at "pm". For a given geometry, the area of the secondary flow will be obtained by ($A_{sm} = A_y - A_{Pm}$) then the second iterative calculation starts from the stagnation point of the secondary flow and the process continues until the mass convergence of the secondary flow at this cross section is obtained. It is then assumed that the two streams mix immediately at the inlet of the constant area duct ("y"). This assumption is in agreement with the experimental work of Zhu et al. [69] for CO_2 two-phase flow. These authors indicated that the mixing of the primary and secondary flows in the mixing chamber is very fast so the completely mixed assumption can be used to analyze transcritical CO_2 ejectors. The properties of mixed flow are then calculated by employing mass, momentum and energy conservations between cross sections "m" and "y". In this case, $F_{ym} = 0$ and the velocity of the mixed flow is determined by the momentum equation according to:

$$u_y(\dot{m}_s + \dot{m}_p) + (P_y - P_m)A_y = (\dot{m}_s u_{sy} + \dot{m}_p u_{py}) \quad (4.7)$$

Constant area duct (cross section "mix")

In this area, stream mixing continues and the static pressure increases resulting in subsonic flow before entering the diffuser. In the proposed model, it is assumed that the shock wave occurs at inlet of the constant area duct unlike other two-phase models. In most existing models for CO_2 ejector the shock wave is not calculated [7], [27], [30] or it is considered at the outlet of the constant area duct [47]. However, it is impossible to capture the shock effects at the outlet ("mix") when the Mach number is low at the inlet ("y"). For CO_2 two-phase flow, the shock wave is not as strong as that in single phase flow [17], [18] and it may diminish before reaching the end of the constant area duct [11] depending on its length. This justifies the assumption that the shock wave occurs at the inlet of the mixing area. Moreover it helps to capture the effect of even not-strong shock waves in CO_2 two-phase ejector.

The properties of flow are calculated after the shock wave by employing mass, momentum and energy conservation between cross sections "sb" and "sa" as follows:

$$\dot{m}_p + \dot{m}_s = \rho_{sa} u_{sa} A_y \tag{4.8}$$

$$h_p + ER\, h_s = (1 + ER) * (h_{sa} + u_{sa}^2/2) \tag{4.9}$$

$$p_{sb} A_{sb} + (\dot{m}_p + \dot{m}_s) * u_{sb} = p_{sa} A_y + (\dot{m}_p + \dot{m}_s) * u_{sa} \tag{4.10}$$

Since the shock wave occurrence is assumed at the inlet of constant area duct, one sets $s_b \equiv y$ in Eqs. (4.4) to (4.6). There are 4 unknowns ($\rho_{sa}, u_{sa}, h_{sa}, p_{sa}$) in theses equations which are coupled with the equation of state and solved iteratively.

After calculating the properties at cross section "sa", the properties of cross section "mix" are calculated. The iteration process is performed on the velocity based on the calculation of the properties at cross section "mix". A velocity at this cross section is estimated and mass, momentum and energy conservation equations are solved to obtain a new velocity. This process continues until convergence for the velocity.

The friction losses are taken into account by employing a wall friction coefficient in the momentum equation. The momentum equation in this area is obtained by following relation:

$$\rho_{sa} u_{sa}^2 + P_{sa} - \Delta P = P_{mix} + \rho_{mix} u_{mix}^2 \tag{4.11}$$

ΔP is the pressure loss between cross sections "sa" and "mix". It is obtained from the Darcy's equation based on the two-phase homogeneous model:

$$\Delta P = \frac{1}{2} f\, (L/D)\, (\bar{\rho}\, \bar{u}^2)/2 \tag{4.12}$$

To evaluate the friction factor, the Prandtl correlation is used as following [12]:

$$1/\sqrt{f} = 2 \log\left(Re\sqrt{f}\right) - 0.8 \tag{4.13}$$

In both above equations, the properties of the flow are determined based on the two-phase homogeneous model principles: average values of density, velocity and viscosity.

The relation between the axial force (F) and the dissipation efficiency (φ_m) was introduced in previous works [12], [26], [31], [33] to account for friction, mixing and pressure losses in the mixing area. It can be obtained by the following relation:

$$F = \left(1 - \varphi_m\right) * \left(\dot{m}_s u_{sm} + \dot{m}_p u_{pm}\right) \tag{4.14}$$

where F is the axial force between cross sections "m" and "mix".

Diffuser (cross section "d")

In the diffuser, the residual kinetic energy of the mixture transforms to the energy linked to the static pressure. To evaluate the conditions at the diffuser outlet, iterations are made by increasing the outlet pressure until the two velocities obtained from the mass and energy conservation converge. For the deceleration process in the diffuser, a polytropic efficiency coefficient is used in the same way of the flow acceleration in the primary and secondary nozzles (Figure 4.5a).

4.4.3 Model of a two-phase ejector for fixed operating conditions (on-design)

The experimental data on CO_2 two-phase ejector are limited in the literature and the design conditions for a two-phase CO_2 ejector are not defined in any of them ([17], [18], [27], [40], [69]). The purpose of the design model is to calculate the geometry of the ejector for given inlet and outlet operating conditions. All dimensions of the ejector are calculated for the base case and then the effects of irreversibilities (polytropic efficiencies) on these dimensions are investigated.

The proposed design procedure for CO_2 two-phase flow is based on the combination of the model proposed by Khennich et al. [34] for a single phase flow and the assumptions presented in section 4.4.1.

Figure 4.6 shows the procedure to evaluate the ejector dimensions. Using this model all cross section areas and lengths of the ejector are calculated. The input parameters are: the primary and secondary operating conditions at inlets ($P_{s0}, T_{s0}, P_{p0}, T_{p0}$); the diffuser outlet conditions (P_d,T_d); the mass flow rate of the primary flow ($\dot{m}_p$); half angles of the converging-diverging parts of the primary nozzle, the mixing chamber and the diffuser ($\alpha_1, \alpha_2, \alpha_3, \alpha_4$). It is worth mentioning that the entrainment ratio as well as the mass flow rate of secondary flow can be determined by satisfying Eq. (4.1).

The model for the primary and secondary nozzles is the same as that described in section 4.4.2. The mass flux maximization criteria and constant polytrophic efficiencies are also used to calculate the properties at their corresponding throats ($P_{th}, D_{th}, P_{sm}, A_{sm}$).

The properties and the area at cross section "p1" are calculated by choosing a small value for the velocity and by using the polytropic efficiency [34]. This value should satisfy the stagnation conditions at the inlet of the primary nozzle. Therefore, the area and the corresponding diameter at the primary inlet are determined (A_{p1}, D_{p1}).

The properties of the primary and secondary flows at cross sections p2 and $s2$ are obtained according the method proposed by Samaké et al. [21]. The pressures of the primary and secondary flows at this cross section are determined as follows:

$$p_{p2} = P_{th} + C_1(p_m - p_{th}) \tag{4.15}$$

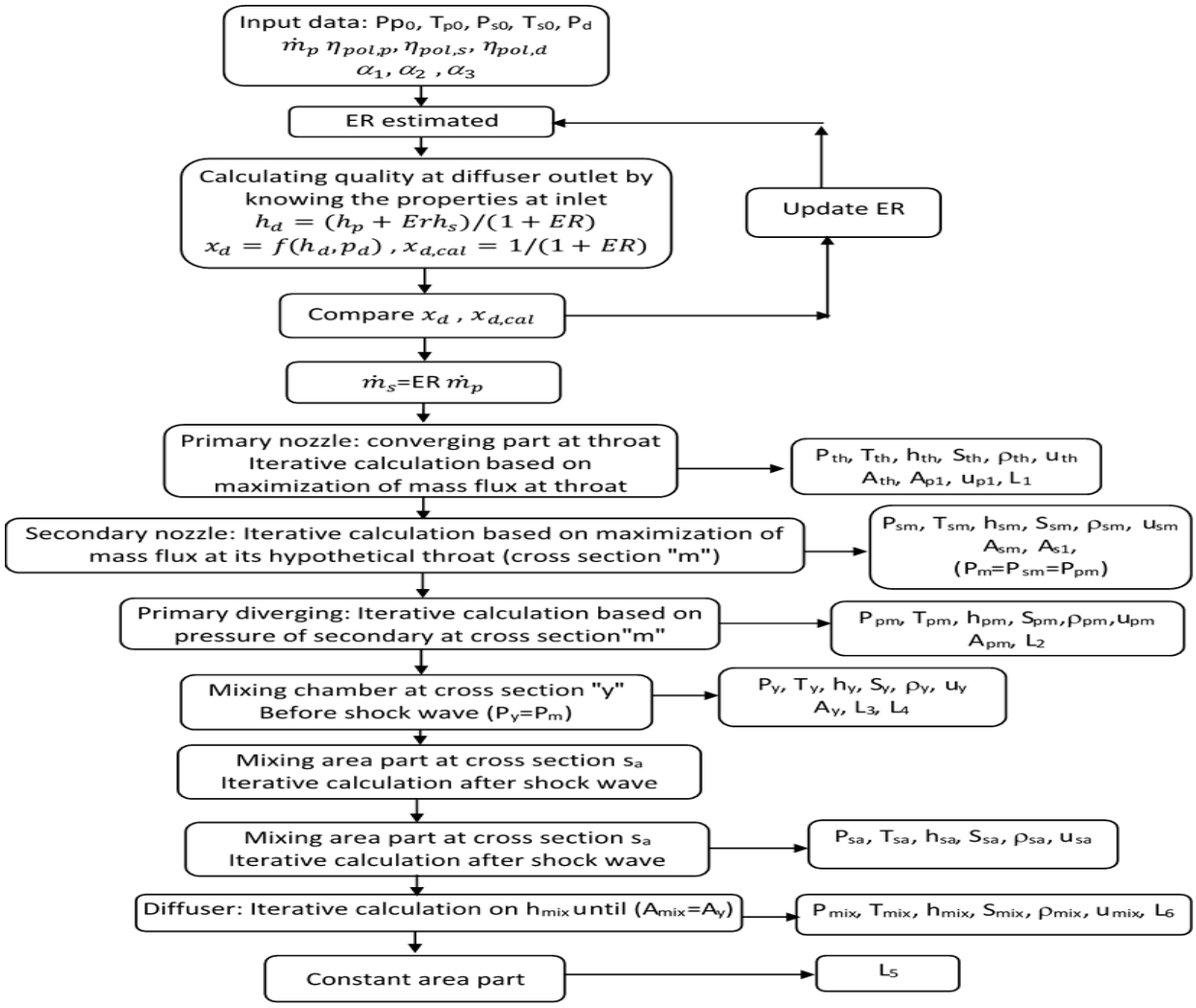

Figure 4.6. Procedure to evaluate the dimensions of a two-phase ejector

$$p_{s2} = P_{s0} + C_2(p_m - p_{s0}) \tag{4.16}$$

Since $p_m < p_{p2} < p_{th}$ and $p_m < p_{s2} < p_{s0}$, the values of c_1 and c_2 range between 0 and 1. These two coefficients are independent of each other except when the mixing takes place at the exit of the primary nozzle. In this case both coefficients are equal to unity. After all diameters have been determined at cross sections p1, "th" and p2, the lengths of the converging and diverging parts of the primary nozzle are obtained from the following relations:

$$L_1 = (D_{p1} - D_{th})/(2 \tan \alpha_1) \tag{4.17}$$

$$L_2 = (D_{p2} - D_{th})/(2 \tan \alpha_2) \tag{4.18}$$

Similar to section 4.4.2 (double choking condition), it is assumed that the choking of the secondary flow occurs at cross section "sm".Therefore the diameter of D_m (corresponding to $A_{pm} + A_{sm}$) is also known.

However, the pressure is assumed constant along the mixing section (unlike off-design condition) to calculate corresponding area as well as properties at cross section "y". By obtaining the area at cross section "y", the lengths of the converging parts are obtained:

$$\mathrm{L3} = (\mathrm{D_2} - \mathrm{D_m})/(2\tan\alpha_3) \tag{4.19}$$

$$\mathrm{L4} = (\mathrm{D_m} - \mathrm{D_y})/(2\tan\alpha_3) \tag{4.20}$$

The properties at cross section "y" are calculated by applying the conservation of mass, momentum and energy between cross sections "m" and "y". Since the mixing takes place under constant pressure, $\mathrm{F_{ym}} = \mathrm{P_m}(\mathrm{A_{pm}} + \mathrm{A_{Sm}} - \mathrm{A_y})$. Substituting this value into Eq. (4.6), the momentum equation becomes:

$$\mathrm{u_{pm}} + \mathrm{ER}\,\mathrm{u_{sm}} = \mathrm{u_y}(1 + \mathrm{ER}) \tag{4.21}$$

where u_y is obtained from the above equation. Then h_y is calculated from energy conservation. The other properties at cross section "y" are obtained by knowing two independent values, h_y and $p_y = p_m$. Similarly to the previous section, the normal shock takes place at the entrance of the constant area duct after completing the mixing process at cross section "y". Therefore, the properties at cross section "sa" after the shock wave can be calculated. The properties at the diffuser outlet ("d") are known since the pressure is fixed at the outlet and the corresponding enthalpy is obtained from energy conservation between inlets and the outlet. The conditions at the diffuser inlet ("mix") can be calculated based on the model described for the diffuser at section 4.4.2. The enthalpy is incrementally reduced until the corresponding area at inlet of constant area duct matches with the known cross section area ("A_y") [34]. The properties and the area at "d1" are calculated by choosing a small value for u_{d1} and by applying mass, momentum and energy equations between "mix" and "d1". Therefore, the length of the diffuser can be calculated by knowing the diameters at "mix" and "d1":

$$\mathrm{L_6} = (\mathrm{D_{d1}} - \mathrm{D_{mix}})/(2\tan\alpha_4) \tag{4.22}$$

Finally, after calculating all of the ejector areas, the length of the constant area duct can be obtained by combining the momentum equation between cross section "sa" and "mix" with Darcy's relation inside a duct (Eqs. 4.8, 4.9).

4.5 Results and discussion

An engineering equation solver (EES) program is used to solve the proposed models described in sections 4.4.2 and 4.4.3, which combines non-linear equations with thermophysical property functions.

4.5.1 Model validation

Table 4.1 compares the calculated primary nozzle mass flow rate with three experimental results available in the literature for refrigerant CO_2. The constant polytropic efficiency of 0.9 is considered for primary nozzle [7], [13], [30], [32].

Regarding the experimental results of Smolka et al. [17] for the converging-diverging primary nozzle with a throat diameter of 1 mm, the discrepancy is less than 13.20 %. Another comparison is made with the experimental results of Zhu et al. [69] for a converging nozzle with throat diameter of 1.1 mm. The results represent the discrepancy between 0.58% and 15.75 %. For the case of Banasiak and Hafner [18], the discrepancy is 6% for the throat diameter of 0.96 mm. This relatively small discrepancy may be due to the use of a constant efficiency and also to the HEM assumption for the expansion of CO_2 through two-phase ejectors. The results show that the accuracy of the HEM varies for different operating conditions [55].

To validate the ejector model for CO_2 two-phase flows, comparisons with the experiments of Smolka et al. [17] are made in terms of the pressure ratio. In all calculations, constant polytropic efficiency coefficients were used as ($\eta_{pol,p} = 0.9, \eta_{pol,s} = 0.9, \eta_{pol,d} = 0.8$) ([7], [30], [32]).

Table 4.1 Comparison of calculated mass flow rates with experimental data for CO_2

			$\dot{m}_p$(g.s^{-1})		
	P_p(kPa)	T_p (˚C)	Present work	Experiment	Error (%)
Experiments of Smolka et al. [17]	9915	29.9	54.68	49.73	9.95
	8668	33.4	34.8	31.94	8.95
	9091	26.7	51.3	48.42	5.95
	9850	35.5	45.85	40.73	12.57
	9455	36.3	39.98	35.69	12.02
	8846	36.5	31.93	29.84	7.004
	8465	35.4	29.51	26.07	13.195
Experiments of Zhu et al. [69]	8002	33.3	33.75	33.95	0.589
	7980	33.2	33.67	33.45	0.658
	7690	33.1	27.54	31.23	11.816
	7300	31.3	24.4	26.74	8.751
	7240	30.5	24.49	24.9	1.647
	8440	33.3	39.11	36.76	6.393
	8390	33.4	38.3	34.97	9.522
	7940	33.4	32.7	32.19	1.584
	7610	31.7	31.88	27.54	15.759
	8910	34.5	43.55	38.46	13.234
	8640	34.1	40.31	36.96	9.064
	8550	34.2	38.92	34.88	11.583
	7910	33.9	30.59	31.02	1.386
	7500	32.1	26.02	27.12	4.056
Experiments of Banasiak and Hafner [18]	10112	39.3	39.56	42.25	6.37

Table 4.2 Validation of the thermodynamic model with experimental data of Smolka et al. [17]

	P_p (kPa)	T_p (˚C)	P_s (kPa)	T_s (˚C)	ER	P_{ratio} Present work	P_{ratio} Experiment	Error (%)
Case 1	9915	29.9	3996	17.4	0.674	1.141	1.096	4.06
Case 2	8668	33.4	3652	6.6	0.57	1.137	1.115	2.01
Case 3	9091	26.7	3595	7.6	0.69	1.132	1.077	5.1
Case 4	9850	35.5	5149	20.7	0.6619	1.103	1.08	2.14
Case 5	9455	36.3	4761	15.1	0.6475	1.107	1.0878	1.78
Case 6	8846	35.6	4255	13.7	0.545	1.113	1.097	1.49
Case 7	8465	35.4	3874	10.3	0.458	1.130	1.106	2.19

As shown in Table 4.2, the pressure ratios are compared for the cases with different entrainment ratios. The discrepancy between the experiments and the model predictions is small (less than 5%). Table 4.3 also presents the model predictions for the pressure at different cross sections of the CO_2 two-phase ejector compared to the experimental study of Banasiak and Hafner [18]. The model prediction is given for the pressure at the inlet and outlet of the constant mixing area as well as the outlet of the diffuser. The results show that the proposed thermodynamic model predicts quite well the pressure at these different locations (discrepancies remain less than 1.34%).

Table 4.3 Comparison of calculated pressures at different cross sections of the ejector with experimental data (Banasiak and Hafner [18])

Pressure (kPa)	Present work	Experiment	Error (%)
P_d	4637	4601.46	0.77
P_y	3912	3940	0.71
P_{mix}	4520	4460	1.34
Operating conditions : P_p=10112 kPa, T_p=39.3˚C, P_s=3952 kPa, T_s=5.5°C, ER=0.42			

4.5.2 Calculating main dimensions

All dimensions of the ejector are calculated with the on-design model described in section 4.4.3. As mentioned before it is assumed that the secondary flow chokes somewhere in the mixing chamber at cross section "sm". Therefore, to calculate L_2, L_3 and L_4, the values of C_1 and C_2 should be determined. Since these two constant parameters depend on the nature of the mixing process and may be different in each case, these parameters should be adjusted in order to calculate D_{2p} and D_2 [21]. Considering the inlet operating conditions and nozzle dimensions in the experiments of Banasiak and Hafner [18], the values of C_1 and C_2 are obtained and are equal to 0.41 and 0.0125 respectively.

Table 4.4 depicts a comparison of the experimental and numerically predicted values for all dimensions of the ejector. The results show that the model predictions are close to the experimental values with a discrepancy for D_{th}, D_{p1}, D_d and L_1 of less than 3.5%. The model predictions for other ejector dimensions are also close to the experimental values. However, the discrepancy between

the calculated and experimental values suggests that the experimental set-up may not work at critical conditions (critical back pressure and entrainment ratio).

The method of calculation of ejector geometry was previously validated for single phase flow by Khennich et al. [34] and Samaké et al. [21], for two different mixing assumptions. In view of these comparisons for two-phase ejectors, this model will be used to investigate the effects of the polytrophic efficiencies on the dimensions of a two-phase ejector.

Table 4.4 Comparison of calculated dimensions with values from literature

D,L (mm)	D_a	D_{th}	D_{pm}	D_2	D_m	D_{mix}	D_d	L_1
Calculation	6.204	0.992	1.44	4.0485	2.137	2.117	6.215	9.726
Experiment [18]	6	0.96	-	-	-	3	6	9.4
D,L (mm)	L_2	L_3	L_4	L_3+L_4	L_5	L_6	L_{tot}	L_5/D_{mix}
Calculation	2.76	2. 58	0.026	2.607	15.54	46.93	77.57	7.344
Experiment [18]	3.72	-	-	2.5	24	34.36	74	8

Table 4.5 depicts the corresponding fluid properties at different ejector cross sections for the "on-design" base case. The amount of void fraction shows that the dominant (continuous) phase is vapor. It means that the CO_2 two-phase flow consists of a gas phase as the continuous phase and droplets as the dispersed phase [33]. The results also show that the pressure increases across the shock wave (P_y to P_{sa}) is more than that in the diffuser (P_{mix} to P_d).

Table 4.5 Calculated flow properties at different ejector cross sections for CO_2 two-phase flow (on-design base case)

status	P (kPa)	T (˚C)	u (m/s)	$\dot{m}$ (kg/s)	x	ϵ_v	Phase
P0	10112	39.3	0	0.04225	-	1	supercritical
P1	10110	39.3	2.15	0.04225	-	1	supercritical
th	7197	29.9	91.49	0.04225	0.0008	0.001	two-phase
p2	5213	16.02	127.1	0.04225	0.329	0.705	two-phase
pm	2357	-14.03	199.7	0.04225	0.448	0.929	two-phase
s0	3952	5.5	0	0.02399	1	1	superheated
s1	3942	5.324	12.59	0.02399	1	1	superheated
s2	3933	5.173	17.23	0.02399	1	1	superheated
sm	2357	-14.03	179.9	0.02399	0.913	0.994	two-phase
y	2357	-14.03	192.6	0.06624	0.617	0.963	two-phase
sa	3824	3.544	114.7	0.06624	0.620	0.931	two-phase
mix	3480	-0.05	127.7	0.06624	0.622	0.94	two-phase
d1	4592	10.8	10.95	0.06624	0.637	0.914	two-phase
d	4601	10.88	0	0.06624	0.638	0.915	two-phase

4.5.3 Effect of polytropic efficiencies on ejector dimensions

Ejector dimensions are calculated for the "on-design" base case in which polytropic efficiency of the primary and secondary nozzles and diffuser are assumed to be 0.9, 0.9 and 0.8 respectively. Four other cases are also considered in the following. The effects of polytropic efficiencies on the dimensions of a two-phase ejector as well as corresponding isentropic and dissipation efficiency are summarized in Table 4.6. In each case, all design variables are equal to their corresponding values of the base case (column 1), expect one of the efficiency coefficients. This is the first time that the dimensions of a two-phase ejector are compared for various polytropic efficiencies. The first column reproduces the dimensions and efficiencies of the ejector for the "on-design" case. The pressure and temperature of the primary flow is considered 10112 kPa and 39.3 ˚C while for secondary flow, they are 3952 kPa and 5.5˚C respectively. The back pressure is assumed 4601 kPa and entrainment ratio is given 0.568.

Table 4.6 Effect of polytropic efficiencies on ejector dimensions and efficiencies

D, L (mm)	$\eta_{pol,p}$=0.9 $\eta_{pol,s}$=0.9 $\eta_{pol,d}$=0.8	$\eta_{pol,p}$=0.85 $\eta_{pol,s}$=0.9 $\eta_{pol,d}$=0.8	$\eta_{pol,p}$=0.9 $\eta_{pol,s}$=0.85 $\eta_{pol,d}$=0.8	$\eta_{pol,p}$=0.9 $\eta_{pol,s}$=0.9 $\eta_{pol,d}$=0.75	$\eta_{pol,p}$=1 $\eta_{pol,s}$=1 $\eta_{pol,d}$=1
D_1	6.204	6.295	6.204	6.204	6.04
D_{th}	0.9921	1.007	0.9921	0.9921	0.9644
D_{p2}	1.088	1.106	1.088	1.088	1.057
D_{pm}	1.44	1.465	1.44	1.44	1.398
D_m	2.137	2.153	2.154	2.137	2.075
D_y (D_{mix})	2.117	2.139	2.127	2.117	2.057
D_d	6.215	6.215	6.215	5.98	6.506
L_1	9.726	9.867	9.726	9.726	9.471
L_2	2.76	2.817	2.757	2.761	2.664
L_3	2.58	2.637	2.565	2.581	2.514
L_4	0.026	0.0188	0.0348	0.026	0.0241
L_3+L_4	2.607	2.656	2.5998	2.607	2.538
L_5	15.54	4.881	9.936	9.778	116.3
L_6	46.93	46.68	46.81	44.25	50.95
L_{tot}	77.57	66.9	71.83	69.12	181.9
(L_5/D_y)	7.344	2.282	4.67	4.62	56.55
$\eta_{is,p}$	0.9014	0.852	0.9014	0.9014	1
$\eta_{is,s}$	0.903	0.903	0.8543	0.903	1
$\eta_{is,d}$	0.7959	0.7962	0.7961	0.7456	1

The results show that the diameters of primary nozzle as well as the lengths are only influenced by the polytropic efficiency of the primary acceleration and increase when the efficiency decreases. The length of the constant area duct decreases by decreasing all polytropic efficiencies (nozzles and diffuser) however its diameter is only influenced by the efficiencies of the primary and secondary nozzles and increases when the efficiencies decrease. The total length of the ejector reduces by decreasing polytropic efficiencies of each component. It is not in agreement with Samaké et al.'s work [21] for R141b, which concluded that the diffuser efficiency has no effect on the total length of the ejector. The length of diverging part of the primary nozzle, as well as the

length of mixing chamber, are not markedly influenced by the efficiencies of secondary nozzle and diffuser. The diffuser efficiency has a small effect on the length of the diffuser .The highest value of constant area and diffuser length is obtained when all polytropic efficiencies equal one while other variables are not varied considerably. These results demonstrate that the ejector becomes larger when all ejector efficiencies increase. The value of isentropic efficiencies of the primary and secondary nozzles and diffuser have also been determined.

4.5.4 Application of the two-phase designed model

In this section, the performance of the ejector has been investigated for some cases with most of the possible operating conditions. They have been considered when the ejector doesn't work in its critical point (off-design). The procedure to calculate ejector properties at off-design conditions is adjusted for two-phase flow based on the designed model proposed in section 4.4.3 using the method introduced by Galanis and Sorin for single-phase flow [33].

4.5.4.1 Double choking with design inlet conditions and ($\mathbf{p_d < p_{cr}}$)

In this case, double chocking occurs when the inlet conditions are identical to their design values and the back pressure is lower than its design value.

This operation refers to the horizontal part of the performance curve (Figure 4.3). The conditions at cross section "y" as well as the conditions before and after shock wave ("sb","sa") are calculated. The properties at cross section "1", "th" and "m" (P_{pm},P_{sm}, P_1, P_{th}) as well as the mass flow rate of the primary and secondary flows are the same as their design values. Therefore, ER is identical to its design condition. The properties at cross sections "d", "mix" and "d_1" are calculated based on the model described at section 4.4.3.

It is observed from experimental and CFD simulations [70]–[75] that the shock occurs downstream of its position at the critical point. Therefore, its position is somewhere in the constant area duct between "y" and "mix". The properties at cross section "sb" and "sa" and the position of the shock can be calculated by employing mass and energy conservation at these cross sections. The momentum equation is also applied between cross sections "y-sb", "sa-mix" and "sb-sa".In both sections "y-sb" and "sa-mix" friction losses are calculated by Eq. (4.13). The position of the shock is dependent on the back pressure, as by decreasing the back pressure the place of shock moves into diffuser. For $P_d = P_{cr}$ the shock occurs at the inlet of the constant area duct at cross section "y" (thus sb ≡ y, $P_{sb} = P_y$).

Figure 4.7 demonstrates the pressure and velocity at different cross sections of the ejector for critical point and 2 other double choked cases. It is shown that, as expected across the shock, the pressure increases and the velocity decreases.

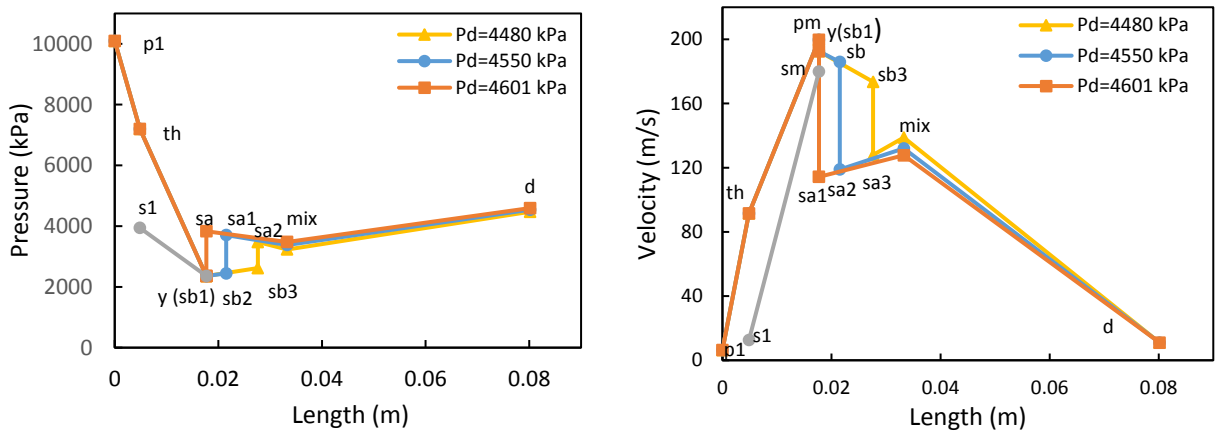

Figure 4.7 Distributions of axial pressure and mean velocity along the axis of the ejector for double chocking conditions and different back pressures P_d.

4.5.4.2 Single chocking with design inlet conditions, different ER and $\mathbf{P_d > P_{cr}}$

This case presents the part of the performance curve in which ER decreases from its design condition (P_{cr}) to maximum pressure (P_{lim}) (Figure 4.3).

To calculate this condition, it is assumed that the primary inlet conditions are the same as the critical point while the mass flow of the secondary flow is lower than its value at the critical point.

{Citation}According to experimental data and CFD simulation [70]–[74], in single choking conditions when the diffuser exit pressure is greater than the critical back pressure, the shock train occurs upstream of cross section "y". Furthermore, the flow at cross section "y" is subsonic in this case [33]. Figure 4.8 shows the pressure, velocity and entropy at different cross sections of the ejector operating at on-design condition (ER=0.568) and three single choking conditions (ER=0.407, ER=0.256 and ER=0.083) for given inlet secondary flow conditions. The results show that by decreasing ER, the pressure increases while the velocity and entropy decrease at cross section "y", "mix" and "d". It should be noted that the lines which join the calculated values at the chosen cross sections are not represented the conditions at the intermediate cross sections.

4.5.4.3 Double chocking with different primary inlet conditions

In this case the inlet operating conditions of the secondary flow are considered the same as theirs design values while the pressure of primary flow is lower or higher than its design value. Therefore the pressure at cross section "m" (P_{sm}) as well as the mass flow rate ($\dot{m}_s$) are not changed for the secondary flow. However, the properties of the primary flow at cross sections "1", "th", "2" and "m" (P_{p1},P_{th}, P_{p2}, P_{pm}) are different from the design conditions and can be calculated by iteration based on the known design area at cross section "m" (A_{pm}). Then the conditions at cross section "mix", "d" and "d_1" are calculated with an assumed value of u_{mix} higher than the design value of u_{sa}. For each value of u_{mix}, the obtained value is checked to satisfy the constraints (between 0 and 1) for the dissipation coefficient applied between cross sections "m" and "mix". The entropy at "mix"

should be lower than that at "d" and the pressure at "d" is less than at its design value [33]. Using this procedure, the corresponding entrainment ratio and critical back pressure are calculated for different primary pressures. Therefore the design condition is obtained for new operating conditions for a given geometry and then single choking conditions can be calculated for each case.

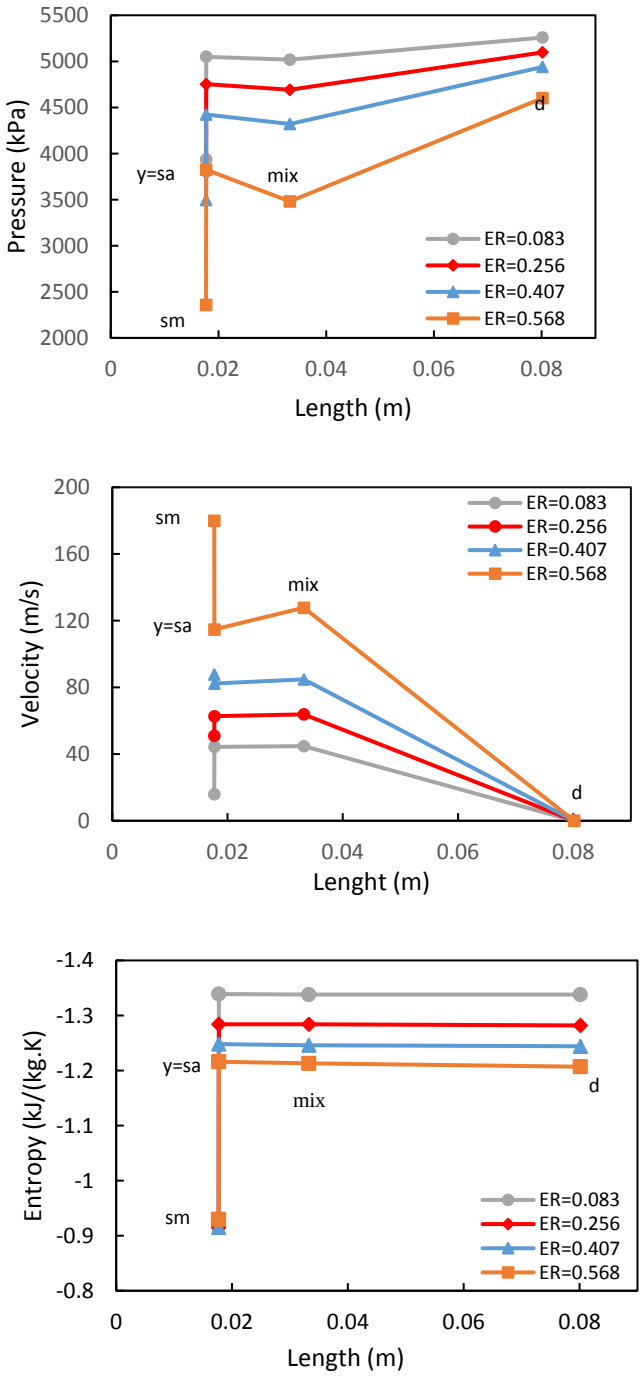

Figure 4.8 Distributions of pressure, velocity and entropy along the axis of the ejector for single choking conditions and different primary flow inlet conditions

Figure 4.9 depicts the relation between the entrainment ratio and the exit pressure for three different primary inlet pressures. It is observed that the difference of P_{cr} for different back pressures is small. It is due to the low pressure ratio of the CO_2 compared to other refrigerants.

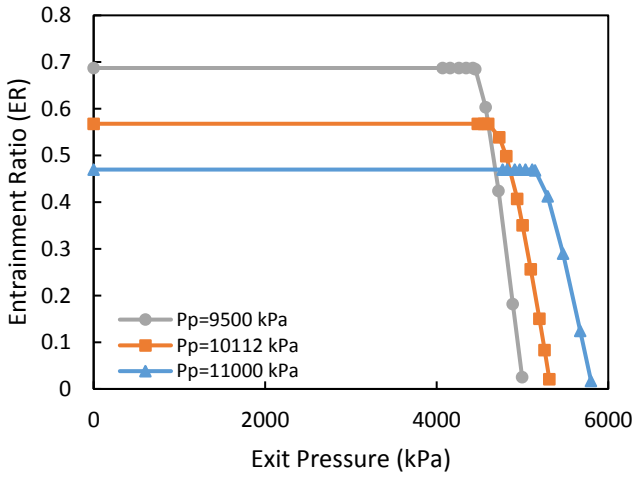

Figure 4.9 Entrainment ratio versus compression ratio for different primary flow pressures

4.6 Conclusion

The new model presented in this work predicts the performance of a CO_2 two-phase ejector for both single and double choking conditions. It is based on the conservation of mass, momentum and energy as well as relations to account for irreversibilities. A model has also been developed to design a two-phase ejector under given operating conditions. The dimensions of different parts of the ejector have been calculated. The performance of a CO_2 two phase ejector has been predicted under different operating conditions for both on-design and off-design conditions. The results have been validated using the data available in the literature. The occurrence of a normal shock wave is assumed at the inlet of the constant area. Unlike other previous models this assumption reveals the effect of a shock wave inside a CO_2 two-phase ejector. Polytropic efficiencies have also been employed to account for the pressure ratio during the acceleration and deceleration processes in the nozzle and diffuser. These have allowed evaluation of the effect of irreversibilities on the dimensions of a two-phase ejector. The newly proposed model has been investigated for different operating conditions typical for a two-phase ejector. It successfully predicts the flow properties at different cross sections of the ejector as well as the relation between entrainment ratio and pressure ratio. The results will be used to develop an optimum design of an ejector heat pump system. The present model will be incorporated into a thermodynamic model describing the whole system. A better understanding of the ejector characteristics will help to better analyse the effects of the different variables on the overall performance of the heat pump system.

4.7 Acknowledgments

This project is a part of the Collaborative Research and Development (CRD) Grants Program at 'Université de Sherbrooke'. The authors acknowledge the support of the Natural Sciences and Engineering Research Council of Canada, Hydro-Québec, Rio Tinto, Alcan and Canmet ENERGY Research Center of Natural Resources Canada.

4.8 Nomenclature

Nomenclature			
A	Cross section area, mm^2	**Subscripts**	
a	Sound velocity, m/s	crit	Critical
D	Diameter, mm	d	Diffuser
ER	Entrainment ratio	is	Isentropic
h	Specific enthalpy, kJ kg^{-1}	l	Liquid
L	Length, m	lim	Limiting
$\dot{m}$	Mass flow rate, kg s^{-1}	m	Choke location of secondary flow
P	Pressure, kPa	mix	Mixing
P_d	Back pressure (discharge pressure), kPa	p	Primary
P_{ratio}	Pressure ratio (pressure lift)	pol	Polytropic
s	Specific entropy, kJ kg^{-1} K^{-1}	s	Secondary
T	Temperature, K	th	Ejector throat
u	Mean axial velocity, m s^{-1}	tot	Total
v	Specific volume, m^3 kg^{-1}	v	Vapor
x	Quality	**Abbreviation**	
c_p	Specific heat at constant pressure, J kg^{-1} K^{-1}	CFD	Computational fluid dynamics
F	Force, N	COP	Coefficient of performance
f	Friction factor	EERC	Ejector expansion recovery cycle
	Greek symbols	EES	Engineering equation solver
α	Half angle, deg	GWP	Global Warming Potential
β	Thermal expansion coefficient, K^{-1}	HEM	Homogeneous equilibrium model
ϵ	Void fraction	IHX	Internal heat exchanger
η	efficiency	SNPD	suction nozzle pressure drop
ρ	Density, kg/m^3		

CHAPTER 5

EXERGY PERFORMANCE OF A TRANSCRITICAL CO_2 TWO-PHASE EJECTOR

5.1 Avant-propos

Auteurs et affiliation:

- Sahar Taslimi Taleghani: étudiante au doctorat, Université de Sherbrooke, Faculté de génie, Département de génie mécanique.
- Mikhail Sorin: professeur, Université de Sherbrooke, Faculté de génie, Département de génie mécanique.
- Sébastien Poncet: professeur, Université de Sherbrooke, Faculté de génie, Département de génie mécanique

Date d'acceptation: 2018

État de l'acceptation: version finale publiée.

Revue: Proceedings of ECOS 2018 - The 31st International conference on efficiency, cost, optimization, simulation and environmental impact of energy systems

Titre français: Performance exergétique d'un éjecteur diphasique au CO_2 transcritique

Contribution au document: Cet article contribue à la thèse par une analyse exergétique évaluant les pertes et l'efficacité exergétique d'un éjecteur diphasique au CO_2.

Résumé en français:

Le dioxyde de carbone est un réfrigérant de remplacement attrayant dans les systèmes de chauffage et de réfrigération qui a un impact minimal sur le changement climatique. Cependant, le cycle de compression transcritique au CO_2 présente une perte d'étranglement importante par rapport aux autres réfrigérants, du fait de la variation de pression élevée pendant la détente dans un processus d'étranglement, du CO_2 supercritique à un état sous-critique. L'intégration d'un éjecteur diphasique offre la possibilité de récupérer partiellement les pertes d'expansion pour le cycle au CO_2 transcritique. Dans cette étude, l'analyse exergétique d'un éjecteur diphasique au CO_2 est réalisée à l'aide d'un modèle 1D pour les régimes "single" et "double-choking". L'impact de la contre-pression sur les pertes et l'efficacité exergétique est présenté. Le comportement de trois mesures thermodynamiques, la production d'exergie, la consommation d'énergie et les pertes d'exergie, est évalué. L'analyse a permis d'évaluer l'impact des variations de température et de pression sur les différents types d'exergie, les irréversibilités et les performances globales de l'éjecteur. Les résultats de deux critères de performance exergétique (efficacité exergétique transitoire et efficacité

exergétique de Grassmann) sont comparés pour trois modes de fonctionnement d'un éjecteur: "double choking", "single choking" et condition au point critique. Un résultat important concernant la conception des éjecteurs est la présence d'une valeur maximale d'efficacité exergétique en transit autour du point critique. Il a également été démontré que l'efficacité exergétique de Grassmann n'était pas un critère approprié pour évaluer les performances d'un éjecteur au CO_2 transcritique.

5.2 Abstract

Carbon dioxide is an attractive alternative refrigerant in heating and refrigeration systems that has minimum impact on climate change. However, transcritical CO_2 compression cycle has a large throttling loss compared to the other refrigerants due to high-pressure change during expansion in a throttling process from a supercritical CO_2 to a subcritical state. The integration of a two-phase ejector offers an opportunity to partially recover the expansion losses for the transcritical CO_2 cycle. In this study, the exergy analysis of a CO_2 two-phase ejector is performed using a 1D model for both single and double choking conditions. The impact of the back pressure on the exergy losses and exergy efficiencies is presented. The behavior of three thermodynamic metrics: exergy produced, exergy consumed and exergy losses are evaluated. The analysis has allowed evaluating the impact of temperature and pressure variations on the different types of exergy, the irreversibilities and the ejector global performance. The results of two exergy performance criteria (transiting exergy efficiency and Grassmann exergy efficiency) are compared for three modes of an ejector functioning: double choking, single choking and at the critical point. An important result concerning the ejector's design, the presence of a maximum value of transiting exergy efficiency around the critical point is illustrated. It is also shown that the Grassmann exergy efficiency is not an appropriate criterion for evaluation of a transcritical CO_2 ejector performance.

5.3 Introduction

The use of two-phase ejector in heating and refrigeration systems has become an interesting issue to investigate performance enhancement of such systems. Carbon dioxide (CO_2) is an appropriate replacement for conventional refrigerants due to its minimal impacts on climate change. However, the transcritical CO_2 compression cycle has lower thermodynamic performance due to large expansion losses of an isenthalpic throttling process from a supercritical to a subcritical state. Among different devices for expansion work recovery, ejector is a favorable device which enables the use of CO_2 and other environmentally friendly refrigerants. It helps to reduce losses by recovering part of the expansion work in a throttling process and improve the cycle's efficiency [6], [16], [76]–[78]. It was determined that the ejector expansion cycle has a higher COP than a basic cycle even at off-design operating conditions [76]. Gay [56] was the first described the performance improvement of a transcritical CO_2 cycle by a two-phase ejector. The first one dimensional and homogeneous model of a two-phase ejector was first developed by Kornhauser [5] using R12 as a refrigerant in the ejector expansion refrigeration cycle (EERC).

An increase in the exergy efficiency (6.6–11.24%) and COP (7.34–12.87%) was obtained experimentally in an ejector expander cycle compared to the basic cycle by Bilir Sag et al. [78] using R134a. They also reported that the range of exergy efficiency of an ejector expansion cycle remains between 0.967 and 0.986.

An exergetic comparison of the ejector transcritical CO_2 cycle with expansion valve and turbine cycles has been presented by Sarkar [16]. He showed 9% exergy efficiency improvement by using ejector over valve for the given operating conditions. The evaluation of COP and exergy destruction of a transcritical CO_2 ejector refrigeration system was performed by Fangtian and Yitai [30]. An improvement of 30% in COP and a decrease of 25% in exergy losses compared to the conventional system were obtained in their analysis.

The effect of the suction nozzle pressure drop (SNPD) on the performance of the ejector transcritical CO_2 refrigeration cycle was investigated by Zhang and Tian [32]. It was recorded a 45% increase in COP compared to the basic cycle and 43% reduction in the ejector exergy losses by an optimized SNPD value.

A comparative study of different transcritical CO_2 ejector cycles has been performed to identify the most efficient one by Taslimi et al. [79].The detail exergy and energy analysis showed that the EERC has the highest COP and exergy efficiency. The amount and location of the irreversibilities within different components of each cycle were also determined and compared to the basic cycle.

An exergy analysis of a one phase ejector was carried out by Khennich et al. [80] for R141b as a refrigerant. An exergy analysis was performed at different sections of a single phase ejector by Croquer et al. [74]. They determined the global ejector efficiency and the main sources of losses.

The effects of ejector component efficiencies on COP and second law performance of EERC were investigated theoretically for a two-phase constant area ejector using the R134a refrigerant [81]. As the ejector component efficiencies increase the COP and exergy efficiency increase while the optimum ejector area ratio (the ratio of the cross-sectional area of the mixing chamber to the motive nozzle exit cross-sectional area) decreases.

Chen et al. [82] employed an advance exergy analysis of an ejector refrigeration system by splitting the exergy destruction into endogenous and exogenous parts for R245fa as the refrigerant. They found that the ejector has the highest exergy destruction compared to other components.

Since the ejector is an important component in the refrigeration and heat pump cycle, in this study, the exergy analysis of a two-phase ejector is carried out at different conditions. Following the concept of the transiting exergy first introduced by Brodyansky et al. [83], Khennich et al. [80] evaluated the transiting exergy efficiencies within different sections of a single phase ejector. The ejectors may work at different operating conditions other than the critical point in double choking or single choking as shown in Figure 5.1. The back pressure that gives the maximum entrainment ratio refers to the critical point. In double choking conditions, both the primary and the secondary flows are choked and the maximum entrainment ratio remains constant while the back pressure decreases. In single choking condition, the secondary flow is not choked and increasing the back pressure results in decreasing the entrainment [84]. In the present paper, the exergetic analysis of a CO_2 two-phase ejector is carried out for the critical point as well as for single and double choking conditions. The effect of the back pressure is investigated on the amount of the exergy losses and the values of two types of performance criteria, namely the transiting exergy efficiency and the Grassmann exergy efficiency.

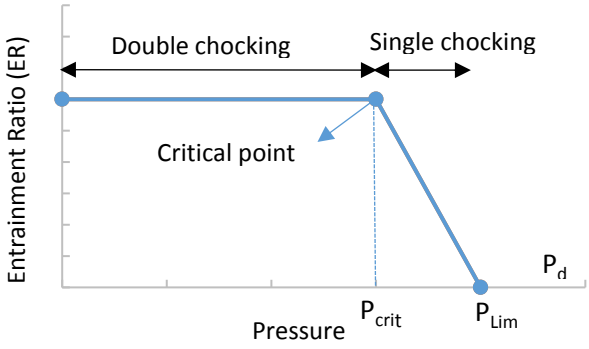

Figure 5.1 Critical mode of an ejector

5.4 Theoretical analysis

A two-phase ejector is employed in an ejector expansion work recovery cycle (EERC) to improve the performance of the cycle by reducing the throttling losses. Figure 5.2 shows the schematic of an ejector used in the cycle. A typical ejector comprises a primary nozzle, a secondary nozzle, a mixing section and a diffuser.

A detailed description of a CO_2 two-phase ejector model for on-design and off-design including both single choking and double chocking conditions is available in [84].

Therefore, a new methodology is employed here to evaluate the exergy efficiency of a two-phase ejector based on the calculation of the transiting exergy through the ejector under different conditions. The ambient temperature is fixed to 20˚C for exergy calculation. The designed dimensions of the ejector are considered for given operating conditions (D_{th}=0.992mm, $L5/D_{mix}$=7.344 and A_{mix}/A_d=0.116).

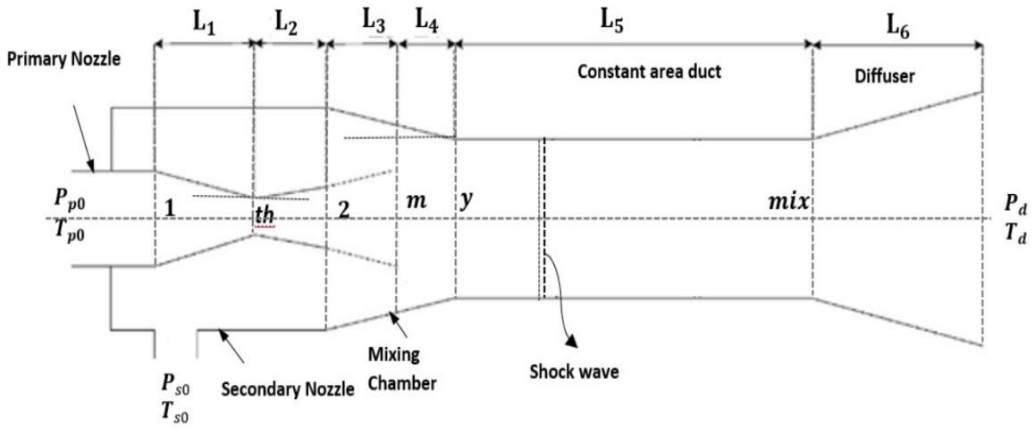

Figure 5.2 Schematic of an ejector with relevant notations

5.4.1 Transiting thermo-mechanical Exergy in a Two-phase ejector

A new definition of exergy efficiency for thermodynamic evaluation of a two-phase ejector is used based on the concept of transiting exergy, introduced by Brodyansky [83] that allows non-ambiguous computation of two thermodynamic metrics: exergy produced and exergy consumed.

$$\eta_{ex,TR} = \frac{E_{out} - E_{tr}}{E_{in} - E_{tr}} = \frac{\Delta E_{out-tr}}{\nabla E_{in-tr}} \tag{5.1}$$

where ΔE and ∇E are exergy produced and consumed in the process, E_{in} ansd E_{out} are the inlet and outlet exergy flows. It should be also mentioned that some authors used a different terminology to express the "exergy produced" and "exergy consumed" in the process. For example, Kotas [85] used "desired output" vs. "necessary input"; Szargut [86] used "exergy of useful products" vs. "feeding exergy", Tsatsaronis [87] and Bejan et al. [88] used "products" vs. "feed".

The difference between the inlet and outlet exergies as well as between the exergy produced and the exergy consumed represents the exergy losses (D).

$$D = \nabla E_{in,tr} - \Delta E_{out,tr} \tag{5.2}$$

The input-output exergy efficiency which was first proposed by Grassmann [89] is defined as follows:

$$\eta_{ex,GR} = \frac{E_{out}}{E_{in}} = 1 - \frac{D}{E_{in}} \tag{5.3}$$

The specific exergy in all states is calculated as:

$$e_k(P,T) = [(h_k + 0.5\,u^2) - h_0) - T_0 \cdot (s_k - s_0)] \tag{5.4}$$

The specific transiting exergy (e_{tr}) is the lowest exergy value of a material stream, which is defined by the pressure and temperature at the inlet and outlet of a system as well as by the ambient temperature T_0. It is illustrated by the following equations:

$$\text{If } (T_{in} > T_0 \text{ and } T_{out} > T_0): E_{tr} = \dot{m}\, e_{tr}(P_{min}, T_{min}, u_{min}) \tag{5.5}$$

$$\text{If } (T_{in} < T_0 \text{ and } T_{out} < T_0): E_{tr} = \dot{m}\, e_{tr}(P_{min}, T_{max}, u_{min}) \tag{5.6}$$

$$\text{If } (T_{in} > T_0 \text{ and } T_{out} < T_0) \text{ OR } (T_{in} < T_0 \text{ and } T_{out} > T_0): E_{tr} = \dot{m}\, e_{tr}(P_{min}, T_0, u_{min}) \tag{5.7}$$

These equations demonstrate that E_{tr} is defined by the minimum values of the pressure and velocity among the inlet and outlet but it is different for temperature based on the processes operating in sub-ambient, sup-ambient or across the ambient temperature.

5.4.2 The Exergy Consumption and Production in a two-phase Ejector

In a two-phase ejector, the primary stream with high pressure (P_{p0}) and temperature ($T_{p0}>T_0$) expands in the primary nozzle into a low pressure and high-velocity stream. This low pressure

entrains a secondary stream at low pressure (P_{s0}) and temperature ($T_{s0}<T_0$) into the mixing section. The two streams exchange momentums and energies inside the mixing section and then the uniform mixture compresses to a higher pressure more than the inlet pressure of the secondary stream ($P_{s0}<P_d<P_{p0}$) and ($T_{so}<T_d<T_0<T_{p0}$). The ejector's performance is evaluated by two parameters: the entrainment ratio ($ER = \dot{m}_s/\dot{m}_p$) defined as the ability to entrain the secondary flow inside the ejector and the pressure ratio ($P_{ratio} = P_d/P_{s0}$), the ability to increase the suction pressure. Figure 5.3 presents the specific exergy-enthalpy diagram for a two-phase ejector.

The e-h diagram shows the expansion of the primary flow and compression of the secondary flow inside the ejector. The primary stream is expanded across T_0 and the secondary stream is compressed at the sub-ambient condition. Eqs. (5.8) and (5.9) are therefore applied to calculate $e_{tr,p}$ and$e_{tr,s}$.

$$e_{tr,p} = e(P_d, T_0) \tag{5.8}$$

$$e_{tr,s} = e(P_{s0}, T_d) \tag{5.9}$$

The total exergies consumed and produced by the primary and secondary flows are obtained by the following equations:

$$\begin{aligned} \nabla E_{p0s0-tr} &= \dot{m}_p\left[e\left(P_{p0}, T_{p0}\right) - e(P_d, T_0)\right] + \dot{m}_s[e(P_{s0}, T_{s0}) - e(P_{s0}, T_d)] \\ &= \dot{m}_p(\nabla e_{P,T}) + \dot{m}_s\,(\nabla e_T)_{P_{s0}} \end{aligned} \tag{5.10}$$

$$\begin{aligned} \Delta E_{d-tr} &= \dot{m}_p[e(P_d, T_d) - e(P_d, T_0)] + \dot{m}_s[e(P_d, T_d) - e(P_{s0}, T_d)] \\ &= \dot{m}_p\,(\Delta e_T)_{P_d} + \dot{m}_s(\Delta e_P)_{T_d} \end{aligned} \tag{5.11}$$

The consumed and produced exergies are linked to both primary and secondary flows. The term ($\nabla e_{P,T}$) in Eq. (5.10) is the decrease of the specific thermo-mechanical exergy due to the expansion process and the temperature drop of the primary flow. The term $(\nabla e_T)_{P_{s0}}$ is the decrease of the specific thermal exergy of the secondary flow due to the temperature rise under sub-environmental conditions and calculated at constant pressure P_{s0}.

The first term of exergy produced, $(\Delta e_T)_{P_d}$ represents the increase of the specific thermal exergy due to the temperature drop of primary flow from T_0 to T_d under constant pressure P_d. The second term represents the increase in mechanical exergy component of the secondary flow due to the pressure rise from P_{s0} to P_d at constant temperature T_d.

The main shortcoming of the Grassmann efficiency is the fact that it cannot reveal the real exergy consumption and production within the process. As an example, $(\nabla e_T)_{P_{s0}}$ represents the exergy consumed due to the temperature rise from T_{s0} to T_d. In fact, this is the partial cold destruction. Because of an important transiting exergy flow, the Grassmann exergy efficiency “does not see” this phenomenon. Meanwhile, the definition based on the concept of transiting exergy allows discovering non-ambiguous computation of exergy consumed and produced and prompts to find the way to recover the amount of the cold destroyed in the ejector.

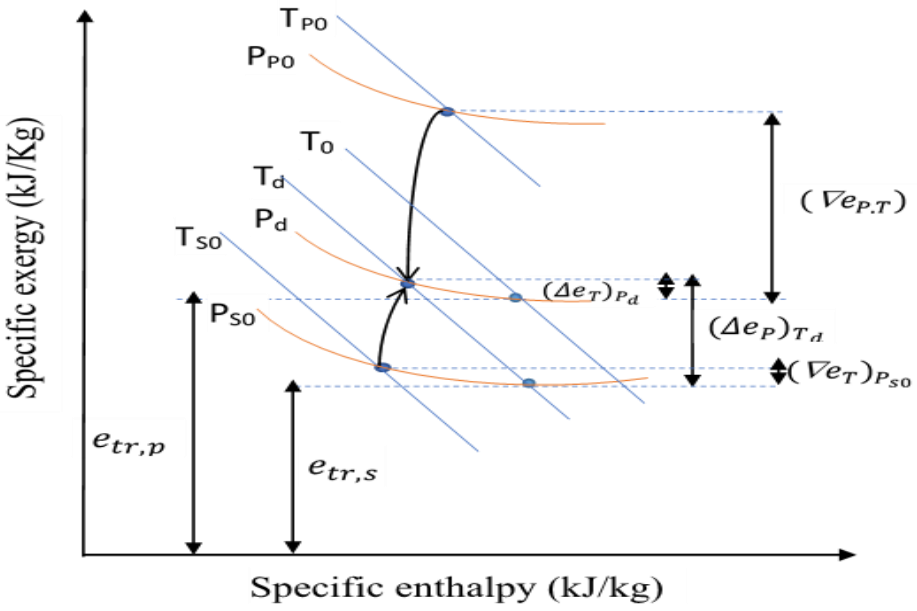

Figure 5.3 Expansion and compression processes on an exergy–enthalpy diagram of a transcritical CO_2 ejector

5.5 Results and discussion

The numerical model for the exergy evaluation of a two-phase CO_2 ejector was developed using the Engineering Equation Solver (EES) software, which combines non-linear equations with thermophysical property functions. This exergy analysis helps to determine the irreversibilities and exergy efficiencies in a two-phase ejector especially when it doesn't work at its design condition.

The calculated parameters of a CO_2 two-phase ejector operating under single choking and double choking conditions, as well as its design condition, are listed in Table 5.1 [84].

The pressures and temperatures of the primary and secondary flows at the inlet are constant for all the cases (P_{p0}=10112 kPa, T_{p0}=39.3˚C, P_{s0}=3952 kPa, T_{s0}=5.5˚C) while the back pressure (diffuser outlet pressure) changes according to the ejector critical conditions.

First row of Table 5.1 refers to the base case, which demonstrates the critical point of the ejector for a fixed geometry. The second row refers to double choking conditions in which the inlet conditions are identical to their design values and the back pressure is lower than its design value. The third row presents the single choking conditions, the part of the performance curve in which ER decreases from its design condition (P_{cr}) to maximum pressure (P_{lim}) (Figure 5.1).

The values of the numerical calculation for double chocking and single chocking conditions are shown in Tables 5.2 and 5.3 respectively. The exergy losses (D), Grassmann exergy efficiency ($\eta_{ex,GR}$) and transiting exergy efficiency ($\eta_{ex,TR}$) are calculated using (5.1-5.3). The first rows refer to the results for the base case (critical or design point).

The corresponding exergy produced and exergy consumed of a two-phase ejector are evaluated as well. The exergy analysis based on both transit and Grassmann definitions are also compared and the effect of ejector's back pressure on the exergy of a two-phase ejector is investigated.

Figure 5.4 also illustrates the variations of the exergy efficiencies and exergy losses within the ejector for various back pressures including critical point, single and double choking conditions.

According to Table 5.2 and Figure 5.4, when the back pressure decreases below the critical pressure, the exergy losses of the ejector increase. The Grassmann exergy efficiency remains approximately constant. The value of $\eta_{ex,GR}$ remains in the range [0.9698;0.9749] (0.5%). While the transiting exergy efficiency ($\eta_{ex,TR}$) decreases by about 5.2 %, $\eta_{ex,TR}$ remains within the range [0.564; 0.595]. The minimum exergy losses (0.34 kW) take place at the critical back pressure (4601 kPa).

The comparison of the Grassmann and transiting exergy efficiencies shows that $\eta_{ex,TR}$ calculated by Eq. (5.1) is lower than the "optimistic" value given by the Grassmann exergy efficiency. This discrepancy is justified by the presence of transiting exergy flow (e_{tr}), which is neglected when using the Grassmann exergy efficiency. This important result indicates the influence of transiting exergy flow (e_{tr}) inside a two-phase ejector.

Table 5.1 Calculated parameters of a CO_2 two-phase ejector for different operating conditions

states	P_d (kPa)	T_d (˚C)	$\dot{m}_p$ (kg/s)	$\dot{m}_s$ (kg/s)	$\dot{m}_d$ (kg/s)	P_{ratio}	ER
Base case (critical point) ($P_d = P_{cr}$)	4601	10.88	0.04225	0.02404	0.06629	1.164	0.568
Double chocking ($P_d < P_{cr}$)	4580	10.61	0.04225	0.02404	0.06629	1.159	0.568
	4520	10.08	0.04225	0.02404	0.06629	1.144	0.568
	4480	9.718	0.04225	0.02404	0.06629	1.134	0.568
	4420	9.162	0.04225	0.02404	0.06629	1.118	0.568
Single choking ($P_d > P_{cr}$)	4730	12.01	0.04225	0.02277	0.06502	1.197	0.539
	4811	12.7	0.04225	0.02106	0.06331	1.217	0.4985
	4939	13.77	0.04225	0.0172	0.05945	1.250	0.4071
	5002	14.3	0.04225	0.01481	0.05706	1.266	0.3505
	5097	15.08	0.04225	0.01083	0.05308	1.290	0.2564
	5198	15.89	0.04225	0.00636	0.04861	1.315	0.1505

Another important result derived from the transiting exergy calculation reveals that the exergy produced (11) increases by decreasing the back pressure while according to the Grassmann exergy definition, the outlet exergy of the ejector stays almost constant. However, the increase in exergy production (ΔE) is surpassed by the increase in exergy consumption (∇E). As a result $\eta_{ex,TR}$ decreases.

Table 5.3 illustrates the variations of exergy losses, $\eta_{ex,\,TR}$ and $\eta_{ex,GR}$ for various back pressures in single choking conditions. It may observe that the transiting exergy efficiency increases slowly from 0.595 to 0.609 (about 2%) with increasing the back pressure from 4601 kPa (critical point) to 4730 kPa and then decrease to about 47% when the back pressures increases to 5198 kPa. The same justification as the previous part holds. Since both exergy consumed and exergy produced decrease by increasing the back pressure, the decrease in exergy consumption (∇E) is surpassed by the decrease in exergy production (ΔE) which results in reducing the exergy efficiency ($\eta_{ex,TR}$). The results also show a minimum value for the exergy losses. The exergy losses decrease from its design value, 0.34 kW to 0.28 kW (17%) and then increase to the value of 0.32 kW when the back pressure increase to a pressure close to its limited pressure (P_{lim}) 5198 kPa. However, its value is still lower than that of the critical point.

The comparison of the exergy losses, ($\eta_{ex,TR}$) and ($\eta_{ex,GR}$) for three different cases (single choking, critical point and double choking) are presented in Figure 5.5. Two important observations can be made from these results. First is that the maximum value of $\eta_{ex,TR}$ is obtained at ejector critical point although the exergy losses are higher at this point compared to the single choking mode.

Table 5.2 Exergy metrics of a two-phase ejector for double choking conditions and different back pressures P_d ($P_d < P_{cr}$)

	Transiting exergy calculation					Grassmann exergy calculation		
Back Pressure (P_d, kPa)	Exergy consumed (∇E, kW)	Exergy Produced (ΔE, kW)	Exergy Losses (D, kW)	Transiting Exergy (E^{tr}, kW)	Exergy Efficiency ($\eta_{ex,TR}$)	Exergy Efficiency ($\eta_{ex,GR}$)	Inlet Exergy (EX_{in},kW)	Outlet Exergy (EX_{out}, kW)
4601	0.8394	0.4998	0.3397	12.718	0.5954	0.9749	13.56	13.22
4580	0.8524	0.5066	0.3458	12.705	0.5943	0.9745	13.56	13.21
4520	0.8847	0.5195	0.3653	12.673	0.5871	0.9731	13.56	13.19
4480	0.9068	0.5221	0.3847	12.65	0.5758	0.9716	13.56	13.17
4420	0.9405	0.5304	0.4101	12.617	0.564	0.9698	13.56	13.15

Table 5.3 Exergy metrics of a two-phase ejector for single choking conditions and different back pressures P_d ($P_d > P_{cr}$) and entrainment ratios.

	Transit exergy calculation					Grassmann exergy calculation		
Back Pressure (P_d, kPa)	Exergy consumed (∇E, kW)	Exergy Produced (ΔE, kW)	Exergy Losses (D, kW)	Transiting Exergy (E^{tr}, kW)	Exergy Efficiency ($\eta_{ex,TR}$)	Exergy Efficiency ($\eta_{ex,GR}$)	Inlet Exergy (E_{in}, kW)	Outlet Exergy (E_{out}, kW)
4601	0.8394	0.4998	0.3397	12.718	0.5954	0.9749	13.56	13.22
4730	0.7628	0.4649	0.2979	12.551	0.6094	0.9776	13.31	13.02
4811	0.7113	0.4262	0.2851	12.276	0.5992	0.978	12.99	12.7
4939	0.6293	0.3481	0.2812	11.618	0.5532	0.977	12.25	11.97
5002	0.5895	0.297	0.2925	11.2	0.5038	0.9752	11.79	11.5
5097	0.533	0.2285	0.3045	10.495	0.4287	0.9724	11.03	10.72
5198	0.4788	0.1551	0.3238	9.693	0.3238	0.9682	10.17	9.848

It is important because the design of the ejectors are usually conducted according to the critical point conditions, what leads to a maximum in transiting exergy efficiency, not a minimum of exergy losses. This is due to the fact that maximum value $\eta_{ex,TR}$ establishes an optimal trade-off between the realization of the ejector's technical purpose (to achieve maximum compression for a given entrainment ratio) and exergy losses. The second observation is that the Grassmann exergy efficiency does not change with the critical pressure variation, because of important transiting exergy flow. It means that $\eta_{ex,GR}$ is not the appropriate criterion to evaluate the exergy efficiency of a two-phase ejector.

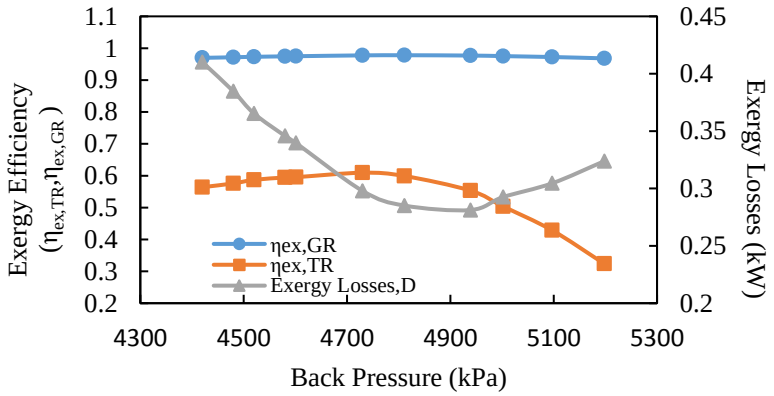

Figure 5.4 Variations of exergy losses; transiting exergy efficiency and Grassmann exergy efficiency of the ejector with the back pressure

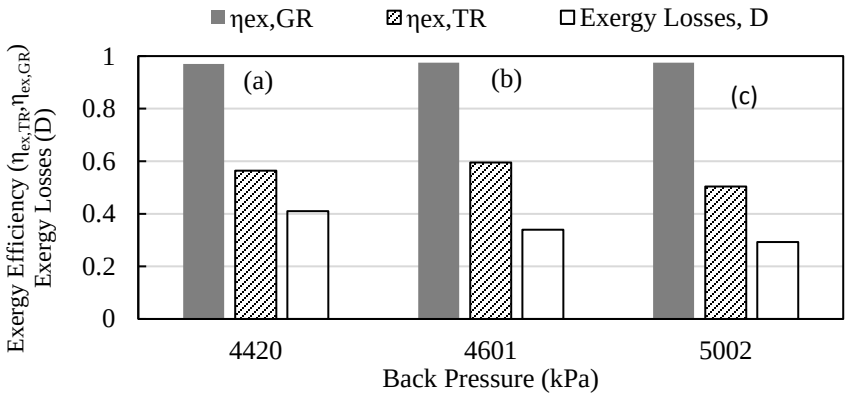

Figure 5.5 Exergy losses, transiting exergy efficiency, Grassmann exergy efficiency of the ejector for different conditions: (a) single choking; (b) critical point; (c) double choking

5.6 Conclusion

An exergy analysis based on the transiting exergy was employed to evaluate the exergy losses and exergy efficiency of a CO_2 two-phase ejector at its critical point as well as under double choking and single choking conditions. The results are compared with the conventional Grassmann exergy analysis.

This application provides the evaluation of exergy losses as well as useful exergy production in the ejector. Two thermodynamically important metrics, exergy produced and exergy consumed are obtained for different ejector working conditions. There is a compromise between exergy losses and useful exergy produced in the ejector to indicate its performance, which cannot be derived from the Grassmann exergy analysis. The Grassmann exergy efficiency is not an appropriate criterion for exergy evaluation of a two-phase ejector.

The ejector back pressure has an important effect on the transiting exergy efficiency and exergy losses. The transiting exergy efficiency achieves the maximum value at the critical pressure corresponding to the critical point, it confirms a well-known heuristics, to design ejectors according to the conditions of the critical point.

5.7 Acknowledgments

This project is a part of the Collaborative Research and Development (CRD) Grants Program at "Université de Sherbrooke". The authors acknowledge the support of the Natural Sciences and Engineering Research Council of Canada, Hydro-Québec, Rio Tinto Alcan and Canmet ENERGY Research Center of Natural Resources Canada (RDCPJ451917-13).

5.8 Nomenclature

A	Cross section area, mm^2	**Greek symbols**	
D	Diameter, mm	η	efficiency
E	Exergy, kW	∇	Consumption
e	Specific exergy, kJ kg^{-1}	Δ	Production
ER	Entrainment ratio	**Subscripts and superscripts**	
h	Specific enthalpy, kJ kg^{-1}	0	Ambient state
L	Length, m	crit	critical
$\dot{m}$	Mass flow rate, kg s^{-1}	d	Diffuser outlet
P	Pressure, kPa	lim	Limiting
P_d	Back pressure (discharge pressure), kPa	mix	mixing
P_{ratio}	Pressure ratio (pressure lift)	out	Outlet
s	Specific entropy, kJ kg^{-1} K^{-1}	p	Primary
T	Temperature, K	s	Secondary
u	Mean axial velocity, m s^{-1}	th	Ejector throat

CHAPTER 6

PERFORMANCE INVESTIGATION OF A TWO-PHASE TRANSCRITICAL CO_2 EJECTOR HEAT PUMP SYSTEM

6.1 Avant-propos

Auteurs et affiliation:

- Sahar Taslimi Taleghani: étudiante au doctorat, Université de Sherbrooke, Faculté de génie, Département de génie mécanique
- Mikhail Sorin: professeur, Université de Sherbrooke, Faculté de génie, Département de génie mécanique
- Sébastien Poncet: professeur, Université de Sherbrooke, Faculté de génie, Département de génie mécanique
- Hakim Nesreddine: PhD, Chercheur-Chargé de projet, Laboratoire des technologies de l'énergie, Shawinigan (Québec), Canada

Date d'acceptation: 5 Février 2019

État de l'acceptation: version finale publiée

Revue: Energy Conversion and Management

Titre français: Étude des performances d'un système de pompe à chaleur à éjecteur au CO_2 transcritique diphasique

Contribution au document: Cet article contribue à la thèse en développant un modèle de simulation détaillé d'un système de pompe à chaleur à éjecteur au CO_2 transcritique afin de prédire les performances du système.

Résumé en français:

Cette étude des performances thermodynamiques d'un cycle de pompe à chaleur à éjecteur au CO_2 transcritique présente une analyse numérique avec pour contrainte une surface de transfert de chaleur totale constante. Un modèle de pompe à chaleur au CO_2 validé expérimentalement et un modèle d'éjecteur diphasique sont combinés pour réaliser l'étude. Les effets de certains paramètres sur les performances du système sont examinés: les conditions de fonctionnement déterminées par les pressions au refroidisseur à gaz et à l'évaporateur; paramètres de conception de l'éjecteur, y compris le diamètre primaire de la gorge, le rapport de surface efficace et le diamètre de sortie du diffuseur; la conception du système telle que définie par le rapport de la surface de transfert de

chaleur. Les résultats de cette analyse permettent de spécifier la plage optimale pour les paramètres de conception afin de maximiser le COP et la capacité de chauffage de la pompe à chaleur. Il a été démontré que le rapport de surface de transfert de chaleur a des effets importants sur le COP et la capacité de chauffage, ainsi que sur la pression optimale du refroidisseur à gaz. Lorsque le rapport de la surface de transfert de chaleur augmente, le COP et la capacité de chauffage augmentent également, tandis que la pression optimale du refroidisseur à gaz diminue. Avec des géométries d'éjecteur et des conditions de fonctionnement données, cette optimisation peut augmenter le COP et la capacité de chauffage de la pompe à chaleur à éjecteur d'environ 17% et 20% respectivement en augmentant le rapport de la surface de transfert de chaleur.

6.2 Abstract

This study of the thermodynamic performance of a transcritical CO_2 ejector heat pump cycle presents a numerical analysis under the constraint of constant total heat transfer area. An experimentally validated model of a CO_2 heat pump system and a model of a two-phase ejector are combined to perform the study. The effects of chosen parameters on system performance are investigated: operating conditions as determined by the gas cooler and evaporator pressures; ejector design parameters including the primary throat diameter, effective area ratio, and diffuser outlet diameter; system design as defined by the heat transfer area ratio. The results of this analysis allow specifying the optimal range for the design parameters in order to maximize the COP and the heating capacity of the heat pump. The heat transfer area ratio is shown to have important effects on the COP and heating capacity as well as the optimal gas cooler pressure. As the heat transfer area ratio increases, COP and heating capacity increase as well, while the optimum gas cooler pressure decreases. At given ejector geometries and operating conditions, this optimization can increase the COP and heating capacity of the ejector heat pump by approximately 17% and 20% respectively by increasing the heat transfer area ratio.

6.3 Introduction

Carbon dioxide, CO_2, is an appropriate replacement for conventional refrigerants due to its minimal impact on climate change. Since CO_2 can operate in a transcritical state, CO_2 heat pumps can work at a higher pressure than most other refrigerants. It has the advantages of high vapor density and high volumetric heating capacity such that a smaller volume of CO_2 can be used to achieve the same heating capacity as compared to other refrigerants.

Unlike subcritical heat pump systems, heat rejection in a CO_2 transcritical cycle is a cooling process that follows a temperature glide, increasing the performance and heat capacity of the system [4], [90]. However, a transcritical CO_2 compression cycle has a lower thermodynamic performance than a subcritical cycle. This is due to the large expansion losses of the isenthalpic throttling process, which occurs as the refrigerant passes from a supercritical to a subcritical state. Among different devices for expansion work recovery, the ejector is a favorable device that enables the use of CO2 and other environmentally friendly refrigerants. An ejector can help to reduce losses by recovering part of the expansion work in the throttling process, and it can improve the cycle’s efficiency [6], [16], [50], [78].

A comparative study by Taslimi et al. [79] of different transcritical CO_2 ejector cycles was performed to identify the most efficient cycle. The detailed exergy and energy analysis showed that the ejector expansion recovery cycle (EERC) has the highest COP and exergy efficiency. This cycle is the most typical layout of the two-phase ejector cycles. Li and Groll [7] and Deng et al. [8] theoretically investigated an ejector in a transcritical CO_2 cooling cycle. Li and Groll [7] employed a two-phase ejector model for a transcritical CO_2 air-conditioning system and reported a COP improvement of up to 16%. Deng et al. [8] showed that the maximum cooling COP in the ejector expansion cycle was up to 22% better than that of the conventional vapor compression cycle respectively. Elbel [11] reported COP and cooling capacity improvements by up to 7% and 8% respectively, by using an ejector. Banasiak et al. [91] performed an experimental and numerical investigation for a small capacity CO_2 ejector heat pump and reported a maximum increase in COP of 8% compared to a conventional expansion valve system. Zhu et al. [92] experimentally investigated the performance of a transcritical CO_2 ejector heat pump water heater system and reported 10.3% COP improvement over the corresponding basic cycle.

In a transcritical cycle, gas cooler pressure has a significant effect on COP. There is an optimum pressure that maximizes the COP of the system [16], [93], [94]. Therefore, the control of gas cooler pressure is important to get optimal system performance. In an ejector cycle, the gas cooler pressure can be controlled with an adjustable throat area of the primary nozzle, because the primary mass flow rate is proportional to the throat area of the nozzle [38].

Furthermore, it is very important for an ejector system that the ejector works in its critical condition, for which it was designed. For a fixed geometry and constant ejector input conditions, the maximum back pressure that gives the maximum entrainment ratio defines the critical condition (double chocking)[84], [95]. Since a fixed ejector geometry has to work under restricted operating conditions to keep the positive effect (critical condition) of the ejector [94], it is not possible to control the high-side pressure and recover the cycle effectively by a fixed ejector geometry [96]. Therefore, an adjustable geometry ejector is proposed to improve the transcritical CO_2 cycle.

According to the literature review, there are two approaches for controlling ejector operation [96]. The first approach is by using a multi-ejector system in which multiple fixed geometry ejectors work in parallel. The second approach is by using a controllable geometry ejector with a needle [96]–[98]. There are two control options for the ejector expansion device in this approach [97], [99]. First, the primary nozzle throat area is adjustable by using a needle in the nozzle via a thread mechanism. Second, the primary nozzle exit position in the mixing chamber thus the secondary nozzle throat area can be adjustable through a thread mechanism [99]. Therefore, the ejector is able to work at its design conditions (double choking) by these two control options which are directly related to the primary nozzle and secondary nozzle throat areas.

He et al. [100] designed an optimal controller for an adjustable ejector with variable nozzle throat area using a dynamic model to increase the performance of a transcritical CO_2 ejector refrigeration system. Chen et al. [101] experimentally investigated a CO_2 heat pump water heater using an adjustable nozzle throat of the ejector and concluded that optimal conditions can be maintained by using an adjustable ejector. The experimental studies of Liu et al. [99], [102] presented the optimization of a CO_2 air conditioner system based on ejector geometries and compressor frequency under specified outdoor and indoor air temperatures and showed that the performance

of a CO_2 air conditioner was improved through nozzle throat adjustment. The experimental study of Bilir Sag and Ersoy [103] on the R134a showed that the maximum COP of the ejector system was achieved by changing the primary nozzle throat area. The COP at optimal points was determined 5-13% higher than a conventional cycle. Liu et al. [104] developed an analytical model to study an air-to-air controllable ejector expansion CO_2 air conditioning system, considering critical flow and the variation of ejector efficiencies. Compared to a conventional expansion valve system, their results showed an improvement of 30.7% and 32.1% respectively in COP and the cooling capacity for particular ejector geometries and an outdoor temperature of 37.8˚C. Xu et al. [105] used an adjustable ejector to experimentally investigate the performance of a transcritical CO_2 heat pump system, aiming for the optimum high-side pressure control. The experiments were performed by varying the primary nozzle throat area at different cooling water flow rates. The results showed the maximal values for COP and heat capacity with increasing high-side pressure. However, according to the ejector model used in their simulation, the ejector critical conditions are not included in their work.

There are still limited comprehensive theoretical analyses of the ejector expansion CO_2 transcritical cycle, especially when an ejector model intended for deas sign purposes is used in the system. Most of the works are limited to off-design conditions [16], [105]. Furthermore, most of the previous studies have investigated the performance enhancement of the transcritical CO_2 cycles based on constant heat transfer coefficients to simplify their theoretical model. However, heat transfer coefficient could be affected by heat exchanger geometries and operating conditions [106].

Since ejectors have better performance at their design conditions [107], and heat transfer coefficients vary under different operating conditions, the objectives of this paper are defined as follows:

(a) To develop a comprehensive simulation model for a two-phase transcritical CO_2 ejector heat pump system based on ejector design conditions (double choking condition).

(b) To investigate the effect of heat exchanger areas on the system performance, under the constraint of constant overall heat transfer area.

(c) To define optimal operating conditions corresponding to maximum COP in order to determine optimal design of a transcritical CO_2 cycle.

(d) To numerically investigate the effects of chosen ejector design parameters on the performance of a two-phase transcritical CO_2 ejector heat pump system.

First, a system model of a transcritical CO_2 heat pump cycle with plate heat exchangers for both the gas cooler and the evaporator is developed and experimentally validated.

Second, a two-phase ejector design model in which the ejector works at its critical condition is integrated within the system model. The goal is to evaluate the system's performance.

Third, a parametric analysis is conducted to evaluate the effects of heat transfer areas, ejector characteristics and operating conditions on system performance. In this study, system performance will refer to the COP and heating capacity of the heat pump system. An engineering equation solver (EES) [108] program is used to solve the developed models.

It should be mentioned that most experimental and theoretical studies on CO_2 transcritical cycles are based on the application of tube-in-tube or other types of heat exchangers. To the best of the authors' knowledge, little information is available on the application of plate heat exchangers for the CO_2 ejector transcritical cycle, and no investigations of the effect of heat transfer area ratios on COP improvement have yet been published. In this study, plate type heat exchangers with different lengths are used for the gas cooler and evaporator to identify the impact of the heat transfer areas on the system performance.

6.4 Experimental set-up

A prototype transcritical CO_2 heat pump system with a heating capacity of 25 kW was used to run the experiments and validate the system model. The test bench corresponds to the model EcoCute Geo 25 of Italian company Enex s.r.l and is currently available in the Hydro Québec's energy technologies laboratory (LTE) in Shawinigan. Figure 6.1 shows the schematic of the experimental set-up. Two plate type heat exchangers were used for the gas cooler and evaporator. A 50%-50% water/glycol mixture was used as heat sink and heat source on the gas cooler and evaporator sides respectively. Hereafter, this fluid mixture will be referred to simply as the 'glycol' or 'external fluid'. The compressor was a Dorin CO_2 single-stage semi-hermetic model (TCS 350/4-D), with a theoretical swept volume of 5.2 m^3/h. The experiments were conducted at given heat exchanger inlet temperatures and mass flow rates for the external fluids. T-type thermocouples with an accuracy of 0.5˚C were used to measure temperatures of CO_2 and glycol. The pressure transducers had an uncertainty 0.6% full scale. The CO_2 mass flow rate was measured by Coriolis mass flow meter (Optimass 6400) with an accuracy of ±0.10% flat for liquid and ±0.35% flat for gas. The glycol flow rates in the gas cooler and evaporator were measured with Turbine flow meters F1110 series, with an accuracy of ±0.5% of the reading value. The electrical power consumption was evaluated using AC watt transducers (PC5 Series) with an accuracy ±0. 1 kW.

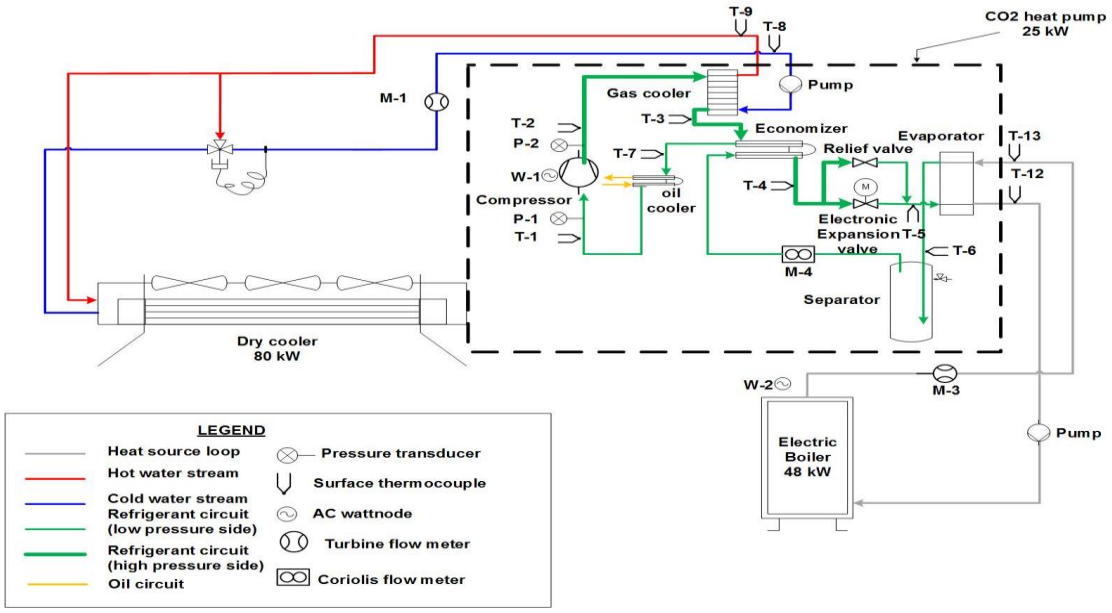

Figure 6.1 Schematic of CO_2 heat pump set-up

6.5 Modeling of the heat pump with plate heat exchangers

The schematic of a basic transcritical CO_2 cycle is shown in Figure 6.2a. Figure 6.2b, c will be discussed in section 4, on ejector integration. In a basic cycle, the subcritical CO_2 vapor at point 1 is compressed in the compressor to a supercritical condition at point 2. The supercritical CO_2 is then cooled in a gas cooler to point 3. After the gas cooler, it is expanded through the throttling valve to the inlet of the evaporator, at point 4. Heat absorption takes place in an evaporator from point 4 to point 1.

The simulation model of the heat pump accounts for the geometries of plate heat exchangers and the compressor. It is based on the energy balance, conservation equations and real properties of the refrigerant. The expansion process is assumed isenthalpic.

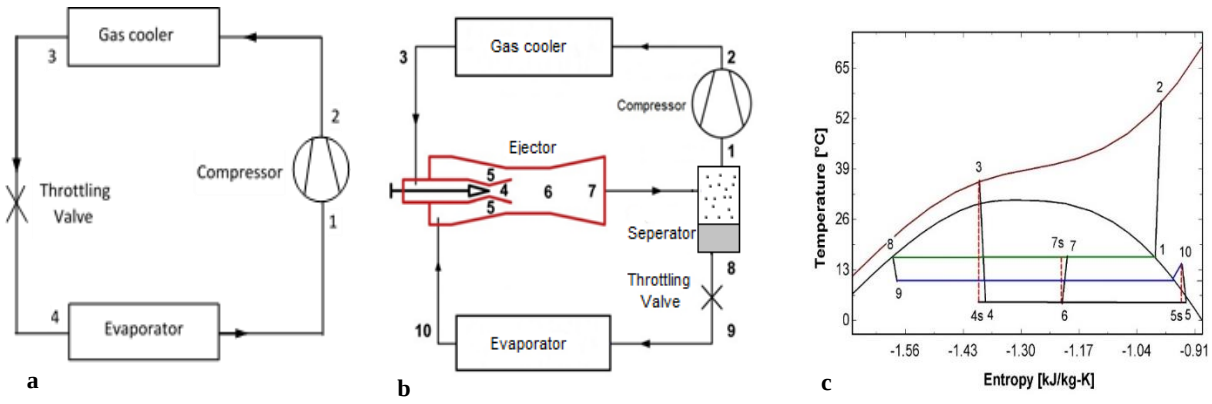

Figure 6.2 a) Basic transcritical CO_2 cycle, b) Transcritical CO_2 ejector cycle, c) Corresponding temperature-specific entropy diagram of the ejector cycle

6.5.1 Compressor model

The compressor model is based on the measured performance of a prototype semi-hermetic carbon dioxide compressor with varying isentropic and volumetric efficiencies based on operating conditions and the equations determined by the manufacturer. The mass flow rate of refrigerant CO_2 is obtained as follows:

$$\dot{m}_{CO_2} = \rho_{comp,in} * \frac{\dot{V}_{pistons}}{3600} * \eta_{vol} \tag{6.1}$$

where $\dot{m}_{CO_2}$ is the mass flow rate of the refrigerant, $\rho_{comp,in}$ is the density at compressor inlet, $\dot{V}_{pistons}$ is the compressor volume swept and η_{vol} is the volumetric efficiency, which is determined from the equation provided by the manufacturer.

6.5.2 Heat exchanger models

The gas cooler and evaporator are modeled as a counterflow plate heat exchangers and based on their actual geometries. Both heat exchangers were simulated using segment-by segment models. The models are based on LMTD methods for counterflow plate heat exchangers. The pressure losses across the gas cooler and evaporator were negligible. The heat transfer coefficient of single-

phase flow in the gas cooler is calculated by the Kim Correlation [109]. This correlation is used for both refrigerant and external fluid (glycol) sides.

$$\mathrm{Nu_{sp}} = 0.05\ \mathrm{Re}^{0.95}\mathrm{Pr}^{1/3} \qquad \text{for } 600 < \mathrm{Re} < 2300 \tag{6.2}$$

Kumar correlation is used for flow of the glycol side in the evaporator [110].

$$\mathrm{Nu_{sp}} = \mathrm{C_1}\mathrm{Re}^{\mathrm{m}}\mathrm{Pr}^{1/3}\,(\mu/\mu_{\mathrm{w}})^{0.17} \tag{6.3}$$

where $\mathrm{C_1}$ and m are constant parameters given according to plate chevron angle and Reynolds number.

The correlations proposed by Martin [111] and Danilova [112] are used for single-phase and two-phase refrigerant side in the evaporator respectively.

$$\mathrm{Nu_{sp}} = 0.122\ \mathrm{Pr}^{1/3}\,(\mu/\mu_{\mathrm{w}})^{1/6}\,[\xi\ \mathrm{Re}^2\sin(2\varphi)]^{0.374} \tag{6.4}$$

where ξ and φ are the friction factor and chevron angle respectively.

$$\mathrm{Nu_{tp}} = 3\ \mathrm{Re_v^{0.3}Bd^{0.33}} \qquad 0.025 < \mathrm{Re}^* < 0.25 \tag{6.5}$$

$$\mathrm{Nu_{tp}} = 4.2\ \mathrm{Re_v^{0.3}Bd^{0.33}Re}^{*0.2} \qquad 0.25 < \mathrm{Re}^* < 2.5 \tag{6.6}$$

where $\mathrm{Re}^* = \mathrm{Bo\ Re_l}$, Bd is the Bond number, Bo is the boiling number and $\mathrm{Re_l}$ and $\mathrm{Re_v}$ are Reynolds numbers of liquid and vapor phases respectively.

In the heat exchanger models, the refrigerant inlet variables for the gas cooler and evaporator are assumed equal to the outlet variables of the compressor and expansion valve respectively. Therefore, CO_2 inlet temperature, pressure and mass flow rates are known. The inlet temperatures and mass flow rate of the external fluids are also known, while the outlet temperatures of CO_2, glycol and heat capacities are unknown. Table 6.1 illustrates the characteristics of heat exchangers used in the simulation.

6.5.3 Experimental validation

Hereafter, the performances of transcritical CO_2 heat pump system are evaluated by two parameters: Heating capacity (Q_h) and coefficient of performance (COP_h). The heating capacity of the refrigerant side is calculated by:

$$\mathrm{Q_h} = \dot{\mathrm{m}}_{\mathrm{gc}}\left(\mathrm{h_{out,gc}} - \mathrm{h_{in,gc}}\right) \tag{6.7}$$

The heating coefficient of performance ($\mathrm{COP_h}$) is obtained using:

$$\mathrm{COP_h} = \frac{\mathrm{Q_h}}{\mathrm{W_{comp}}} \tag{6.8}$$

where $\mathrm{W_{comp}}$ is the compressor work.

Table 6.1 Characteristics of the heat exchangers

Component	Type	characteristics
Gas cooler	Plate type	Total number of plates: 45 vertical port distance (plate length): 390 mm Horizontal port distance: 115 mm Effective channel width: 90 mm Number of passes: 2 Plate thickness: 0.5 mm Enlargement factor: 1.17
Evaporator	Plate type	Total number of plates: 29 vertical port distance (plate length): 500 mm Horizontal port distance: 125 mm Effective channel width: 75 mm Number of passes: 2 Plate thickness: 0.2 mm Enlargement factor:1.17

In this study, the inlet temperatures and mass flow rates of the external fluid at the evaporator and gas cooler are independent parameters, which are fixed at the beginning of the experiments. The inlet temperatures of the external fluid at the evaporator and gas cooler are set on two different PID controllers, while the mass flow rates through both the evaporator and gas cooler are manually controlled by means of throttling valves. Table 6.2 shows independent variables and their associated dependent ones used as the experimental and simulation operating conditions of the heat pump. The heat pump simulation model is validated by a comparison between the simulation and experiment results. Figure 6.3 shows that the simulation model predicts the COP_h within ±5% of the measured COP_h and the heating capacity within ±3% of the measured heating capacity. Based on the accuracies of the measurement instruments given in section 2 and the experimental results, the uncertainties of COP_h and heating capacity can be calculated. The measurement uncertainties for the heating capacities and COPs were ±0.4 kW and ±0.15, respectively.

Table 6.2 Experimental and simulation operating conditions of the heat pump

Cases	$T_{gc,in,ex}$ (˚C)	$T_{ev,in,ex}$ (˚C)	P_{gc} (kPa)	P_{ev} (kPa)	$\dot{m}_{gc,ex}$ (kg/s)	$\dot{m}_{ev,ex}$ (kg/s)	$\dot{m}_{CO2}$ (kg/s)
1	18.04	27.39	10621.69	2780.36	0.081	0.764	0.058
2	24.47	18.34	10615.86	2665.51	0.086	0.604	0.054
3	22.05	27.09	10698.89	2701.24	0.086	0.763	0.055
4	21.81	21.58	10501.73	2675.69	0.087	0.755	0.055
5	19.18	12.83	9919.73	2597.37	0.085	0.751	0.055
6	15.83	17.69	9862.84	2601.32	0.083	0.745	0.055
7	12.43	17.77	10094.63	2736.76	0.074	0.745	0.060
8	12.50	17.65	10668.26	2762.26	0.063	0.744	0.058
9	18.86	17.77	11222.70	2984.54	0.208	0.741	0.067
10	18.65	18.01	11341.68	3052.54	0.208	0.741	0.070
11	18.78	18.19	11134.95	3017.43	0.291	0.738	0.069

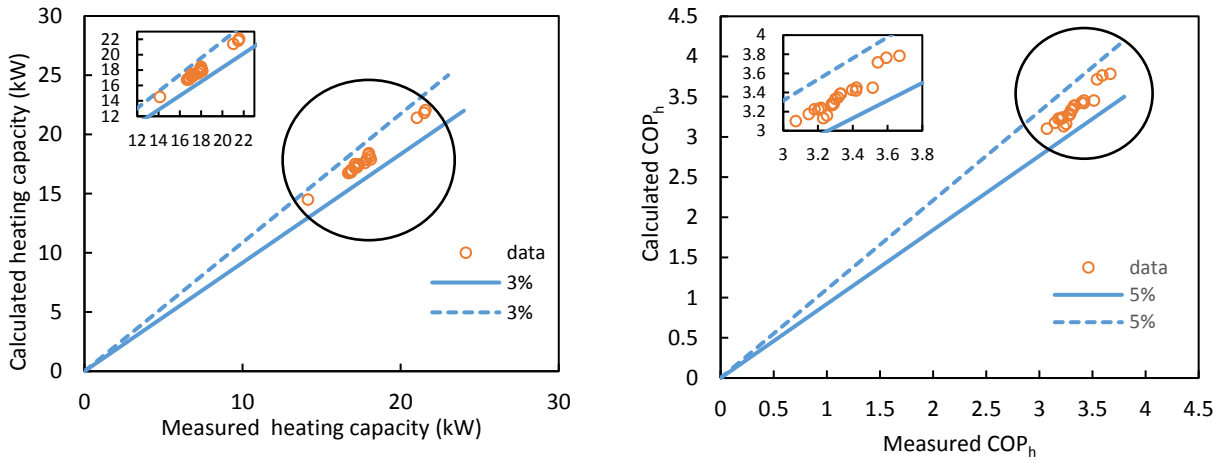

Figure 6.3 Comparison between predicted and measured COP_h and heating capacity of the transcritical CO_2 heat pump

6.6 Ejector integration

In an ejector expansion recovery cycle, the expansion valve is replaced by a two-phase ejector to reduce the throttling losses. It consists of a two-phase ejector, a separator, a compressor, an expansion valve, a gas cooler and an evaporator.

As shown in Figure 6.2b, c, the subcritical CO_2 exiting the vapor port of the separator (state 1) is compressed to supercritical state at high pressure and temperature (state 2). It releases heat in the gas cooler (state 3). After the gas cooler exit, the stream enters the ejector primary nozzle and expands after exiting the primary nozzle as it enters the mixing chamber (state 4). The secondary vapor stream accelerates into the mixing section (state 5). The mixture (state 6) then flows through the diffuser where it is compressed before entering the separator (state 7). The vapor portion of the two-phase flow returns to the compressor, whereas the liquid portion is reduced in pressure through the metering valve before entering the evaporator. The CO_2 absorbs heat in the evaporator before it enters the ejector.

6.6.1 Ejector model

A two-phase ejector is employed in an ejector expansion work recovery cycle (EERC) to improve the performance of the cycle by reducing the throttling losses. A two-phase ejector model is incorporated with the existing compressor and heat exchanger models into an ejector heat pump simulation model.

Figure 6.4 shows the schematic of an ejector used in the cycle. A typical ejector comprises a primary nozzle, a secondary nozzle, a mixing chamber and a diffuser.

Unlike most previous works [16], the ejector model used in this study is developed based on its design or critical condition. It is assumed that the primary flow expands after exiting primary nozzle and creates a hypothetical throat (effective area) for the secondary flow, downstream of the primary nozzle exit, where the secondary flow reaches sonic velocity and chokes inside the mixing chamber

(cross section "sm") [23], [84]. After the choking of the secondary flow, the mixing of two streams starts and completes before the inlet of constant area duct, in which a normal shock wave takes place.

Some of the important assumptions used in the ejector model are:

- Flow is one dimensional, adiabatic and steady state throughout the ejector;
- The homogeneous equilibrium model is assumed for two-phase flow.
- The real fluid properties are used for CO_2 thermodynamic and transport properties;
- The stagnation conditions are considered at both primary and secondary inlets;
- Constant polytropic efficiency coefficients are used to account for friction losses in the nozzles and the diffuser;
- The friction losses in the mixing chamber are negligible, however a friction factor is calculated for constant area duct.
- Mass flux maximization criterion is used for both nozzles.
- Both primary and secondary flows are choked at design condition (double choking) [113], [114].
- A normal shock wave takes place at the inlet of constant area duct.

A detailed description of a CO_2 two-phase ejector model for on-design and off-design, including both single choking and double choking conditions, is available in the authors' previous work [84]. In all calculations, constant polytropic efficiency coefficients are used to account for friction losses in the nozzles and the diffuser ($\eta_{pol,p}$ = 0.9, $\eta_{pol,s}$ = 0.9, $\eta_{pol,d}$ = 0.8). The effects of polytropic efficiencies on the dimensions of a two-phase ejector as well as corresponding isentropic efficiencies are summarized in the authors' previous work [84]. The concept of polytropic efficiency was first introduced by Galanis and Sorin [33] for single-phase ejectors working with perfect gases. It was later used successfully for real gases by other researchers [21], [34], [35]. The polytropic efficiency coefficient is obtained as the isentropic efficiency of an elemental process and takes into account the effect of pressure ratio on the entropy increase during expansion and compression processes. The selected values in this work are in the ranges determined by Zheng and Deng [115] for a CO_2 two-phase ejector in their combined experimental and theoretical study. These values are also used in other works for CO_2 two-phase ejectors [30], [32], [81], [116].

In this study, the diameter of the constant area duct is fixed to 4 mm based on the results of our simulation model. This value is less than the calculated diameter of the cross section "m" in the simulation. The length of the constant area duct is fixed to 32 mm to satisfy the fully developed flow based on the former works [18], [65], [98], [99]. The diffuser outlet diameter is assumed to be 8.94 mm (A_{mix}/A_d=0.2), which corresponds to an optimum value as pointed out by Liu et al. [98], and Banasiak et al. [117].

The primary nozzle throat diameter changes between 1.1 to 2.6 mm, according to different operating conditions based on the mass flow rates and choking conditions of the primary flow in the nozzle throat.

Two common parameters are used to evaluate the ejector's performance: the ability to entrain the secondary flow inside the ejector, defined as the entrainment ratio ($ER = \dot{m}_s/\dot{m}_p$); the ability to increase the suction pressure, known as the pressure ratio ($P_{ratio} = P_d/P_s$). The ejector efficiency is defined as the amount of expansion work recovery divided by the maximum amount that could be recovered [27].

$$\eta_{ejec} = \frac{W_{rec}}{W_{rec,max}} = ER\left[\frac{h(P_d, s_s) - h_s}{h_p - h(P_d, s_p)}\right] \tag{6.9}$$

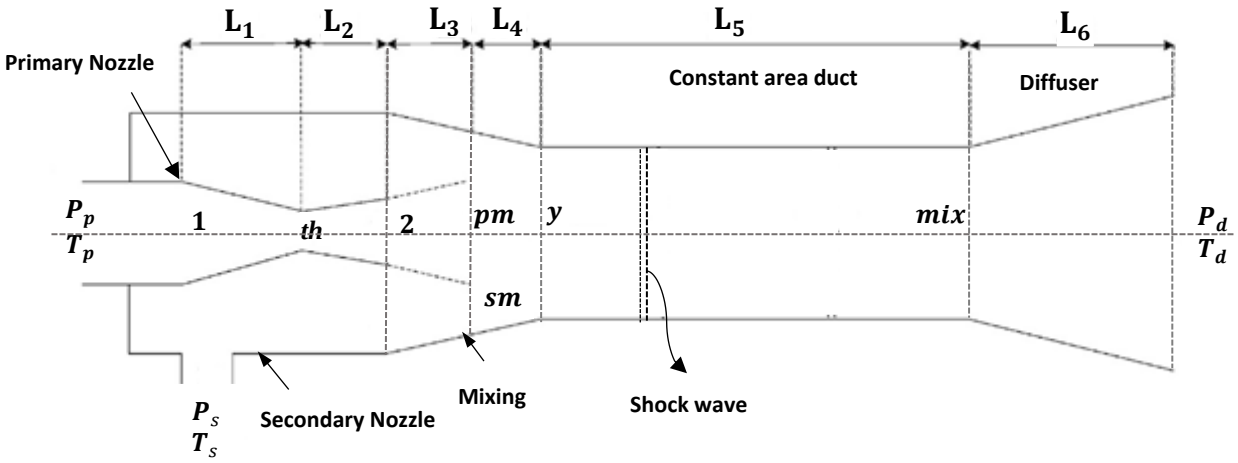

Figure 6.4 Schematic of an ejector with relevant notations

By changing the gas cooler and evaporator operating conditions in the cycle, two geometric parameters that can be adjusted to maintain the ejector at its design condition are the primary nozzle throat area [101] and the secondary nozzle exit area in the mixing chamber [81]. In this work the primary nozzle throat diameter (D_{th}) and ejector effective area ratio ($A_{r,ejec} = A_m/A_{th}$) are considered as variables that are changed by operating conditions. A_m is defined as the total area of primary and secondary flows at cross section 'm' and A_{th} is the area of the primary flow at cross section 'th'.

6.6.2 Numerical procedure

The input parameters of the model for the transcritical CO_2 cycle are: temperatures, pressures and mass flow rates of the external fluids at the gas cooler and evaporator inlets and the CO_2 pressure of heat exchangers. The total area of heat exchangers is considered as a constraint in cycle simulation and it is constant in all calculations ($A_{gc} + A_{ev}$=4.13 m^2). The characteristics of each heat exchanger (Table 6.1) remain fixed, except that the lengths of evaporator and gas cooler change to keep the total area constant.

According to Sahin and Kodal [118], the total cost of the system, including the annual investment cost of the system and the annual energy consumption cost, is $C=a\ (A_H+A_L)+b\ (Q_H-Q_L)$.

The annual investment cost of the system is proportional of areas of heat exchangers and compressor work. Therefore, by keeping the total area of heat exchangers constant, the compressor work is the only factor to affect the economic optimization. This means that the design conditions that maximize COP correspond approximately to the economically optimal conditions.

Unlike most previous works, where total thermal conductivity (UA) was considered as a quantity to determine the capital and operational cost of the system [100], in this work the total area is considered as the constraint that is more realistic than the product of UA. Heat transfer area ratios used in the simulation are given in Table 6.3.

The theoretical model of a two-phase ejector heat pump cycle (Figure 6.2b) was developed to investigate the effect of different parameters on the performance of the cycle. Figure 6.5 shows the flowchart for the iterative calculation of the transcritical CO_2 ejector heat pump system. The calculation procedure is as follows:

1. The calculation starts with a preliminary value for pressure at ejector outlet (point 7) which is the same as the separator and compressor inlet pressure (point 1& 8).The inlet streams to the compressor and expansion valve are saturated vapor and saturated liquid respectively.

2. Based on the gas cooler pressure (discharge pressure) and using the compressor model, the mass flow rate of the refrigerant , compressor work and properties at inlet temperature of the gas cooler (point 2) are determined.

3. The heat capacity, outlet temperature of the external flow and properties at gas cooler outlet (point 3) are determined using the gas cooler model.

4. Based on an isenthalpic process through the throttling valve from ejector outlet pressure to evaporator pressure, the properties at evaporator inlet (point 9) are determined. By assuming a value for entrainment ratio, the CO_2 mass flow rate through the evaporator is determined. By using the evaporator model, the cooling capacity and properties at evaporator outlet (point 10) are determined.

5. By using the inlet conditions of the primary and secondary flows to the ejector model, the ejector outlet conditions (point 7) are determined. The new value for entrainment ratio is obtained from $ER= (1-X_7)/X_7$. If the calculated value is different with the assumed value, steps 4 and 5 are repeated until convergence of the entrainment ratio. This relation is satisfied to maintain a balance between liquid and vapor in the expansion recovery cycle.

6. After convergence of the entrainment ratio, the calculated pressure of ejector outlet is compared to the assumed value. If the pressures are not equal, the assumed pressure is updated and steps 1 to 6 are repeated until the solution converges.

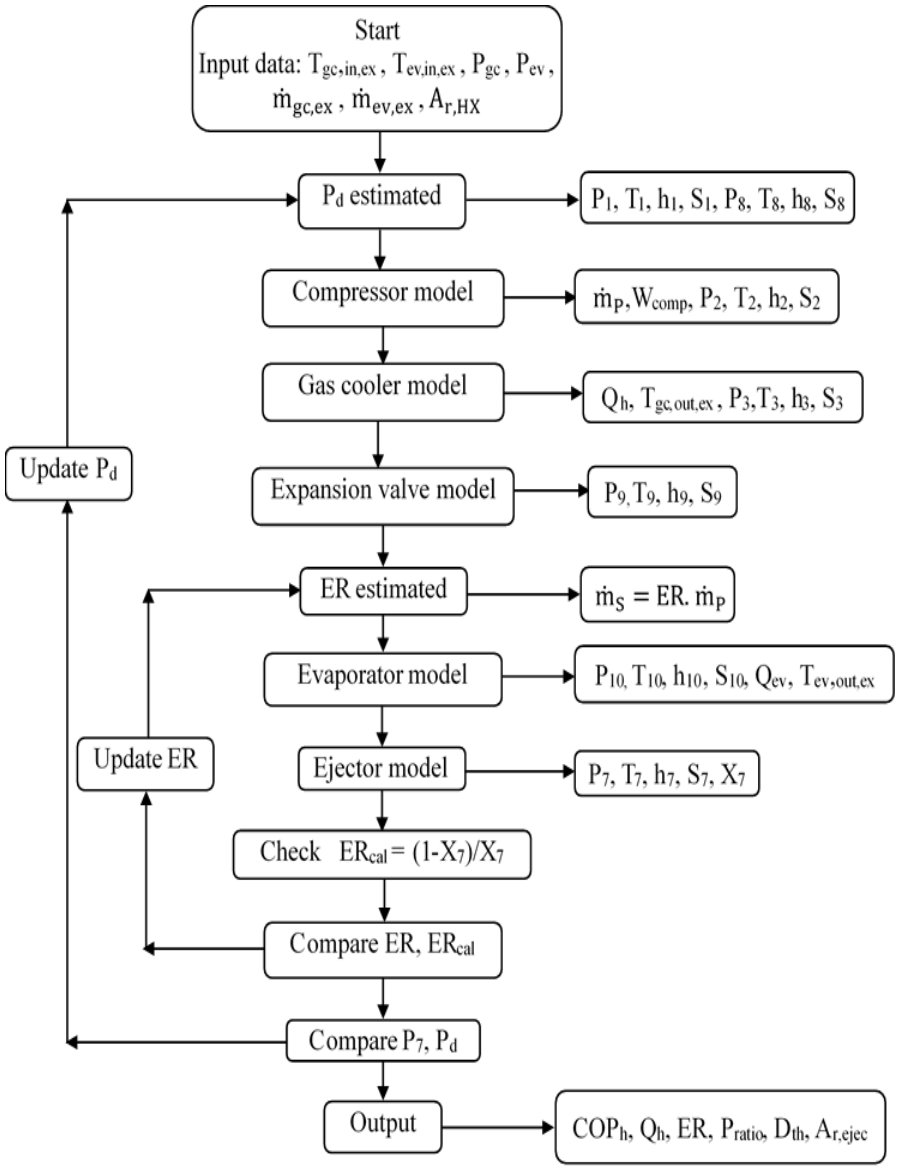

Figure 6.5 Calculation flowchart for transcritical CO_2 ejector cycle

Table 6.3 Heat transfer area ratio of simulated heat exchangers

	gas cooler		evaporator		
Case	Plate length (mm)	Heat transfer Area (m^2)	Plate length (mm)	Heat transfer Area (m^2)	Heat transfer area ratio (A_{gc}/A_{ev})
1	300	1.678	632	2.456	0.683
2	390	2.199	500	1.935	1.136
3	480	2.719	368	1.414	1.923
4	550	3.124	266	1.009	3.096
5	600	3.414	192	0.72	4.742

In this study, a validated ejector model [84] is integrated into the heat pump system. Table 6.4 shows the comparison of the simulation model of the ejector heat pump cycle with the experiments of Bilir Sag et al. [78]. The discrepancy between the experiments and the model predictions is small (less than 6%). Since there is insufficient available data in the literature, absolute values comparison with other experimental results is not possible.

Table 6.4 Validation of the simulation model with experimental data of Bilir Sag et al. [78] with the same capacity, operating conditions, and ejector geometry

	Case 1			Case 2			Case 3		
	Experiment	Simulation	Error (%)	Experiment	Simulation	Error (%)	Experiment	Simulation	Error (%)
COP	3.87	3.82	1.20	3.18	3.38	6.12	2.629	2.70	3.17
P_d , kPa	354.27	361.51	2.05	380	373.63	1.68	397	387.03	2.51
ER	0.78	0.79	0.64	0.79	0.77	2.03	0.73	0.75	3.15
W_{comp}	1.18	1.19	1.21	1.35	1.27	5.70	1.492	1.44	3.26

6.7 Results and discussion

6.7.1 Comparison of basic and ejector cycle

Table 6.5 illustrates the energy analysis simulation results for the basic and ejector transcritical cycles.

It can be seen that for the given operating conditions in Table 6.2 and heat exchangers geometries of Table 6.1, the ejector improves the COP by up to 12% compared to the basic cycle and increases the heating capacity by up to 25%. This difference can be justified by an increase in compressor power. Although the compressor pressure ratio decreases in the ejector cycle, the mass flow rate of the refrigerant through the compressor may increase compared to the basic cycle.

Table 6.5 Comparison of energy performance between basic and ejector heat pump cycles

	COP_h			Q_{gc} (kW)			W_{comp} (kW)		
	Basic cycle	Ejector cycle	Difference (%)	Basic cycle	Ejector cycle	Difference (%)	Basic cycle	Ejector cycle	Difference (%)
1	3.387	3.749	10.70	18.29	22.12	20.91	5.399	5.899	9.26
2	3.176	3.556	11.98	16.74	20.92	24.95	5.271	5.881	11.58
3	3.269	3.662	12.04	17.43	21.63	24.10	5.33	5.906	10.81
4	3.283	3.662	11.55	17.27	21.24	22.97	5.259	5.799	10.27
5	3.334	3.678	10.32	16.81	20.18	20.02	5.041	5.485	8.81
6	3.42	3.764	10.07	17.21	20.48	19.06	5.03	5.442	8.18
7	3.428	3.769	9.94	17.89	21.15	18.21	5.219	5.612	7.52
8	3.24	3.545	9.42	17.47	21.10	20.79	5.392	5.952	10.39
9	3.715	4.062	9.34	21.40	24.10	12.62	5.761	5.933	2.99
10	3.764	4.122	9.50	22.05	24.85	12.69	5.858	6.029	2.91
11	3.784	4.133	9.22	21.82	24.46	12.08	5.767	5.918	2.61

6.7.2 Performance analysis

In this part, a parametric study is performed in order to investigate the effect of the heat exchanger area ratio on COP_h, optimal discharge pressure, and heating capacity. The heat transfer areas are varied by changing the lengths of the plate heat exchangers.

The effects of gas cooler and evaporator pressures and design parameters of a two-phase ejector on the optimum performance of an ejector heat pump system are investigated.

For different gas cooler and evaporator pressures, the optimal ejector values will be obtained; namely, the values for primary nozzle throat diameter, effective area ratio, entrainment ratio and pressure ratio of the ejector that yield maximum heating capacity and COP. The knowledge of these parameters will be useful for proper ejector design and optimal adjustment of the primary and secondary nozzle areas in system operation to assure maximal performance.

The parametric analysis is based on the operating conditions shown in Table 6.2. Inlet temperatures of the external fluid at the evaporator and gas cooler are fixed at 27.39 and 18.04°C respectively, and external fluid mass flow rates are fixed at 0.764 kg/s and 0.117 kg/s for the evaporator and gas cooler respectively. The gas cooler pressure is varied from 9000 kPa to 11500 kPa and the evaporator pressure is varied from 2600 kPa to 4000 kPa.

The evaporator pressure is held at 2780 kPa when the gas cooler pressure is varied; the gas cooler pressure is held at 10000 kPa when the evaporator pressure is varied.

6.7.2.1 Effect of heat transfer area ratio on system performance and the optimal gas cooler pressure

Figure 6.6 presents the variation of COP_h and heat capacity with respect to gas cooler pressure for different heat transfer area ratios. As shown in Figure 6.6, there exists a maximum COP_h and heating capacity corresponding to an optimum gas cooler pressure for each different heat transfer area ratio. The optimal gas cooler pressures are lower for COP_h than they are for heating capacity, and they vary with heat transfer area ratio. As the heat transfer area ratio increases, the optimal gas cooler pressure decreases. The same result was observed by Wang et al. [106] for a tube in tube gas cooler in an air source CO_2 water heat pump system when the gas cooler area increased.

It can be seen that the larger heat transfer area ratio increases COP_h .When the length of the gas cooler increases from 300 mm ($A_{r,HX}$=0.68) to 600 mm ($A_{r,HX}$=4.7), the optimal gas cooler pressure decreases from 11500 to 10000 kPa, while the maximum COP_h increases from 3.55 to 3.96 (11.46%). The COP_h enhancement is also higher (9.5%) at lower heat transfer area ratio compared to higher heat transfer area ratio (4.7%). The maximum increase in COP_h (16.5%) and heating capacity (20%) are obtained with a gas cooler pressure of 9000 kPa.

Figures 6.7 and 6.8 present the variations of compressor work and gas cooler outlet temperature as a function of gas cooler pressure.

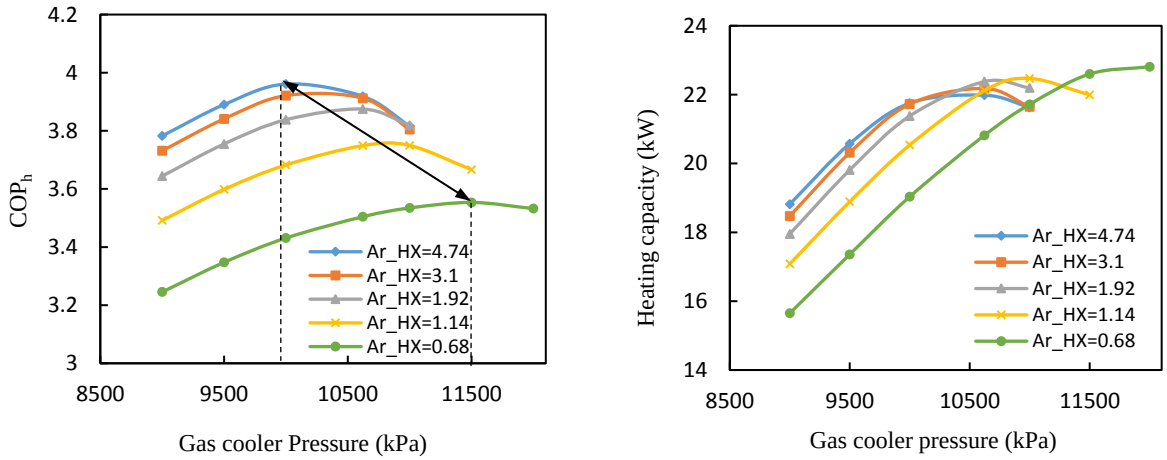

Figure 6.6 COP_h and heating capacity versus gas cooler pressure for different heat transfer area ratios

It can be seen from Figure 6.7 that the effect of gas cooler pressure on compressor work is more significant than the effect of heat transfer area ratio. The heat transfer area ratio has no significant effect on the compressor work at lower gas cooler pressure, below around 10000 kPa. However, at higher gas cooler pressure, the increase in compressor work is dependent on the heat exchanger area ratio. By increasing the gas cooler pressure from 9000 kPa to 11000 kPa, the minimum increase in compressor work is about 13.9% for larger heat transfer area ratio while the maximum increase is 27.4% for lower heat transfer area ratio.

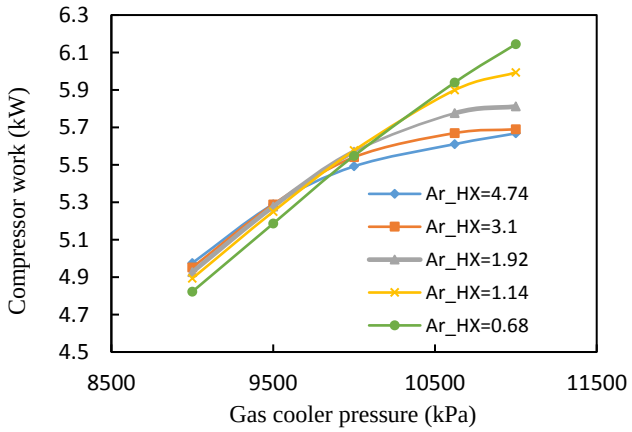

Figure 6.7 Compressor work versus gas cooler pressure for different heat transfer area ratios

Figure 6.8 shows that at larger heat transfer area ratio, the variations of gas cooler outlet temperature increases. The gas cooler pressure has less impact on gas cooler outlet temperature at lower heat transfer area ratio. It is worth mentioning that the gas cooler outlet temperature is constrained by the external fluid inlet temperature in the gas cooler in a counter flow heat exchanger. It means that the improvement of heat capacity is limited at higher heat transfer area ratios.

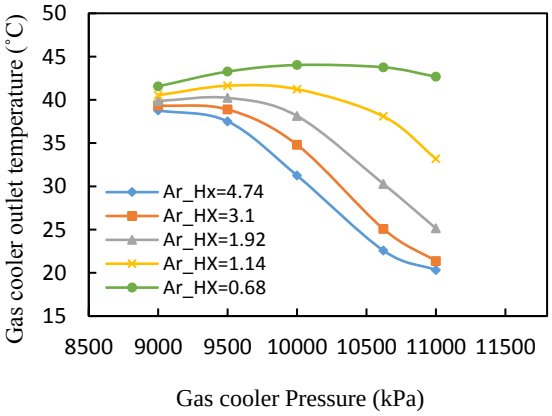

Figure 6.8 Gas cooler outlet temperature versus gas cooler pressure for different heat transfer area ratios

6.7.2.2 Optimal characteristics of the ejector at different heat transfer area ratios

Figure 6.9 and 6.10 show the variation of the primary nozzle throat diameter and ejector effective area ratio with respect to the gas cooler pressure for different heat transfer area ratios. It can be seen in Figure 6.9 that the primary nozzle throat diameter decreases, for constant heat transfer area ratio, with increasing gas cooler pressure. This occurs because the mass flow rate in the primary nozzle decreases. Comparing Figures 6.6 and 6.9, the optimal values of primary nozzle throat diameter, corresponding to maximum COP_h and optimum gas cooler pressure for different heat transfer area ratios, were obtained in range 1.35-1.5 mm. The results also show that the ejector has larger throat diameters at lower heat transfer area ratio due to larger primary mass flow rates and lower secondary mass flow rates, corresponding to lower gas cooler area and higher evaporator area.

As illustrated in Figure 6.10 the ejector effective area ratio increases as the gas cooler pressure increases. However, the values of effective area ratio are not the same for all heat transfer area ratios.

The minimum heat transfer area ratio, corresponding to minimum gas cooler area and maximum evaporator area, and thus maximum primary mass flow rate and minimum secondary mass flow rate, is found to yield the minimum ejector effective area ratio.

There is an optimal range for ejector effective area ratio (7.8-8.3), corresponding to maximum COP_h (Figure 6.6) at the respective optimum gas cooler pressures. This confirms the previous finding that showed the existence of an optimal area ratio yielding maximum capacity [119].

The variation of the ejector entrainment ratio and pressure ratio with the gas cooler pressure for various heat transfer area ratios is shown in Figure 6.11. It can be seen that the ejector entrainment ratio increases with increasing gas cooler pressure and increasing heat transfer area ratio, however the pressure ratio decreases. This is because that by decreasing the evaporator heat transfer area, the mass flow rate of the evaporator increases while the mass flow rate of the gas cooler decreases. As a result, entrainment ratios increase and the pressure ratios decrease.

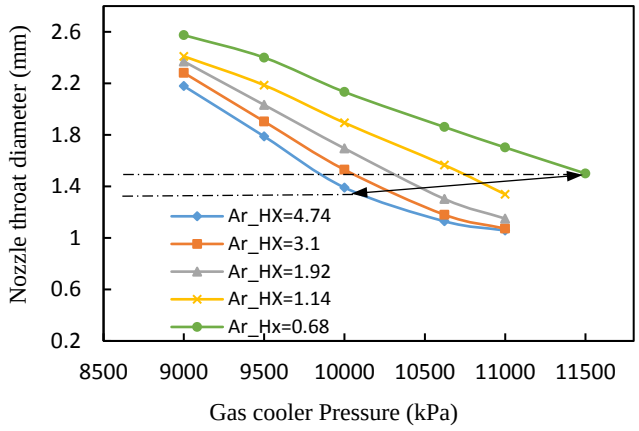

Figure 6.9 Primary nozzle throat diameter versus gas cooler pressure for different heat transfer area ratios

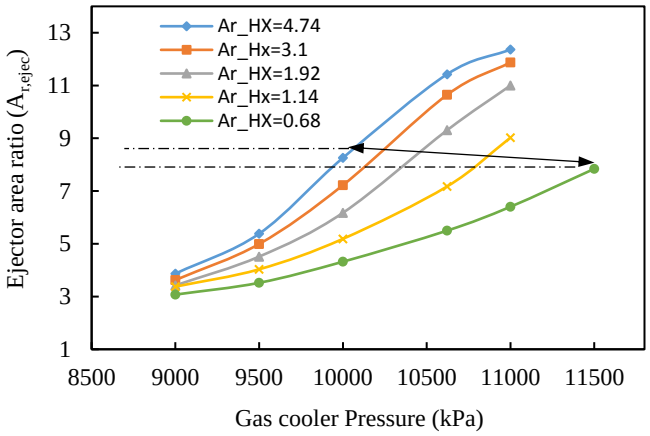

Figure 6.10 Ejector area ratio versus gas cooler pressure for different heat transfer area ratios

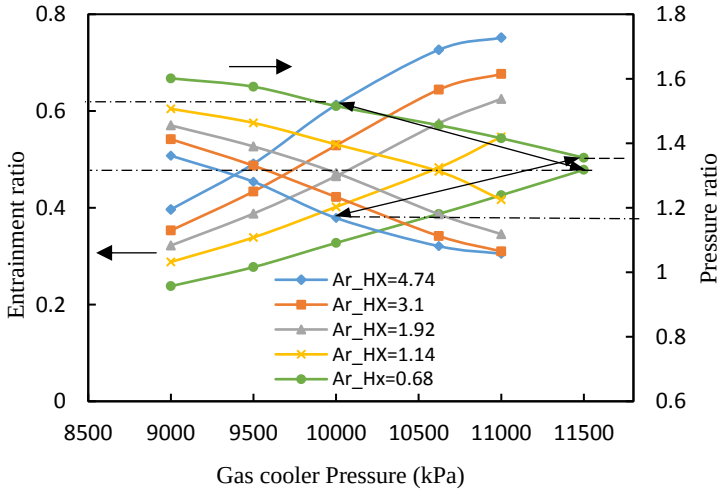

Figure 6.11 Entrainment ratio and pressure ratio versus gas cooler pressure for different heat transfer area ratios

The optimal values of entrainment ratio vary between 0.47 and 0.61 while the optimal pressure ratios are in the range of 1.16-1.35. When the gas cooler pressure increases, the primary mass flow rate decreases, which makes the primary nozzle throat decrease while the secondary mass flow rate increases, leading to an increase in the ejector effective area ratio and entrainment ratio. Thus, the entrainment ratio and ejector area ratio have the same change direction while the pressure ratio has an inverse change direction of that entrainment ratio.

The effect of gas cooler pressure on ejector efficiency is shown in Figure 6.12. The results establish the existence of optimal values for the gas cooler pressure that maximize the ejector efficiency. However, the highest ejector efficiency occurred at a pressure lower than the optimum gas cooler pressure corresponding to the maximum COP_h. These results show a similar trend when compared with the experimental results of Elbel and Hrnjak [27]. The range of maximum ejector efficiency is between 0.38 and 0.49, depending on the heat transfer area ratios. The lower ejector efficiency at different gas cooler pressure was obtained when the gas cooler heat transfer area is larger than the evaporator heat transfer area.

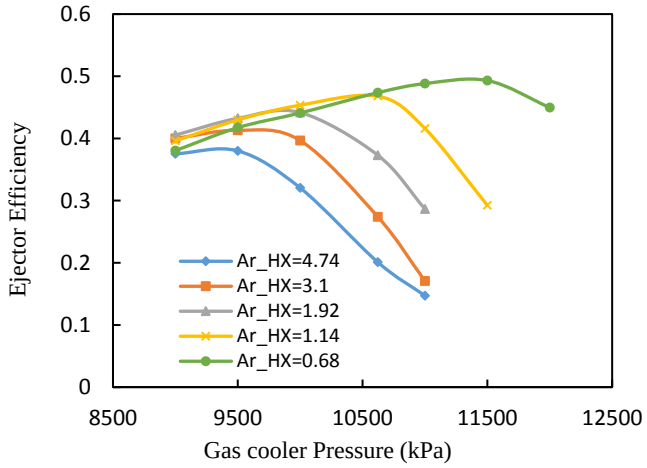

Figure 6.12 Ejector efficiency versus gas cooler pressure for different heat transfer area ratios

6.7.2.3 Effect of diffuser outlet area on the system performance

Figure 6.13 shows the variation of COP_h, heating capacity, and compressor work as a function of diffuser outlet diameter, for different heat transfer area ratios. The gas cooler and evaporator pressures are 10000 kPa and 2780 kPa respectively. It can be seen that the diffuser outlet diameter has an insignificant effect on system performance. This is because of the small change in entrainment ratio (8-11%) and pressure ratio (5-9%) when the ejector outlet diameter increases from 6.3mm to 12.6 mm.

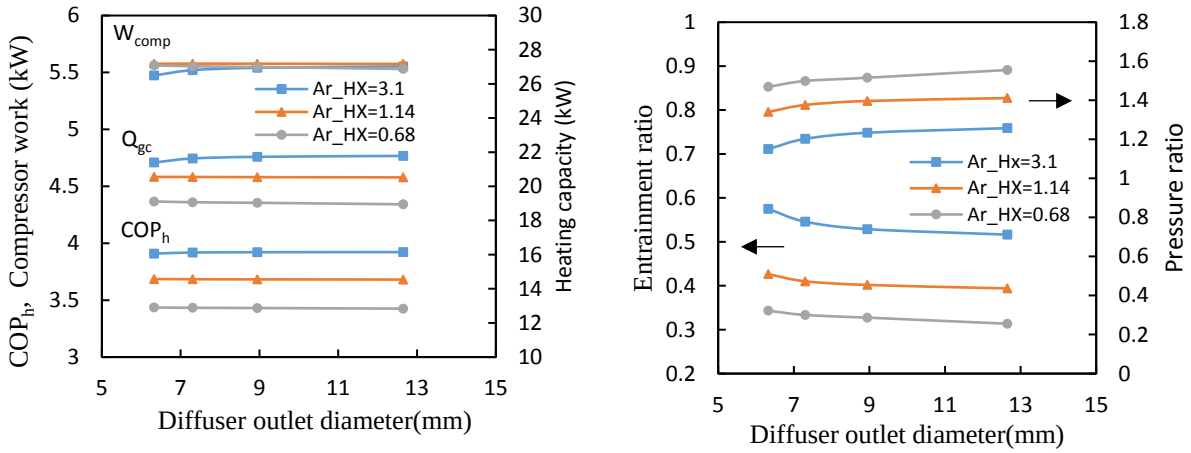

Figure 6.13 COP_h, heating capacity and compressor work; (b) entrainment ratio and pressure ratio versus diffuser outlet diameter, for different heat transfer area ratios

6.7.2.4 Effect of evaporator pressure on system performance and ejector characteristics

Figure 6.14 shows the variation of COP_h and heating capacity for various evaporator pressures and heat transfer area ratios. It can be seen that the COP_h and heating capacity of the ejector heat pump cycle increase slowly at lower evaporator pressure and then decrease when the evaporator pressure increases from 3000 to 4000 kPa. This result is in contrast to previous works [8], [16] which investigated the effects of the evaporator temperature and gas cooler outlet temperature as two independent design variables. They concluded that COP improved with increasing evaporator temperature and decreasing gas cooler exit temperature. However, in this study the gas cooler exit temperature is a dependent variable, and it changes with the gas cooler inlet operating conditions.

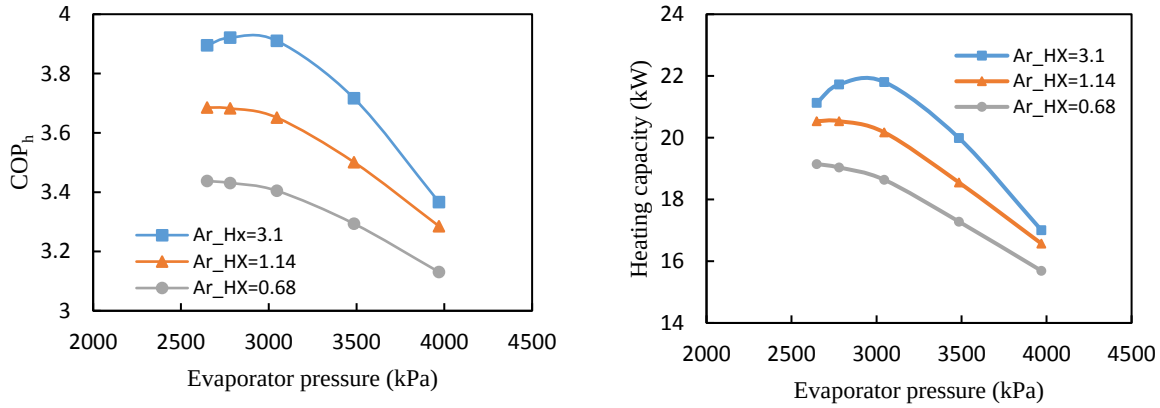

Figure 6.14 (a) COP_h and (b) heating capacity versus evaporator pressure for different heat transfer area ratios

As shown in Figure 6.15, the gas cooler outlet temperature increases as the evaporator pressure increases. Therefore, the effect of increasing evaporator pressure is surpassed by the effect of gas cooler outlet temperature. As a result, the COP_h and heating capacity decrease (Figure 6.14). This result confirms that the gas cooler outlet temperature has a more significant effect than the evaporator temperature, in terms of system performance [16]. The same results as the previous

section hold, where higher heat transfer area ratio yields higher COP_h and heating capacity for various evaporator pressures. It can be seen that with an increase in the heat transfer area ratio, there is a steeper increase in gas cooler outlet temperature as the evaporator pressure increases.

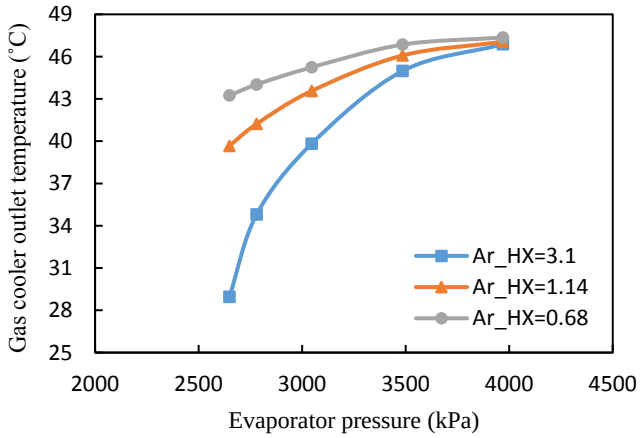

Figure 6.15 Gas cooler outlet temperature versus evaporator pressure for different heat transfer area ratios

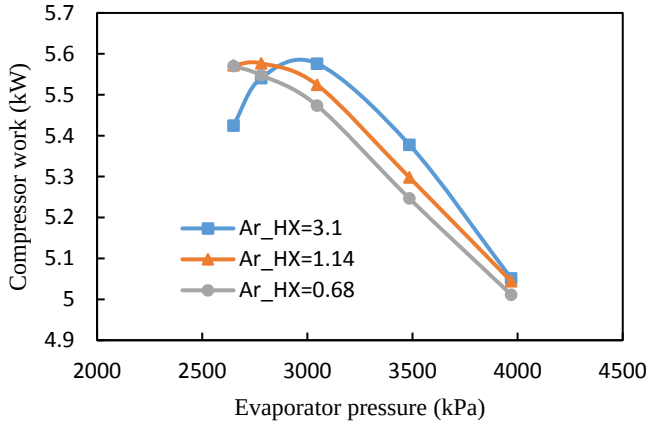

Figure 6.16 Compressor work versus evaporator pressure for different heat transfer area ratios

Figure 6.16 depicts that by increasing the evaporator pressure, the compressor work slightly increases and then decreases. This reduction is because that higher evaporator pressure is associated with higher gas cooler outlet temperature, the increase in primary mass flow rate is surpassed by the increase in ejector pressure lift, which reduces the pressure difference between the compressor suction and discharge pressures and thus lowers the compressor work. The effect of heat transfer area ratio, as shown in Figure 6.16 is insignificant compared to evaporator pressure.

Figure 6.17 shows the variation of primary nozzle throat diameter and ejector effective area ratio as a function of evaporator pressure. Unlike the effect of the gas cooler pressure on primary nozzle throat diameters and ejector area ratio (Figures 6.9, 6.10), the primary nozzle throat diameter increases while the ejector area ratio decreases, both occurring with increasing evaporator pressure. This is due to the increase of primary mass flow rates that results in higher throat diameters and

lower ejector area ratios. It can be seen that the larger throat diameter and lower ejector area ratio is obtained at lower heat transfer area ratio. The variation of entrainment ratio and pressure ratio with evaporator pressure is shown in Figure 6.18. It can be seen that the ejector pressure ratio increases with evaporator pressure at different heat transfer area ratio, while the entrainment ratio decreases. It is apparent that the changes of entrainment ratio and pressure ratio are more significant at higher heat transfer area ratio.

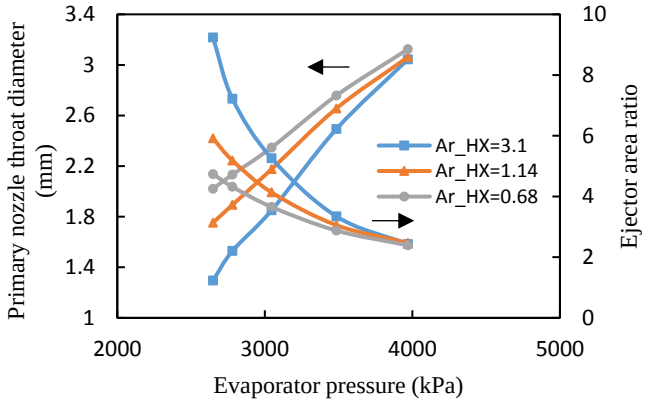

Figure 6.17 Primary nozzle throat diameter and ejector area ratio versus evaporator pressure for different heat transfer area ratios

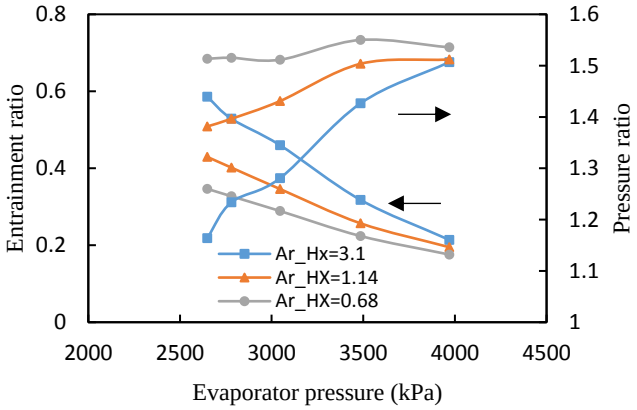

Figure 6.18 Entrainment ratio and pressure ratio versus evaporator pressure for different heat transfer area ratios

6.8 Conclusion

In this work, a detailed simulation model based on actual heat transfer areas was developed to predict the performance of a transcritical CO_2 ejector heat pump system. An ejector design model varies the primary nozzle throat diameter and effective area ratio to adjust to the gas cooler and evaporator pressures. The effects of the heat exchanger area ratio are presented, namely its impact on COP_h, heating capacity, and optimal gas cooler pressure. A constraint of constant total heat exchanger area was imposed. This constraint permits the results to be used as a thermo-economic

optimization. The corresponding optimal values of the ejector characteristics are also obtained for different operating parameters.

The results show that the heat transfer area ratio has important effects on COP_h, heating capacity as well as the optimal gas cooler pressure.

An increase in heat transfer area ratio improves system performance, although it has an inverse effect on the ejector efficiency. By increasing heat transfer area ratio, COP_h and heating capacity increase, while the corresponding optimal gas cooler pressure decreases. For fixed heat transfer area ratio, the optimal gas cooler pressure corresponding to maximal COP_h is slightly lower than that corresponding to maximal heating capacity, but slightly higher than that for ejector efficiency.

The ejector characteristics have significant effects on the optimal performance of the system. The primary nozzle throat diameter and effective area ratio are two important parameters to consider as controllable and adjustable parameters for the design of ejector cycles. In contrast, the diffuser outlet diameter has no significant effect on system performance. The desired throat diameter and effective area ratio of the ejector at the given operating conditions in this work are in the range of 1.35-1.5 mm and 7.8-8.3 respectively. The optimal ranges of entrainment ratio and pressure ratio are 0.47-0.61 and 1.16-1.35 respectively.

The results show that the effect of gas cooler outlet temperature on the system performance is predominate compared to evaporator pressure. This is because the increase of evaporator pressure is surpassed by the increase in gas cooler outlet temperature. The gas cooler outlet temperature has a different separate trend as a function of either gas cooler pressure or evaporator pressure. It decreases as either the gas cooler pressure increases or as the evaporator pressure decreases. The established results will be helpful for the optimal design of a transcritical CO_2 ejector heat pump cycle.

6.9 Acknowledgments

This project is a part of the Collaborative Research and Development (CRD) Grants Program at Université de Sherbrooke. The authors acknowledge the support of the Natural Sciences and Engineering Research Council of Canada, Hydro-Québec, Rio Tinto Alcan and Canmet ENERGY from Research Center of Natural Resources Canada (RDCPJ451917-13).

6.10 Nomenclature

A	Area , mm²	d	Diffuser
A_r	Area ratio	ejec	Ejector
D	Diameter , mm	ev	Evaporator
ER	Entrainment ratio	ex	External fluid
h	Enthalpy	gc	Gas cooler
H	Heat sink	h	heating
L	Heat source	HX	Heat exchanger
$\dot{m}$	Mass flow rate, kg s^{-1}	in	Inlet
Nu	Nusselt number	m	Choke location of secondary flow
P	Pressure, kPa	max	maximum
Pr	Prandtl number	mix	Mixing
P_d	Ejector back pressure, kPa	out	outlet
P_{ratio}	Pressure ratio (pressure lift)	p	Primary
Q	Capacity , kW	pol	Polytropic
Re	Reynolds Number	rec	Recovery
s	Specific entropy, kJ kg^{-1} K^{-1}	s	Secondary
T	Temperature , K	sp	Single Phase
UA	Total thermal conductivity	th	Ejector throat
W	Work rate, kW	tp	Two-phase
X	Quality	v	Vapor
Greek symbols		w	Wall
η	efficiency	**Abbreviation**	
μ	Dynamic viscosity , N m^{-2} s	COP	Coefficient of performance
Subscripts		EERC	Ejector expansion recovery cycle
comp	compressor	EES	Engineering equation solver

CHAPTER 7

CONCLUSION

7.1 Conclusion de la thèse

Les cycles de réfrigération avec éjecteur diphasique ont retenu l'attention des chercheurs ces dernières années. Le dioxyde de carbone est l'un des réfrigérants naturels appropriés pour remplacer les réfrigérants classiques de par leur faible impact environnemental. Cependant, les pertes dues à l'étranglement au cours du processus isenthalpique à travers la valve de détente sont très élevées dans un cycle transcritique au CO_2 et entraînent un faible coefficient de performance (COP). L'utilisation de l'éjecteur en tant que dispositif de construction simple et robuste permet d'améliorer les performances du système de refroidissement transcritique au CO_2 et de la pompe à chaleur.

Une étude détaillée d'un système de pompe à chaleur à éjecteur au CO_2 transcritique a été réalisée. L'analyse numérique a été réalisée pour évaluer les effets des conditions de fonctionnement, des caractéristiques de l'éjecteur ainsi que des zones de transfert de chaleur sur les performances du système.

Au chapitre 3, les performances énergétiques et exergétiques de différentes configurations de cycles d'éjecteurs au CO_2 transcritiques ont été étudiées afin d'identifier le cycle le plus efficace. Le COP, l'efficacité exergétique et les destructions exergétiques d'un cycle de récupération du travail d'expansion de l'éjecteur (EERC), d'un cycle de recirculation de liquide (LRC), d'un cycle de pression de refoulement du compresseur (CDPC) et d'un cycle de réfrigération à jet de vapeur (VJRC) ont été comparés. Il a été constaté que le CO_2 peut tirer davantage profit de l'EERC par rapport aux autres cycles. Le COP et l'efficacité exergétique optimaux ont été atteints dans l'EERC. Pour la même capacité de refroidissement, le COP de l'EERC était de 23,3%, 24,9% et 5,6 fois supérieur à celui de LRC, CDPC et VJRC. Le COP et l'efficacité exergétique ont été améliorés jusqu'à 23% et 24%, respectivement, par rapport au cycle d'étranglement de base. Pour l'EERC, l'utilisation d'un éjecteur peut réduire considérablement la perte irréversible du processus de détente et augmenter l'efficacité exergétique. L'analyse exergétique a révélé que les principales pertes d'exergie dans l'EERC se sont produites dans l'évaporateur (environ 33% de la destruction totale du cycle), suivi du compresseur (25,5%) et de l'éjecteur (24,4%).

Dans les systèmes transcritiques avec un éjecteur, la compréhension des effets des caractéristiques de l'éjecteur sur les performances est un facteur impératif pour parvenir à une conception optimale du système. Par conséquent, au chapitre 4, un modèle d'éjecteur diphasique spécialement conçu pour prévoir les performances de l'éjecteur dans des conditions de géométrie et de fonctionnement donnés a été développé. Un modèle 1-D détaillé d'un éjecteur au CO_2 diphasique a été présenté pour les régimes « single or double choking ». Le modèle développé basé sur les principes de conservation de la masse, de la quantité de mouvement et de l'énergie résout le flux dans différentes sections de l'éjecteur. Il est plus complet que d'autres modèles publiés précédemment car il inclut

les paramètres géométriques de l'éjecteur ainsi que l'effet d'onde de choc. Des rendements polytropiques constants ont été utilisés pour représenter les irréversibilités des processus de détente et de compression dans les tuyères et le diffuseur. De plus, le modèle d'éjecteur a été validé en comparant les résultats avec les données expérimentales disponibles dans la littérature ainsi qu'avec celles fournies par le laboratoire des technologies de l'énergie (LTE) d'Hydro Québec, données à l'annexe A. La comparaison avec les données expérimentales a montré un bon accord en termes de débits massiques, de rapports de pression ainsi que de pressions à différentes sections de l'éjecteur. Le modèle d'éjecteur développé a été utilisé aux chapitres 5 et 6 pour l'analyse exergétique d'un éjecteur diphasique et l'étude d'un système de pompe à chaleur à éjecteur au CO_2 transcritique, respectivement.

Au chapitre 5, les performances exergétiques d'un éjecteur transcritique diphasique au CO_2 ont été étudiées pour le point critique ainsi que pour les conditions de "choking" simple et double. L'effet de la contre-pression sur les pertes d'exergie et l'efficacité exergétique a été évalué sur la base de deux critères de performance (efficacité exergétique transitoire et efficacité exergétique de Grassmann). Deux paramètres thermodynamiques importants, l'exergie produite et l'exergie consommée, ont également été calculés. Les résultats de la comparaison de deux efficacités exergétiques ont révélé que l'efficacité exergétique de Grassmann ne changeait pas avec la variation de la contre-pression. Ceci est dû à la présence d'un flux d'exergie en transit qui est négligé lors de l'utilisation de l'efficacité exergétique de Grassmann. Par conséquent, l'efficacité exergétique de Grassmann ne peut pas être un critère approprié pour évaluer les performances d'un éjecteur transcritique. Un autre résultat important a été la présence d'une valeur maximale d'efficacité exergétique en transit autour du point critique. Il confirme l'importance de la conception de l'éjecteur en fonction des conditions critiques.

Au chapitre 6, les performances thermodynamiques d'un système de pompe à chaleur à éjecteur au CO_2 transcritique ont été étudiées. Tout d'abord, un modèle de simulation du cycle de pompe à chaleur au CO_2 avec échangeurs de chaleur au refroidisseur à gaz et à l'évaporateur a été réalisé et validé expérimentalement à partir des données fournies par le laboratoire des technologies de l'énergie d'Hydro-Québec. Un modèle de conception d'éjecteur diphasique décrit au chapitre 4 a été intégré au modèle de pompe à chaleur pour évaluer les performances du système. Un modèle de simulation détaillé du cycle de pompe à chaleur à éjecteur a été développé sur la base des zones de transfert de chaleur réelles. La surface totale de transfert de chaleur a été considérée comme la principale contrainte pour l'analyse numérique. Le COP et la capacité de chauffage de la pompe à chaleur à éjecteur ont été améliorés de 12% et 25% respectivement par rapport au cycle de base pour des conditions de fonctionnement et des rapports de surface de transfert de chaleur donnés. Les effets des conditions de fonctionnement, des rapports de surface de transfert de chaleur et des différentes caractéristiques sur le COP et la capacité de chauffage ont également été étudiés.

Il a été constaté que les rapports de surface de transfert de chaleur ont des effets importants sur le COP et la capacité thermique, ainsi que sur la pression optimale du refroidisseur à gaz. Une augmentation du rapport de la surface de transfert de chaleur a amélioré les performances du système alors que cela avait un effet inverse sur l'efficacité de l'éjecteur. En augmentant la longueur du refroidisseur de gaz de 300 mm ($A_{r,HX}$ = 0.68) à 600 mm ($A_{r,HX}$ = 4.7), le COP maximum est passé de 3.55 à 3.96 (+11.46%), tandis que la pression optimale du refroidisseur de gaz a été réduite

de 11500 à 10000 kPa. L'efficacité maximale de l'éjecteur a également diminué de 0.49 à 0.38. L'augmentation maximale du COP et de la capacité de chauffage a également été obtenue à une pression de refroidissement à gaz de 9000 kPa (16.5%). Deux paramètres géométriques de l'éjecteur, le diamètre de la gorge de la tuyère primaire et le rapport de surface effective ont été ajustés pour fournir les conditions optimales de débit. Il a été déterminé que le diamètre de sortie du diffuseur n'avait pas d'effet significatif sur les performances du système. Les valeurs optimales pour les caractéristiques de l'éjecteur (diamètre de la gorge de la tuyère primaire, rapports de surface effective, taux d'entraînement et taux de pression) correspondant au COP maximum à une pression optimale du refroidisseur à gaz ont été obtenues. Les diamètres de gorge désirés et le rapport de surface efficace de l'éjecteur dans des conditions de fonctionnement données étaient compris entre 1.35 et 1.5 mm et entre 7.8 et 8.3 respectivement. Les plages optimales du rapport d'entraînement et du rapport de pression étaient également de 0.47-0.61 et de 1.16-1.35 respectivement.

Les résultats indiquent que l'effet de la sortie du refroidisseur à gaz est prédominant par rapport à la pression de l'évaporateur. Dans les conditions de fonctionnement données, les performances du système diminuaient avec l'augmentation de la pression de l'évaporateur. La température de sortie du refroidisseur à gaz a augmenté à mesure que la pression de l'évaporateur augmentait. Par conséquent, l'effet de l'augmentation de la température de sortie du refroidisseur à gaz a surpassé l'effet de l'augmentation de la pression de l'évaporateur, qui a entraîné une baisse du travail du compresseur. Par conséquent, la capacité de chauffage et le COP ont diminué.

L'intégration d'un éjecteur diphasique dans les pompes à chaleur au CO_2 transcritiques peut améliorer les performances du système. Cette thèse montre que la conception appropriée, un réglage optimal de la géométrie de l'éjecteur et les caractéristiques de conception des échangeurs de chaleur sont à considérer pour obtenir des performances optimales.

7.2 Conclusion of thesis

The two-phase ejector expansion recovery cycles have received the significant attention of the researchers in recent years. Carbon dioxide is one of the appropriate natural refrigerants with environmentally friendly characteristics to replace conventional refrigerants. However, the throttling losses during the isenthalpic process through the expansion valve are very high in a transcritical CO_2 cycle and result in a low coefficient of performance (COP). Using ejector as a device with simple construction and robust operation helps to improve the transcritical CO_2 refrigeration and heat pump system performance.

A detail investigation of a transcritical CO_2 ejector heat pump systems was performed. The numerical analysis was carried out to evaluate the effects of operating conditions, ejector characteristics as well as heat transfer areas on the system performance.

In chapter 3, the energy and exergy performance of different configurations of the transcritical CO_2 ejector cycles under the same cooling capacity were performed in order to identify the most efficient cycle. The COP, exergy efficiency and exergy destructions of an ejector expansion work recovery cycle (EERC), a liquid recirculation cycle (LRC), a compressor discharge pressure cycle

(CDPC) and a vapor jet refrigeration cycle (VJRC) were compared. It was found that CO_2 can gain more benefit from EERC compared to other cycles. The maximum COP and exergy efficiency were achieved in EERC. For the same cooling capacity, the COP of EERC was 23.3%, 24.9% and 5.6 times higher than that of LRC, CDPC and VJRC. The COP and exergy efficiency were improved up to 23% and 24%, respectively, compared to the basic throttling cycle. In EERC, using ejector can significantly reduce the irreversibility loss of the expansion process and increase the exergy efficiency. The exergy analysis implied that the major exergy losses in EERC occurred in the evaporator (about 33% of the total exergy destruction of the cycle) followed by the compressor (25.5%) and the ejector (24.4%).

In ejector transcritical systems, understanding the effects of ejector characteristics is an imperative factor to reach an optimum design of the system. Therefore, in Chapter 4, a two-phase ejector model has been specifically developed to predict ejector performances under given geometry and operating conditions (off-design and design conditions). A detailed 1-D model of a two-phase CO_2 ejector was presented for single choking and double choking conditions. The developed model based on mass, momentum and energy conservation principles solves the flow in different sections of the ejector. It is more complicated than other previous models since it includes ejector geometrical parameters as well as the shock wave effect. The constant polytropic efficiencies were used to represent the irreversibilities of the expansion and compression processes in the nozzles and the diffuser. Furthermore, the ejector model was validated by comparing the results with the experimental data available in the literature as well as that provided at Hydro Québec's energy technologies laboratory (LTE) given in Appendix A. The comparison with the experimental data showed a good agreement in terms of mass flow rates, pressure ratio as well as the pressures at different cross sections of the ejector. The developed ejector model has been used in chapter 5 and 6, for the exergy analysis of a two-phase ejector and the investigation of a transcritical CO_2 ejector heat pump system, respectively.

In chapter 5, the exergy performance of a transcritical CO_2 two-phase ejector was studied for the critical point as well as for single and double choking conditions. The effect of back pressure on the exergy losses and exergy efficiency was evaluated based on two exergy performance criteria (transiting exergy efficiency and Grassmann exergy efficiency). Two important thermodynamic parameters, exergy produced and exergy consumed, were also computed. The comparison results of two exergy efficiencies revealed that Grassmann exergy efficiency did not change with the back pressure variation. This is due to the presence of transiting exergy flow, which is neglected when using the Grassmann exergy efficiency. Therefore Grassmann exergy efficiency cannot be an appropriate criterion for the evaluation of the transcritical ejector performance. Another important result was the presence of a maximum value of transiting exergy efficiency around the critical point. It confirms the importance of the ejector's design according to the critical point conditions.

In chapter 6, the thermodynamic performance of a transcritical CO_2 ejector heat pump system was investigated. First, a simulation model of CO_2 heat pump cycle with gas cooler and evaporator plate heat exchangers was performed and experimentally validated by the data provided in the Hydro Québec's energy technologies laboratory. A two-phase ejector design model described in chapter 4 was integrated into the heat pump model to evaluate the system performance. A detailed simulation model of the ejector heat pump cycle was developed based on the actual heat transfer areas. The total heat transfer area was considered as the constraint in the numerical analysis. The COP and heating capacity of the ejector heat pump cycle were improved by up to 12% and 25%

respectively compared to the basic cycle for the given operating conditions and heat transfer area ratios. The effects of operating conditions, heat transfer area ratios and ejector characteristics on COP and heating capacity were also obtained.

It was found that heat transfer area ratios have important effects on COP and heat capacity as well as optimum gas cooler pressure. An increase in the heat transfer area ratio improved the system performance while it had an inverse effect on the ejector efficiency. By increasing the length of the gas cooler from 300 mm ($A_{r,HX}$=0.68) to 600 mm ($A_{r,HX}$=4.7), the maximum COP increased from 3.55 to 3.96 (+11.46%) while the optimal gas cooler pressure decreased from 11500 to 10000 kPa. The maximum ejector efficiency also decreased from 0.49 to 0.38. The maximum increase in COP and heating capacity was also obtained at a gas cooler pressure of 9000 kPa (16.5%). Two ejector geometric parameters, the primary nozzle throat diameter and effective area ratio were adjusted to provide the optimum flow conditions. It was determined that the diffuser outlet diameter had an insignificant effect on system performance. The optimum values for ejector characteristics (primary nozzle throat diameter, effective area ratios, entrainment ratio and pressure ratio) corresponding to maximum COP at optimum gas cooler pressure were obtained. The desired throat diameters and the effective area ratio of the ejector at given operating conditions in this work, were in the range of 1.35-1.5 mm and 7.8-8.3, respectively. The optimum range of entrainment ratio and pressure ratio were also 0.47-0.61 and 1.16-1.35, respectively.

The results indicated the predominate effect of the gas cooler outlet compared to evaporator pressure. For the given operating conditions of this work, the system performance decreased with increasing evaporator pressure. The gas cooler outlet temperature increased as the evaporator pressure increased. Therefore the effect of increasing evaporator pressure which resulted in lower compressor work was surpassed by the effect of increasing gas cooler outlet temperature. As a result, COP and heating capacity decreased.

Although the integration of a two-phase ejector in the transcritical CO_2 heat pumps can improve the system performance, this thesis shows the proper design and optimal adjustment of the ejector geometry and also that heat exchangers design characteristics can be useful to get maximum performance.

7.3 Suggested future work

Since carbon dioxide is one of the natural refrigerants which can replace CFCs and HCFCs in refrigeration and heat pump systems, CO_2 technology is developing drastically to improve the efficiency of the CO_2 systems. Ejector application is one of the innovative ideas regarding the development of new system designs. Considering the previous studies on transcritical CO_2 ejector systems and also the results obtained in this study, the high potential enhancement in the performance of CO_2 ejector refrigeration and heat pump systems has been demonstrated. In this section, few recommendations are proposed as future works and improvements regarding ejector expansion transcritical systems.

The validation of the numerical results against experimental data is very important specifically for ejector applications due to the large range of geometries and operating conditions that ejectors can undergo. Experimental studies including the optimum ejector performance are still limited in the

literature. So, more experimental studies have to be carried out in order to evaluate the effects of geometric parameters, operating conditions as well as a control strategy.

The experimental test bench of CO_2 heat pump in LTE can be extended by integrating a two-phase ejector.

Although the 1-D model is simple and can be easily integrated into a system compared to a CFD model, the CFD analysis of a CO_2 two-phase ejector can be helpful to investigate the effects of flow characteristics, shock waves as well as ejector component efficiencies on the ejector performance. Therefore, it can help to improve the ejector design and its performance prediction.

Through a simulation model, two ejector geometric parameters, namely the primary nozzle throat diameter and the effective area ratio were identified as the most important ones which can be adjusted according to operating conditions in a transcritical system. The experimental study of a transcritical CO_2 heat pump system with a controllable ejector in which the nozzle throat diameter and nozzle exit position are adjustable is suggested to validate the results of the simulation model. It would be possible to control the gas cooler pressure and the choking of the secondary flow with a moving needle in the primary nozzle and a moving primary nozzle respectively.

In this study, the influence of different heat transfer area ratios on the system performance revealed the significant effect of the heat exchanger characteristics on the optimal design of the system. The different lengths of the plate heat exchangers were considered to quantify the effects of heat exchanger's area. However, different configurations of the plate heat exchangers including other geometries and the number of plates can lead to more results. Further research could be suggested to investigate the effects of heat exchangers design characteristics on the improvement of ejector cycles. A thermo-economic optimization algorithm with multiple constraints will help also to demonstrate the potential of two-phase CO_2 ejector in a heat pump cycle.

The study of the control strategy of the ejector cycles can be considered as a future perspective to improve the system performance under different operating conditions.

Therefore, by considering the results achieved in this thesis and previous reviews, there is still much potential for further investigation regarding two-phase transcritical CO_2 ejector systems to be used in real applications.

APPENDIX A

COMPARISON OF THE EJECTOR MODEL WITH EXPERIMENTAL DATA (LTE)

The experimental test bench presented at Hydro-Québec laboratory is shown in Figure A.1. A CO_2 ejector test rig was used to test the two-phase CO_2 operation conditions within the ejector. The experimental tests were carried out to find flow features of an ejector by measuring pressure, at the inlet and outlet of the ejector as well as static pressure along the wall.

Figure A.2 shows the ejector drawing including the pressure indicators. The pressure indicators and the corresponding cross sections are also given in Table A.1. The comparison results of the two-phase ejector model with experiments are given in Tables A.2 and A.3. The ejector inlet operating conditions (pressure, temperature and mass flow rate of the primary and secondary streams) and ejector geometry were used as the input parameters of the ejector simulation model. Then the pressures at different cross sections of the ejector as well as the pressure at ejector outlet were predicted and compared with the experimental results.

Temperatures were measured with K-type thermocouples in both refrigerant and water/coolant lines with an accuracy of 1.1˚C. The refrigerant side pressures were measured with analog manometers and pressure transducers installed by Obrist. The pressure transducers had an uncertainty 0.25% full scale. Two Coriolis mass flow meters were used to measure the refrigerant mass flow rates with an accuracy of 0.15~0.5% of the reading value.

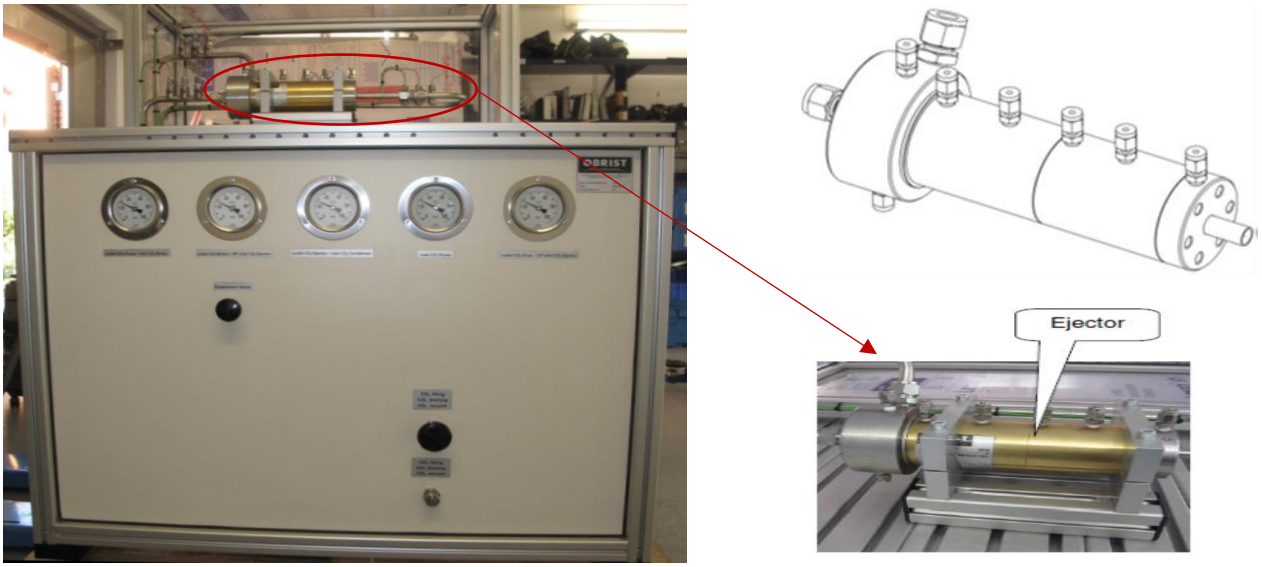

Figure A.1 Installed CO_2 ejector test rig at Hydro-Québec

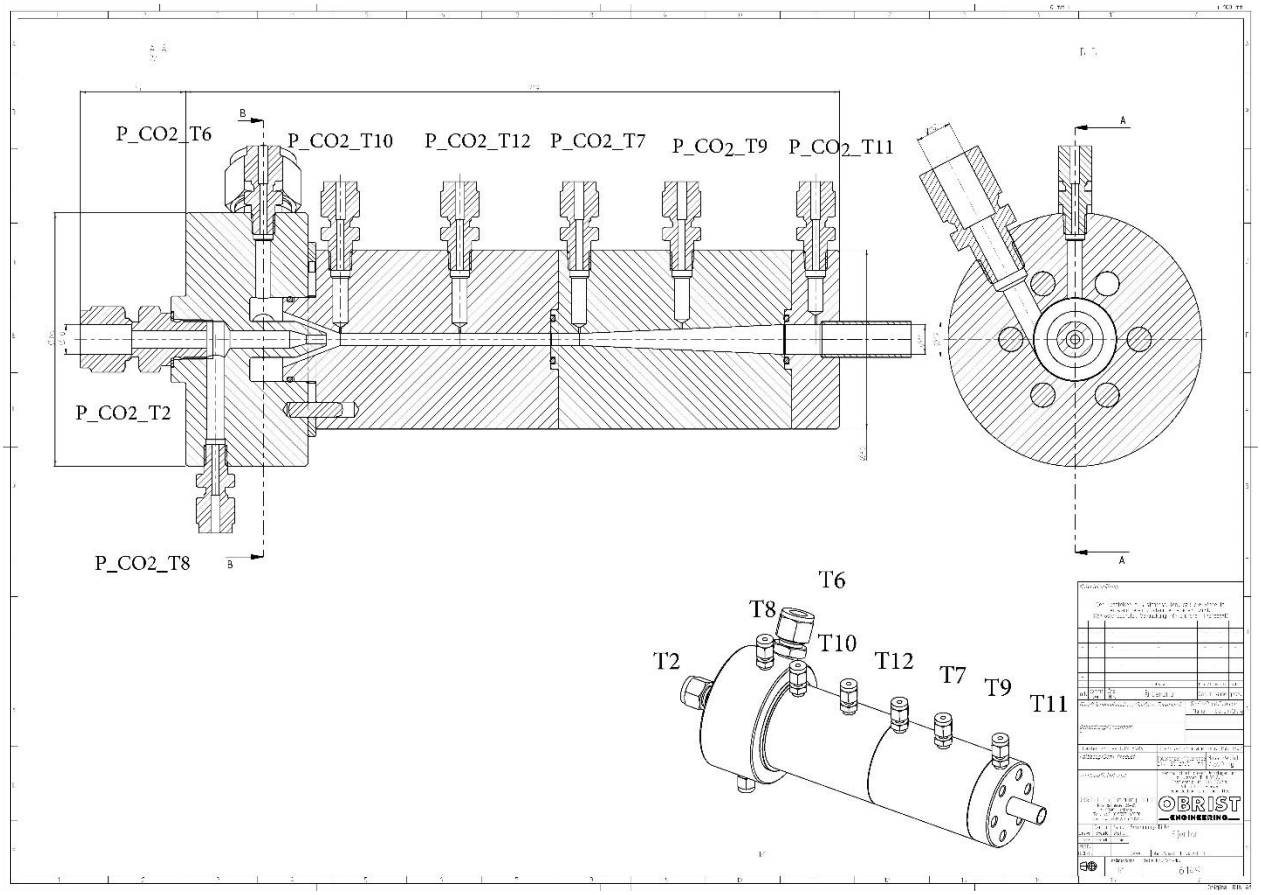

Figure A.2 Ejector drawing (Obrist Engineering)

Table A.1 Pressure indicators and the corresponding cross sections

Pressure indicators acc. to Figure A.1	Corresponding cross section acc. to Figure 4.1	Description
$P\_CO_2\_T_2$	P_p	Pressure at primary inlet
$P\_CO_2\_T_6$	P_s	Pressure at secondary inlet
$P\_CO_2\_T_{10}$	P_m	Pressure at constant area inlet
$P\_CO_2\_T_{12}$	-	Pressure at middle of constant area
-	P_y	Pressure after mixing
$P\_CO_2\_T_7$	P_{mix}	Pressure at outlet of constant area
$P\_CO_2\_T_{11}$	P_{d1}	Pressure at diffuser outlet
$P\_CO_2\_T_3$	P_d	Pressure at ejector outlet

Table A.2 Comparison of simulations with experiments –Series 1 (20-03-2018) for D_{th}=3mm

	Pressure indicators (Figure A.1)	**P_CO₂_T₂**	**P_CO₂_T₆**	**P_CO₂_T₁₀**	**P_CO₂_T₁₂**		**P_CO₂_T₇**	**P_CO₂_T₁₁**	**P_CO₂_T₃**	**F₂/F₁**	
	Description	**Primary inlet**	**secondary inlet**	**Constant area inlet**	**Constant area middle**	**After mixing**	**Constant area outlet**	**Diffuser outlet**	**Ejector outlet**		
	Cross sections (Figure 4.1)	**P_p (kPa)**	**P_s (kPa)**	**P_m (kPa)**		**P_y (kPa)**	**P_{mix} (kPa)**	**P_{d1} (kPa)**	**P_d (kPa)**	**ER**	**P_{ratio}**
1	**Expriment**	7599.78	4608.05	4585.51	5539.96	-	5601.51	5678.30	5681.82	0.128	1.233
	Model	7599.78	4608.05	4538.05	-	5408.05	5321.58	5798.00	5782.53	0.128	1.255
	Error	-	-	1.03	-	-	5.00	2.11	1.77	-	1.772
2	**Expriment**	7573.69	4682.33	4659.53	5628.94	-	5686.25	5770.07	5773.07	0.132	1.233
	Model	7573.69	4682.33	4612.33	-	5427.33	5340.56	5845.00	5828.50	0.132	1.245
	Error	-	-	1.01	-	-	6.08	1.30	0.96	-	0.960
3	**Expriment**	7372.86	4550.64	4527.57	5405.95	-	5472.76	5530.76	5535.55	0.121	1.216
	Model	7372.86	4550.64	4480.60	-	5402.60	5274.60	5637.03	5622.79	0.121	1.236
	Error	-	-	1.04	-	-	3.62	1.92	1.58	-	1.576
4	**Expriment**	7412.16	4008.54	3981.25	4978.57	-	5043.22	5133.07	5134.81	0.123	1.281
	Model	7412.16	4008.54	3913.50	-	4832.50	4725.46	5236.20	5220.42	0.123	1.302
	Error	-	-	1.70	-	-	6.30	2.01	1.67	-	1.667
5	**Expriment**	7699.07	4184.56	4159.86	5229.77	-	5290.85	5388.61	5391.66	0.129	1.288
	Model	7699.07	4184.56	4089.56	-	5079.56	4974.74	5511.40	5494.74	0.129	1.313
	Error	-	-	1.69	-	-	5.97	2.28	1.91	-	1.912
6	**Expriment**	7590.79	4223.31	4198.53	5231.57	-	5293.21	5381.33	5383.76	0.126	1.275
	Model	7590.79	4223.31	4138.31	-	5092.31	4994.04	5506.01	5489.99	0.126	1.300
	Error	-	-	1.43	-	-	5.65	2.32	1.97	-	1.973
7	**Expriment**	7242.68	3950.23	3911.01	4828.49	-	4888.06	4990.32	4990.89	0.158	1.263
	Model	7242.68	3950.23	3790.23	-	4608.23	4484.20	5044.00	5027.15	0.158	1.273
	Error	-	-	3.09	-	-	8.26	1.08	0.73	-	0.727
8	**Expriment**	7237.90	3907.50	3871.16	4804.19	-	4863.38	4963.58	4963.58	0.153	1.270
	Model	7237.90	3907.50	3757.50	-	4590.50	4467.35	5024.00	5007.30	0.153	1.281
	Error	-	-	2.94	-	-	8.14	1.22	0.88	-	0.881

Table A.3 Comparison of simulations with experiments –Series 2 (30-03-2018) for D_{th}=1mm

	Pressure indicators (Figure A.1)	**P_CO2_T2**	**P_CO2_T6**	**P_CO2_T10**	**P_CO2_T12**		**P_CO2_T7**	**P_CO2_T11**	**P_CO2_T3**	**F2/F1**	
	Description	**Primary inlet**	**secondary inlet**	**Constant area inlet**	**Constant area middle**	**After mixing**	**Constant area outlet**	**Diffuser outlet**	**Diffuser outlet**		
	Cross sections (Figure 4.1)	**P_p (kPa)**	**P_s (kPa)**	**P_m (kPa)**		**P_y (kPa)**	**P_{mix} (kPa)**	**P_{d1} (kPa)**	**P_d (kPa)**	**ER**	**P_{ratio}**
1	**Expriment**	9261.17	4084.62	4058.88	4774.39	-	4826.99	4834.34	4839.53	0.055	1.185
	Model	9261.17	4084.62	4079.62	-	4465.62	4462.24	4479.00	4477.99	0.055	1.096
	Error	-	-	0.51	-	-	7.56	7.35	7.47	-	7.471
2	**Expriment**	8589.57	3870.60	3845.91	4496.41	-	4548.14	4547.09	4552.44	0.058	1.176
	Model	8589.57	3870.60	3865.60	-	4209.60	4206.50	4221.00	4220.25	0.058	1.090
	Error	-	-	0.51	-	-	7.51	7.17	7.30	-	7.297

LIST OF REFERENCES

[1] P. Neksa, "CO_2 heat pump systems," International Journal of Refrigeration, vol. 25, no. 4, pp. 421–427, 2002.

[2] M. H. Kim, J. Pettersen, and C. W. Bullard, "Fundamental process and system design issues in CO_2 vapor compression systems," Progress in Energy and Combustion Science, vol. 30, no. 2, pp. 119–174, 2004.

[3] A. Cavallini, L. Cecchinato, M. Corradi, E. Fornasieri, and C. Zilio, "Two-stage transcritical carbon dioxide cycle optimisation: A theoretical and experimental analysis," International Journal of Refrigeration, vol. 28, no. 8, pp. 1274–1283, 2005.

[4] B. T. Austin and K. Sumathy, "Transcritical carbon dioxide heat pump systems: A review," Renewable and Sustainable Energy Reviews, vol. 15, no. 8, pp. 4013–4029, 2011.

[5] A. A. Kornhauser, "The use of an ejector as a refrigerant expander," in Proceedings of the 1990 USNC/IIR – Purdue Refrigeration Conference, Purdue University, West Lafayette, IN, USA, 1990, pp. 10–19.

[6] G. Besagni, R. Mereu, and F. Inzoli, "Ejector refrigeration: a comprehensive review," Renewable and Sustainable Energy Reviews, vol. 53, pp. 373–407, 2016.

[7] D. Li and E. A. Groll, "Transcritical CO_2 refrigeration cycle with ejector-expansion device," International Journal of Refrigeration, vol. 28, no. 5, pp. 766–773, 2005.

[8] J. Deng, P. Jiang, T. Lu, and W. Lu, "Particular characteristics of transcritical CO_2 refrigeration cycle with an ejector," Applied Thermal Engineering, vol. 27, no. 2, pp. 381–388, 2007.

[9] A. Pearson, "Carbon dioxide—new uses for an old refrigerant," International Journal of Refrigeration, vol. 28, no. 8, pp. 1140–1148, 2005.

[10] E. A. Groll and J. H. Kim, "Review article: review of recent advances toward transcritical CO_2 cycle technology," HVAC&R Research, vol. 13, no. 3, pp. 499–520, 2007.

[11] S. Elbel, "Historical and present developments of ejector refrigeration systems with emphasis on transcritical carbon dioxide air-conditioning applications," International Journal of Refrigeration, vol. 34, no. 7, pp. 1545–1561, 2011.

[12] K. Ameur, Z. Aidoun, and M. Ouzzane, "Modeling and numerical approach for the design and operation of two-phase ejectors," Applied Thermal Engineering, vol. 109, pp. 809–818, 2016.

[13] S. W. Elbel and P. S. Hrnjak, "Effect of internal heat exchanger on performance of transcritical CO_2 systems with ejector," in International Refrigeration and Air Conditioning Conference, Purdue, USA, 2004, pp. R166-1-R166-8.

[14] D. Li, “Investigation of an ejector-expansion device in a transcritical carbon dioxide cycle for military ECU applications, Purdue University,” Ph. D. Dissertation, West Lafayette, IN, USA, 2006.

[15] E. Nehdi, L. Kairouani, and M. Bouzaina, “Performance analysis of the vapour compression cycle using ejector as an expander,” International Journal of Energy Research, vol. 31, no. 4, pp. 364–375, 2007.

[16] J. Sarkar, “Optimization of ejector-expansion transcritical CO_2 heat pump cycle,” Energy, vol. 33, no. 9, pp. 1399–1406, 2008.

[17] J. Smolka, Z. Bulinski, A. Fic, A. J. Nowak, K. Banasiak, and A. Hafner, “A computational model of a transcritical R744 ejector based on a homogeneous real fluid approach,” Applied Mathematical Modelling, vol. 37, no. 3, pp. 1208–1224, 2013.

[18] K. Banasiak and A. Hafner, “1D Computational model of a two-phase R744 ejector for expansion work recovery,” International Journal of Thermal Sciences, vol. 50, no. 11, pp. 2235–2247, 2011.

[19] K. Banasiak, A. Hafner, and M. Palacz, “State of the art in the identification of two-phase transonic flow phenomena in transcritical CO_2 ejectors,” in Proceedings of the 24th IIR International Congress of Refrigeration, Yokohama, Japan, 2015.

[20] J. H. Keenan, E. P. Neumann, and F. Lustwerk, “An investigation of ejector design by analysis and experiment,” Journal of Applied Mechanics, vol. 17, pp. 299–309, 1950.

[21] O. Samaké, N. Galanis, and M. Sorin, “On the design and corresponding performance of steam jet ejectors,” Desalination, vol. 381, pp. 15–25, 2016.

[22] A. Dahmani, Z. Aidoun, and N. Galanis, “Optimum design of ejector refrigeration systems with environmentally benign fluids,” International Journal of Thermal Sciences, vol. 50, no. 8, pp. 1562–1572, 2011.

[23] J. T. Munday and D. F. Bagster, “A new ejector theory applied to steam jet refrigeration,” Industrial & Engineering Chemistry Process Design and Development, vol. 16, no. 4, pp. 442–449, 1977.

[24] B. J. Huang, J. M. Chang, C. P. Wang, and V. A. Petrenko, “A 1-D analysis of ejector performance,” International Journal of Refrigeration, vol. 22, no. 5, pp. 354–364, 1999.

[25] S. Varga, A. C. Oliveira, and B. Diaconu, “Numerical assessment of steam ejector efficiencies using CFD,” International Journal of Refrigeration, vol. 32, no. 6, pp. 1203–1211, 2009.

[26] F. Liu and E. A. Groll, “Study of ejector efficiencies in refrigeration cycles,” Applied Thermal Engineering, vol. 52, no. 2, pp. 360–370, 2013.

[27] S. Elbel and P. Hrnjak, “Experimental validation of a prototype ejector designed to reduce throttling losses encountered in transcritical R744 system operation,” International Journal of Refrigeration, vol. 31, no. 3, pp. 411–422, 2008.

[28] N. Lawrence and S. Elbel, “Mathematical modeling and thermodynamic investigation of the use of two-phase ejectors for work recovery and liquid recirculation in refrigeration cycles,” International Journal of Refrigeration, vol. 58, pp. 41–52, 2015.

[29] E. B. L. Ksayer, “Study and design of systems with improved energy efficiency operating with CO_2 as refrigerant,” Ph. D. Dissertation, École Nationale Supérieure des Mines de Paris, 2007.

[30] S. Fangtian and M. Yitai, “Thermodynamic analysis of transcritical CO_2 refrigeration cycle with an ejector,” Applied Thermal Engineering, vol. 31, no. 6, pp. 1184–1189, 2011.

[31] F. E. Manjili and M. A. Yavari, “Performance of a new two-stage multi-intercooling transcritical CO_2 ejector refrigeration cycle,” Applied Thermal Engineering, vol. 40, pp. 202–209, 2012.

[32] Z. Zhang and L. Tian, “Effect of suction nozzle pressure drop on the performance of an ejector-expansion transcritical CO_2 refrigeration cycle,” Entropy, vol. 16, no. 8, pp. 4309–4321, 2014.

[33] N. Galanis and M. Sorin, “Ejector design and performance prediction,” International Journal of Thermal Sciences, vol. 104, pp. 315–329, 2016.

[34] M. Khennich, N. Galanis, and M. Sorin, “Effects of design conditions and irreversibilities on the dimensions of ejectors in refrigeration systems,” Applied Energy, vol. 179, pp. 1020–1031, 2016.

[35] P. Haghparast, M. V. Sorin, and H. Nesreddine, “Effects of component polytropic efficiencies on the dimensions of monophasic ejectors,” Energy Conversion and Management, vol. 162, pp. 251–263, 2018.

[36] ASHRAE, Handbook: Equipment, Chapter 13, Steam jet refrigeration equipment. 1983.

[37] M. Nakagawa, H. Takeuchi, and M. Nakajima, “Performance of two-phase ejector in refrigeration cycle,” in Proceedings of the 3rd International Conference on Multiphase Flow, Lyon, France, 1998, vol. 382, pp. 1–8.

[38] Y. Ozaki, H. Takeuchi, and T. Hirata, “Regeneration of expansion energy by ejector in CO_2 cycle,” in Proceedings of the 6th IIR-Gustav Lorentzen Conference on Natural Working Fluids, Glasgow, UK, 2004, pp. 10–15.

[39] D. Butrymowicz, J. Karwacki, and M. Trela, “Investigation of two-phase ejector in application in compression refrigeration systems,” in Proceedings of the IIR International Conference on Thermophysical Properties and Transfer Processes of Refrigerants, Vicenza, Italy, 2005.

[40] M. Nakagawa, A. R. Marasigan, T. Matsukawa, and A. Kurashina, "Experimental investigation on the effect of mixing length on the performance of two-phase ejector for CO_2 refrigeration cycle with and without heat exchanger," International Journal of Refrigeration, vol. 34, no. 7, pp. 1604–1613, 2011.

[41] M. Palacz, J. Smolka, W. Kus, A. Fic. Z. Bulinski, A.J. Nowak, K. Banasiak and A. Hafner, "CFD-based shape optimisation of a CO_2 two-phase ejector mixing section," Applied Thermal Engineering, vol. 95, pp. 62–69, 2016.

[42] A. B. Wood, A textbook of sound. G. Bell, London, 1964.

[43] M. Yazdani, A. A. Alahyari, and T. D. Radcliff, "Numerical modeling of two-phase supersonic ejectors for work-recovery applications," International Journal of Heat and Mass Transfer, vol. 55, no. 21, pp. 5744–5753, 2012.

[44] C. E. Brennen, Fundamentals of multiphase flow. New York, USA: Cambridge university press, 2005.

[45] M. Nakagawa, A. Harada, and M. S. Berana, "Analysis of expansion waves appearing in the outlets of two-phase flow nozzles," HVAC&R Research, vol. 15, no. 6, pp. 1065–1079, 2009.

[46] H. Lund and T. Flatten, "Equilibrium conditions and sound velocities in two-phase flows," in SIAM Annual Meeting, Pittsburg, Pennsylvania, USA, 2010.

[47] L. Zheng, J. Deng, Y. He, and P. Jiang, "Dynamic model of a transcritical CO_2 ejector expansion refrigeration system," International Journal of Refrigeration, vol. 60, pp. 247–260, 2015.

[48] P. Gullo, A. Hafner, and K. Banasiak, "Transcritical R744 refrigeration systems for supermarket applications: Current status and future perspectives," International Journal of Refrigeration, vol. 93, pp. 269–310, 2018.

[49] H. Takeuchi, Y. Kume, H. Oshitani, and G. Ogata, Ejector cycle system. Google Patents, 2002.

[50] S. Elbel and N. Lawrence, "Review of recent developments in advanced ejector technology," International Journal of Refrigeration, vol. 62, pp. 1–18, 2016.

[51] C. Ju, J. Yang, and H. Qu, "Performance Analysis of CO_2 Heat Pump Water Heater with an Ejector," in 2012 Asia-Pacific Power and Energy Engineering Conference, Shanghai, China, 2012, pp. 1–5.

[52] J. Sarkar, S. Bhattacharyya, and M. R. Gopal, "Simulation of a transcritical CO_2 heat pump cycle for simultaneous cooling and heating applications," International Journal of Refrigeration, vol. 29, no. 5, pp. 735–743, 2006.

[53] M. Nakagawa, M. S. Berana, and A. Kishine, "Supersonic two-phase flow of CO_2 through converging–diverging nozzles for the ejector refrigeration cycle," International Journal of Refrigeration, vol. 32, no. 6, pp. 1195–1202, 2009.

[54] W. Angielczyk, J.-M. Seynhaeve, D. Butrymowicz, and Y. Bartosiewicz, "1-D modeling of supersonic carbon dioxide two-Phase flow through ejector motive nozzle," in International Refrigeration and Air Conditioning Conference, Purdue, USA, 2010, pp. 2362-1-2362–8.

[55] M. Palacz, J. Smolka, A. Fic, Z. Bulinski, A.J. Nowak, K. Banasiak and A. Hafner, "Application range of the HEM approach for CO_2 expansion inside two-phase ejectors for supermarket refrigeration systems," International Journal of Refrigeration, vol. 59, pp. 251–258, 2015.

[56] N. H. Gay, Refrigerating system. Google Patents, 1931.

[57] S. Elbel and P. Hrnjak, "Ejector refrigeration: an overview of historical and present developments with an emphasis on air-conditioning applications," in International Refrigeration and Air Conditioning Conference, Purdue, USA, 2008, pp. 2350-1-2350–8.

[58] H. A. Phillips, Refrigeration system. Google Patents, 1938.

[59] G. Lorentzen, "Throttling, the internal haemorrhage of the refrigeration process, Proceedings of the Institute of Refrigeration," in Proceedings of the Institute of Refrigeration, London, UK, 1983, vol. 80, pp. 39–47.

[60] M. J. Bergander, "New regenerative cycle for vapor compression refrigeration, Final Scientific Report, Magnetic Development Inc., Madison, CT, USA," 2005.

[61] M. J. Bergander, "Refrigeration cycle with two-phase condensing ejector," in International Refrigeration and Air Conditioning Conference, Purdue, USA, 2006, pp. R008-1-R008-8.

[62] A. Khalil, M. Fatouh, and E. Elgendy, "Ejector design and theoretical study of R134a ejector refrigeration cycle," International Journal of Refrigeration, vol. 34, no. 7, pp. 1684–1698, 2011.

[63] A. Selvaraju and A. Mani, "Analysis of an ejector with environment friendly refrigerants," Applied Thermal Engineering, vol. 24, no. 5, pp. 827–838, 2004.

[64] Y. He, J. Deng, and Z. Zhang, "Thermodynamic study on a new transcritical CO_2 ejector expansion refrigeration system with two-stage evaporation and vapor feedback," HVAC&R Research, vol. 20, no. 6, pp. 655–664, 2014.

[65] J. H. Keenan and E. P. Neumann, "A simple air ejector," ASME, Journal of Applied Mechanics, vol. 9, no. 2, pp. A75–A81, 1942.

[66] F. Giacomelli, F. Mazzelli, and A. Milazzo, "Evaporation in supersonic CO_2 ejectors: analysis of theoretical and numerical models," in International Conference on Multiphase Flow, Firenze, Italy, 2016.

[67] M. Yazdani, A. A. Alahyari, and T. D. Radcliff, "Numerical Modeling and Validation of Supersonic Two-Phase Flow of CO_2 in Converging-Diverging Nozzles," Journal of Fluids Engineering, vol. 136, no. 1, p. 14503, 2014.

[68] R. Span and W. Wagner, “A new equation of state for carbon dioxide covering the fluid region from the triple-point temperature to 1100 K at pressures up to 800 MPa,” Journal of Physical and Chemical Reference Data, vol. 25, no. 6, pp. 1509–1596, 1996.

[69] Y. Zhu, Z. Wang, Y. Yang, and P.-X. Jiang, “Flow visualization of supersonic two-phase transcritical flow of CO_2 in an ejector of a refrigeration system,” International Journal of Refrigeration, vol. 74, pp. 352–359, 2017.

[70] B. J. Huang, C. B. Jiang, and F. L. Hu, “Ejector performance characteristics and design analysis of jet refrigeration system,” Journal of Engineering for Gas Turbines and Power, vol. 107, no. 3, pp. 792–802, 1985.

[71] K. Chunnanond and S. Aphornratana, “An experimental investigation of a steam ejector refrigerator: the analysis of the pressure profile along the ejector,” Applied Thermal Engineering, vol. 24, no. 2, pp. 311–322, 2004.

[72] T. Sriveerakul, S. Aphornratana, and K. Chunnanond, “Performance prediction of steam ejector using computational fluid dynamics: Part 1. Validation of the CFD results,” International Journal of Thermal Sciences, vol. 46, no. 8, pp. 812–822, 2007.

[73] T. Sriveerakul, S. Aphomatana, and K. Chunnanond, “Performance prediction of steam ejector using computational fluid dynamics: Part 2. Flow structure of a steam ejector influenced by operating pressures and geometries,” International Journal of Thermal Sciences, vol. 46, pp. 823–833, 2010.

[74] S. Croquer, S. Poncet, and Z. Aidoun, “Turbulence modeling of a single-phase R134a supersonic ejector. Part 2: Local flow structure and exergy analysis,” International Journal of Refrigeration, vol. 61, pp. 153–165, 2016.

[75] Y. Fang, S. Croquer, S. Poncet, Z. Aidoun, and Y. Bartosiewicz, “Drop-in replacement in a R134 ejector refrigeration cycle by HFO refrigerants,” International Journal of Refrigeration, vol. 77, pp. 87–98, 2017.

[76] N. Bilir Sag and H. K. Ersoy, “Performance improvement of the vapour compression refrigeration cycle by a two-phase constant area ejector,” International Journal of Energy Research, vol. 33, no. 5, pp. 469–480, 2009.

[77] J. Chen, S. Jarall, H. Havtun, and B. Palm, “A review on versatile ejector applications in refrigeration systems,” Renewable and Sustainable Energy Reviews, vol. 49, pp. 67–90, 2015.

[78] N. Bilir Sag, H. K. Ersoy, A. Hepbasli, and H. S. Halkaci, “Energetic and exergetic comparison of basic and ejector expander refrigeration systems operating under the same external conditions and cooling capacities,” Energy Conversion and Management, vol. 90, pp. 184–194, 2015.

[79] S. Taslimi Taleghani, M. Sorin, and S. Poncet, “Energy and exergy efficiencies of different configurations of the ejector-based CO_2 refrigeration systems,” International Journal of Energy Production and Management, vol. 3, no. 1, pp. 22–33, 2018.

[80] M. Khennich, M. Sorin, and N. Galanis, “Exergy flows inside a one phase ejector for refrigeration systems,” Energies, vol. 9, no. 3, p. 212, 2016.

[81] H. K. Ersoy and N. Bilir Sag, “Performance characteristics of ejector expander transcritical CO_2 refrigeration cycle,” Proceedings of the Institution of Mechanical Engineers, Part A: Journal of Power and Energy, vol. 226, no. 5, pp. 623–635, 2012.

[82] J. Chen, H. Havtun, and B. Palm, “Conventional and advanced exergy analysis of an ejector refrigeration system,” Applied Energy, vol. 144, pp. 139–151, 2015.

[83] V. M. Brodyansky, M. Sorin, and P. Le Goff, The efficiency of industrial processes: exergy analysis and optimization, Elsevier Science B. V: Amsterdam, The Netherlands, 1994.

[84] S. Taslimi Taleghani, M. Sorin, and S. Poncet, “Modeling of two-phase transcritical CO_2 ejectors for on-design and off-design conditions,” International Journal of Refrigeration, vol. 87, pp. 91–105, 2017.

[85] T. J. Kotas, The exergy method of thermal plant analysis. 2nd ed. Malabar, Florida: Krieger Publishing, 1995.

[86] J. Szargut, D. R. Morris, and F. R. Steward, “Exergy analysis of thermal, chemical, and metallurgical processes,” New York: Hemisphere Publishing Corporation, 1988.

[87] G. Tsatsaronis, “Thermoeconomic analysis and optimization of energy systems,” Progress in Energy and Combustion Science, vol. 19, no. 3, pp. 227–257, 1993.

[88] A. Bejan and G. Tsatsaronis, Thermal design and optimization. John Wiley & Sons, 1996.

[89] P. Grassmann, “Towards the general definition of efficiency (in German),” Chemie Ingenieur Technik, vol. 22, no. 4, pp. 77–80, 1950.

[90] Y. Ma, Z. Liu, and H. Tian, “A review of transcritical carbon dioxide heat pump and refrigeration cycles,” Energy, vol. 55, pp. 156–172, 2013.

[91] K. Banasiak, A. Hafner, and T. Andresen, “Experimental and numerical investigation of the influence of the two-phase ejector geometry on the performance of the R744 heat pump,” International Journal of Refrigeration, vol. 35, no. 6, pp. 1617–1625, 2012.

[92] Y. Zhu, Y. Huang, C. Li, F. Zhang, and P.-X. Jiang, “Experimental investigation on the performance of transcritical CO_2 ejector–expansion heat pump water heater system,” Energy Conversion and Management, vol. 167, pp. 147–155, 2018.

[93] C. Lucas and J. Koehler, “Experimental investigation of the COP improvement of a refrigeration cycle by use of an ejector,” International Journal of Refrigeration, vol. 35, no. 6, pp. 1595–1603, 2012.

[94] Y. He, J. Deng, F. Yang, and Z. Zhang, "An optimal multivariable controller for transcritical CO_2 refrigeration cycle with an adjustable ejector," Energy Conversion and Management, vol. 142, pp. 466–476, 2017.

[95] P. Haghparast, M. V. Sorin, and H. Nesreddine, "The impact of internal ejector working characteristics and geometry on the performance of a refrigeration cycle," Energy, vol. 162, pp. 728–743, 2018.

[96] J. Smolka, M. Palacz, J. Bodys, K. Banasiak, A. Fic, Z. Bulinski, A.J. Nowak, A. Hafner, "Performance comparison of fixed-and controllable-geometry ejectors in a CO_2 refrigeration system," International Journal of Refrigeration, vol. 65, pp. 172–182, 2016.

[97] F. Liu and E. A. Groll, "Analysis of a two phase flow ejector for transcritical CO_2 cycle," in Refrigeration and Air Conditioning Conference, Purdue, USA, 2008, pp. 1–10.

[98] F. Liu, E. A. Groll, and D. Li, "Investigation on performance of variable geometry ejectors for CO_2 refrigeration cycles," Energy, vol. 45, no. 1, pp. 829–839, 2012.

[99] F. Liu, Y. Li, and E. A. Groll, "Performance enhancement of CO_2 air conditioner with a controllable ejector," International Journal of Refrigeration, vol. 35, no. 6, pp. 1604–1616, 2012.

[100] Y. He, J. Deng, L. Zheng, and Z. Zhang, "Performance optimization of a transcritical CO_2 refrigeration system using a controlled ejector," International Journal of Refrigeration, vol. 75, pp. 250–261, 2017.

[101] G. Chen, L. Liang, L. Tang, X. Xu, Z. Zhu, and Q. Chen, "Experimental investigation of an adjustable ejector for CO_2 heat pump water heaters," Journal of Zhejiang University SCIENCE A, vol. 10, no. 11, pp. 1678–1682, 2009.

[102] F. Liu, E. A. Groll, and J. Ren, "Comprehensive experimental performance analyses of an ejector expansion transcritical CO_2 system," Applied Thermal Engineering, vol. 98, pp. 1061–1069, 2016.

[103] N. Bilir Sag and H. K. Ersoy, "Experimental investigation on motive nozzle throat diameter for an ejector expansion refrigeration system," Energy Conversion and Management, vol. 124, pp. 1–12, 2016.

[104] F. Liu, E. A. Groll, and D. Li, "Modeling study of an ejector expansion residential CO_2 air conditioning system," Energy and Buildings, vol. 53, pp. 127–136, 2012.

[105] X. X. Xu, G. M. Chen, L. M. Tang, and Z. J. Zhu, "Experimental investigation on performance of transcritical CO_2 heat pump system with ejector under optimum high-side pressure," Energy, vol. 44, no. 1, pp. 870–877, 2012.

[106] S. Wang, Y. He, H. Tuo, F. Cao, and Z. Xing, "Effect of heat transfer area and refrigerant mass flux in a gas cooler on heating performance of air-source transcritical CO_2 heat pump water heater system," Energy and Buildings, vol. 67, pp. 1–10, 2013.

[107] S. Taslimi Taleghani, M. Sorin, and S. Poncet, "Exergy performance of a transcritical CO_2 two-phase ejector," in Proceedings of ECOS 2018 - The 31st International Conference on Efficiency, Cost, Optimization, Simulation and Environmental Impact of Energy Systems, Guimaraes, Portugal, 2018.

[108] S. A. Klein, "EES, Engineering Equation Solver, Academic Commercial V8.400, McGraw Hill, http://www.fchart.com/ees/." 2009.

[109] I. K. Kim, J. H. Park, Y. H. Kwon, and Y. S. Kim, "Experimental study on R-410a evaporation heat transfer characteristics in oblong shell and plate heat exchanger," Heat Transfer Engineering, vol. 28, no. 7, pp. 633–639, 2007.

[110] Z. H. Ayub, "Plate heat exchanger literature survey and new heat transfer and pressure drop correlations for refrigerant evaporators," Heat Transfer Engineering, vol. 24, no. 5, pp. 3–16, 2003.

[111] H. Martin, "A theoretical approach to predict the performance of chevron-type plate heat exchangers," Chemical Engineering and Processing: Process Intensification, vol. 35, no. 4, pp. 301–310, 1996.

[112] D. N. Danilova, "Heat transfer in different plate geometries," Kholodilnaya Tekhnika, vol. 4, pp. 25–31, 1981.

[113] J. X. Wang, Y. Z. Li, J. X. Li, C. Li, Y. Zhang, and X. W. Ning, "A gas-atomized spray cooling system integrated with an ejector loop: ejector modeling and thermal performance analysis," Energy Conversion and Management, vol. 180, pp. 106–118, 2019.

[114] J. X. Wang, Y. Z. Li, J. X. Li, C. Li, K. Xiong, and X. W. Ning, "Enhanced heat transfer by an original 'immersed spray cooling system'integrated with an ejector," Energy, 2018.

[115] L. Zheng and J. Deng, "Research on CO_2 ejector component efficiencies by experiment measurement and distributed-parameter modeling," Energy Conversion and Management, vol. 142, pp. 244–256, 2017.

[116] J. Cen, P. Liu, and F. Jiang, "A novel transcritical CO_2 refrigeration cycle with two ejectors," International Journal of Refrigeration, vol. 35, no. 8, pp. 2233–2239, 2012.

[117] K. Banasiak, A. Hafner, E.E. Kriezi, K.B. Madsen, M. Birkelund, K. Fredslund, R. Olsson, "Development and performance mapping of a multi-ejector expansion work recovery pack for R744 vapour compression units," International Journal of Refrigeration, vol. 57, pp. 265–276, 2015.

[118] B. Sahin and A. Kodal, "Finite time thermoeconomic optimization for endoreversible refrigerators and heat pumps," Energy Conversion and Management, vol. 40, no. 9, pp. 951–960, 1999.

[119] J. Sarkar, "Geometric parameter optimization of ejector-expansion refrigeration cycle with natural refrigerants," International Journal of Energy Research, vol. 34, no. 1, pp. 84–94, 2010.